eCAM Evidence-Based Complementary and Alternative Medicine

Traditional Medicine for Wound Management

Lead Guest Editor: Ipek Suntar
Guest Editors: Satyajit D. Sarker, Lutfun Nahar, and Norazah Basar

Traditional Medicine for Wound Management

Evidence-Based Complementary and Alternative Medicine

Traditional Medicine for Wound Management

Lead Guest Editor: Ipek Suntar
Guest Editors: Satyajit D. Sarker, Lutfun Nahar, and Norazah Basar

Editorial Board

Contents

Hindawi
Evidence-Based Complementary and Alternative Medicine
Volume 2017, Article ID 4214382, 1 page
https://doi.org/10.1155/2017/4214382

Editorial
Traditional Medicine for Wound Management

Ipek Suntar,[1] Satyajit D. Sarker,[2] Lutfun Nahar,[2] and Norazah Basar[3]

[1]*Department of Pharmacognosy, Faculty of Pharmacy, Gazi University, Etiler, 06330 Ankara, Turkey*
[2]*Medicinal Chemistry and Natural Products Research Group, School of Pharmacy and Biomolecular Sciences, Liverpool John Moores University, Faculty of Science, James Parsons Building, Byrom Street, Liverpool L3 3AF, UK*
[3]*Chemistry Department, Faculty of Science, Universiti Teknologi Malaysia, Johor, Malaysia*

Correspondence should be addressed to Ipek Suntar; ipesin@gazi.edu.tr

Received 13 June 2017; Accepted 13 June 2017; Published 17 July 2017

Nature is the main source of traditional medicine, which is based on the knowledge gained over generations. The development of novel drugs through the scientific investigation of biological activities and phytochemical features of traditional medicines is fundamental for the treatment of human ailments. Indeed, ethnobotanical knowledge has been recorded in folklore medicines in certain parts of the world. Ethnobotanical data are the starting point of such ethnopharmacognostic research endeavors, proceeding with an experimental part at the later stage for the verification of this information using appropriate scientific approaches.

As various natural remedies, especially from medicinal plants, are affordable and easily available, they are widely used for wound healing and to treat other skin diseases. Although the popularity of traditional and complementary medicine has increased in recent years, an awareness regarding their quality, efficacy, and safety needs to be raised through scientific standardization and safety evaluation before their clinical use.

To date, many scientific studies have revealed the wound healing active components from natural products. This special issue includes seven research articles addressing the effectiveness of natural remedies used for wound healing purposes. A research regarding the antiadhesive effect of Traditional Chinese Medicinal plants, namely, *Atractylodes macrocephala* Koidz., *Aucklandia lappa* Decne., *Cannabis sativa* L., *Citrus aurantium* L., *Codonopsis pilosula* Franch., *Magnolia officinalis* Rehd. et Wils., *Paeonia lactiflora* Pall., *Prunus persica* Batsch., and *Rheum palmatum* L. in intra-abdominal adhesion-induced rat model takes a part. Moreover, hemostatic activity of *Bletilla striata* Rchb.f. micron particles and potential wound healing activities of *Periplaneta americana* L., *Abrus cantoniensis* Hance, *Prunus yedoensis* Matsum., grape seed, sesame, and fenugreek oils as well as traditionally used medicinal plants in Ghana are also presented herein. These articles represent *in vivo* and *in vitro* bioactivity tests, phytochemical analysis, and activity mechanism assays, all of which are essential for scientific confirmation of natural product utilization in complementary medicine.

We would like to express our gratitude to all authors for their contributions. We hope the readers will benefit from this special issue as an academic reference.

Ipek Suntar
Satyajit D. Sarker
Lutfun Nahar
Norazah Basar

Hindawi
Evidence-Based Complementary and Alternative Medicine
Volume 2017, Article ID 5821706, 12 pages
https://doi.org/10.1155/2017/5821706

Research Article

Periplaneta americana Extracts Promote Skin Wound Healing via Nuclear Factor Kappa B Canonical Pathway and Extracellular Signal-Regulated Kinase Signaling

Qin Song,[1] Qiheng Gou,[2] Yuxin Xie,[3] Zhen Zhang,[4] and Chaomei Fu[4]

[1]*College of Pharmacy and Bioengineering, Chengdu University, Chengdu, Sichuan 610106, China*
[2]*State Key Laboratory of Biotherapy/Collaborative Innovation Center of Biotherapy, West China Hospital, Sichuan University, Chengdu 610041, China*
[3]*Departments of Head and Neck and Mammary Gland Oncology and Medical Oncology, Cancer Center and State Key Laboratory of Biotherapy, Laboratory of Molecular Diagnosis of Cancer, West China Hospital, Sichuan University, Chengdu, Sichuan 610041, China*
[4]*College of Pharmacy, Chengdu University of Traditional Chinese Medicine, Chengdu, Sichuan 610106, China*

Correspondence should be addressed to Chaomei Fu; chaomeifu@126.com.cn

Received 31 October 2016; Revised 14 February 2017; Accepted 7 March 2017; Published 23 May 2017

Academic Editor: Ipek Suntar

Periplaneta americana extracts (PAEs) exhibit wound healing properties. However, the underlying molecular mechanisms are not well understood. Here, we treated human skin fibroblasts (HSF) with PAE and the proliferation was determined by 3-(4,5-dimethylthiazol-2-yl)-2,5-diphenyltetrazolium bromide (MTT) assay. The wound healing and transwell migration assays were used to detect cell migration. Nuclear factor kappa B (NF-κB) and extracellular signal-regulated kinase (ERK) pathways were analyzed by Western blot (WB). Immunofluorescence staining was used to detect the key molecular localization in the cells. The results showed that PAE enhanced the proliferation and migration of HSF cells. The expression and activation of key proteins such as RelA and p-ERK were increased in NF-κB and ERK pathways followed by nuclear translocation. In vivo, both WB and immunohistochemical (IHC) staining showed that PAE enhanced p-IκBα and p-ERK activation and the nuclear translocation of RelA. Our study suggests that the protective function of PAE is mediated via enhanced NF-κB and ERK signaling.

1. Introduction

Skin wound healing is a complex process including cell proliferation, migration, and matrix synthesis. It is commonly divided into three stages including: (1) inflammatory cell phase, (2) cell proliferation, and (3) tissue remodeling [1]. Various types of cells including epithelial and mesenchymal cells and fibroblasts play a key role in wound healing [2]. Thermal injury of skin is caused by tissue lesions following exposure to flames, hot surfaces and liquids, extreme cold, chemicals, radiation, or friction [3]. Even with improved prognosis and therapeutic intervention via biological skin substitutes, burns represent an important cause of mortality.

Periplaneta americana exhibits therapeutic effects in wound healing. In 1985, the *Periplaneta americana* extract (PAE), also designated as W11-a12 or Kangfuxin, was first used clinically. Subsequently, it has been widely used in China to heal severe ulcers and burns. It is administered intravenously and orally or directly applied on the wounds topically [4, 5]. The mechanisms underlying the healing effect of PAE are not fully established. Early studies suggested that PAE promoted healing in rats sustaining combined radiation (6 Gy) [3] and wound injury [6]. In the present study, we focused on the molecular mechanisms of PAE applied topically on skin wounds in mice following to thermal injury.

ERK belongs to the mitogen-activated protein kinase (MAPK) family. ERK1 and ERK2 form a central component in the MAPK cascade and play a crucial role in signal transduction from surface receptors to the nucleus. Activated ERK dimers translocate to the nucleus and regulate several gene transcriptions, such as Elk-1, ATF, NF-κB, Ap-1, and c-fos, leading to cell proliferation and differentiation,

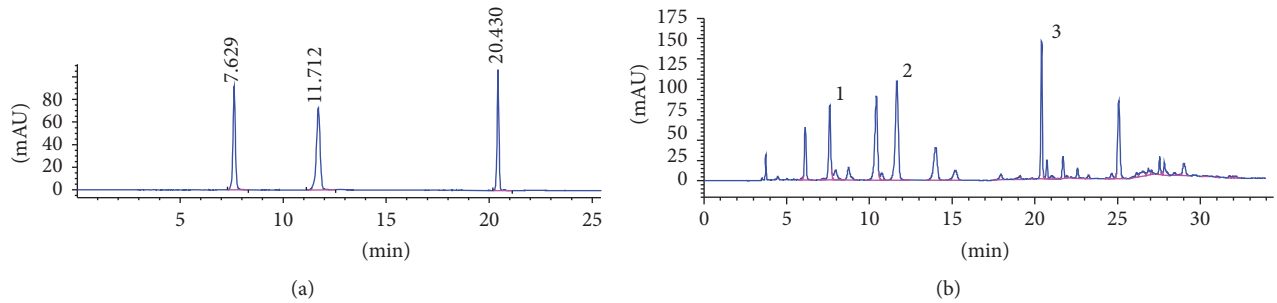

Figure 1: Chromatographic separation of PAE. (a) HPLC chromatogram of authentic standards tested. (b) HPLC chromatogram of PAE at 254 nm: peak 1, uracil (1.140 mg/g); peak 2, hypoxanthine (4.257 mg/g); and peak 3, inosine (8.158 mg/g). Identification was based on retention time and UV spectra compared with commercial standards.

cytoskeletal structure, cell apoptosis, and other biological reaction [7, 8]. The biological effect, in turn, dictates whether ERK-expressing cells enter a program of cell death, survival, or differentiation [9, 10].

NF-κB is a transcription factor regulating the expression of multiple genes and cellular functions, including migration and survival [11]. NF-κB activation is regulated by negative feedback mediated by IκB, an inhibitor that binds to NF-κB, but undergoes ubiquitin-mediated proteasomal degradation, releasing NF-κB for nuclear translocation and transcription [12]. NF-κB triggers cell proliferation and migration. Abnormal NF- κB expression induces autoimmune disease, chronic inflammation, metabolic disease, and cancer [13]. Early evidence reveals three separate pathways: the canonical NF- κB pathway; the alternative NF- κB pathway; and an independent pathway [14, 15]. The canonical pathway is involved in the fibroblast migration and progression of wound healing. Furthermore, NF-κB is a redox-sensitive transcription factor acting as a sensor of oxidative stress [16]. Thermal injury induces local tissue hypoxia. We hypothesize that PAE treatment improves NF-κB signaling via activation of wound healing. Thus, in the present study, we investigated the biological function and mechanisms of PAE in human skin fibroblast and rat skin injury models to facilitate the clinical application of PAE.

2. Materials and Methods

2.1. Cell Lines. Human skin fibroblast (HSF) cell line purchased from the American Type Cell culture/ATCC CRL-2522™ was cultivated in DMEM with 10% fetal bovine serum (Gibco Life Science, Grand Island) and 1% penicillin-streptomycin (Sigma, V900929) at 37°C in a humidified incubator with 5% carbon dioxide.

2.2. Preparation of PAE. *P. americana* was obtained from the Good Agriculture Practice (GAP) breeding base, Sichuan, China. The powdered dried *P. americana* (200 g) was extracted with 90% EtOH (1.2 L) twice at 80°C. After solvent evaporation, the ethanol extract was recovered. The extract (20 g) was suspended in water (200 mL) at 80°C. After filtration through 0.22 μm filter membranes at appropriate concentrations, it was stored at −20°C until use. The HPLC-diode array detector (HPLC-DAD) was used to study *P. americana* extraction. The compounds in PAE were analyzed (Figure 1) using Diamonsil C18 (250 × 4.6 mm; 5 μm) as the chromatography column. The optimized mobile phase consisted of solvent A (3% v/v methanol in water containing 0.07% v/v acetic acid) and solvent B (methanol). The following gradient of time (min)/mobile phase A (%)/mobile phase B (%) was used: 0.0/100/0, 10/100/0, 20/70/30, 21/50/50, and 35/0/100, at a flow rate of 0.6 mL/min at 25°C and detection wavelength 254 nm with 10 μL injection volume.

2.3. MTT Cell Proliferation Assays. The in vitro cell proliferation induced by PAE was determined using MTT assay. Briefly, cells were seeded in a volume of 200 μL (3,000 cells/well) on 96-well plates after cultivation with different concentrations of PAE. The culture medium containing serum was replaced by MTT every 24 h. A final MTT concentration of 0.5 mg/mL was added to the wells followed by incubation for 4 h at 37°C. The supernatant was discarded and replaced with DMSO (150 μL/well). The optical densities (OD) were measured at 570 nm with a NOVOstar microplate reader. The experiment was repeated in triplicate. The viable concentration was calculated using GraphPad Prism 5.0.

2.4. Transwell Migration Assay. To assay the migratory behavior of HSF cells following PAE treatment in the Transwell Milicells (8 μm pore size, Millipore, USA), a 90% confluent T-25 flask of HSF cells was treated with or without PAE (0.3125 mg/mL). A 600 μl 10% FBS growth medium was added to the lower chamber, followed by trypsinization using standard procedures. The final pellet was resuspended in 2 mL of serum-free medium (SF-EMEM) and seed cells (2×10^4/cells) in the upper chamber. After incubation for 24 h, the chambers were fixed with 4% paraformaldehyde for 30 min and stained with hematoxylin for 15 min. We counted the cells using optical microscope.

2.5. Cell Scratch Tests. Cell scratch test is particularly appropriate for studies investigating the effect of cell-matrix and cell-cell interactions on cell migration. HSF were seeded in the 6-well plate and the 10% FBS growth medium

containing the serum-free medium supplemented with the PAE (0.3125 mg/mL) was grown to 90% confluence. After treatment for 48 h, the culture medium was removed and the monolayers were scratched using a 200 μL pipette to create a uniform cell-free wound area. Debris was removed by gently washing with sterile PBS. Cell movement into the wound area was monitored and photographed at 0, 24, and 48 h using an optical microscope.

2.6. Western Blot. Total protein extracts (30 to 50 μg) from cells lysates were prepared. Each sample was subjected to electrophoresis on 12% SDS-polyacrylamide gels. Then, the protein was blotted onto a PVDF membrane (Millipore, Billerica, MA) at 230 mA for 2 h. Primary antibodies against IKK β (1 : 1,000; Cell Signaling Technology, Beverly, MA, USA), p-IκBα (1 : 1,000; Cell Signaling Technology, Danvers, MA, USA), IκBα (1 : 1,000; Cell Signaling Technology, Beverly, MA, USA), RelA (1 : 1,000; Cell Signaling Technology, Beverly, MA, USA), p-ERK (1 : 1000; Cell Signaling Technology, Beverly, MA, USA), ERK (1 : 1000; Cell Signaling Technology, Beverly, MA, USA), and β-actin (1 : 1,000; Sigma-Aldrich, St. Louis, MO, USA) were used, according to the manufacturer's instructions. After washing the membrane, the secondary antibody (HRP-conjugated anti-mouse/rabbit IgG) was used for detection. The bands were visualized with the ECL detection system.

2.7. Immunofluorescence Staining. After seeding the cells on sterile slides for 24 h, different doses of PAE were added for 48 h. Each group of HSF cells was washed twice with PBS and fixed with 4% paraformaldehyde (pH 7.4) in 6-well plates and incubated with 0.5% Triton X-100 for 30 min at room temperature, followed by blocking with 5% BSA for 1 h. The slides were incubated with the following primary antibodies: RelA (dilution 1 : 100; Cell Signaling Technology, Beverly, MA, USA), phospho-ERK (Cell Signaling Technology, Beverly, MA, USA), and ERK (Cell Signaling Technology, Beverly, MA, USA) overnight at 4°C. The cells were incubated with the corresponding fluorescent dye-conjugated secondary antibodies (dilution 1 : 200; Cell Signaling Technology, Beverly, MA, USA) at 37°C for 1 h and protected from light. The cells were visualized using fluorescence microscopy.

2.8. Mouse Model of Thermal Burn. Eight healthy adult C57 male mice were purchased from the West China School of Preclinical and Forensic Medicine, Sichuan University, China. All the experiments were conducted according to the Guide for the Care and Use of Laboratory Animals at the Animal Experimental Center of Sichuan. Initially, 8 animals were weighed and intramuscularly injected with atropine sulfate (0.04 mg/kg). After 10 minutes, they were injected with anesthetic combination of 10% ketamine (90 mg/kg) and 2% xylazine (10 mg/kg) intramuscularly. When the animals properly anesthetized, their backs were treated with 1% polyvinylpyrrolidone iodine. Thermal injuries were created with a solid aluminum bar (φ10 mm) previously heated in boiling water (100°C). The bar was maintained symmetrically in contact with the skin on the dorsal flank for 15 s. The pressure exerted on the animal skin corresponded to the mass of 50 g. Immediately after the procedure, analgesia with sodium dipyrone (40 mg/kg) was performed intramuscularly and was maintained with sodium dipyrone (200 mg/kg) in the drinking water for three consecutive days. The left dorsal skin was wiped with PAE (5 mg/mL), while the right was treated with equal amounts of normal saline. In the course of 21-day treatments, wound healing rates were measured at day points 0, 7, 14, and 21 after treatment. The wound healing rates were measured and the complete wound healing time was calculated using the formula: healing rate = original wound area/original wound area [17]. Mice were sacrificed after 21 days.

2.9. Immunohistochemical and Immunocytochemical Staining. Briefly, the skin tissues were fixed in formalin and embedded in paraffin. Consecutive paraffin sections (4 μm-thick) of tissue samples were prepared and incubated overnight at 4°C with primary antibodies, followed by incubation with peroxidase-labeled polymer conjugated to goat anti-rabbit immunoglobulins (EnVision/HRP, Dako, Denmark). All the IHC assays were carried out according to the manufacturer's instructions.

2.10. Statistical Analyses. Statistical analyses were performed using SPSS 11.5 (SPSS Inc., Chicago, IL, USA) or Prism 6.0 (GraphPad Software, La Jolla, CA, USA). Quantitative data were evaluated with a two-tailed Student's t-test, and one-way analysis of variance (ANOVA). Differences were considered statistically significant at $p < 0.05$.

3. Results

3.1. PAE Promotes Cell Proliferation In Vitro. MTT cell proliferation assay was used to detect the appropriate concentration of PAE and the time point on the HSF cell line at early passages (passage 8–10). The assays performed at 24 h, 48 h, and 72 h showed that the low (0.3125 mg/mL) dose of the PAE promoted cell growth (Figure 2), especially at 48 h of treatment ($p < 0.05$; one-way ANOVA). Interestingly, the data presented in Figure 2 indicated that the PAE at higher concentration (1.25 mg/mL) could inhibit the cell proliferation. Above all, we selected the optimal concentration of 0.3125 mg/mL with the time of 48 h treatment in subsequent assay.

3.2. PAE Facilitates Migration of HSF. Cell migration into a "wound" created on a monolayer of cells revealed the effects of wound healing. Denudation of part of the HSF induced epidermal cell migration to close the wound with loosely connected cell populations, which also mimicked the behavior of cells during migration in vivo [18].

To determine whether PAE promoted HSF cell migration in skin, we performed transwell and wound healing assays. Human skin fibroblasts were treated with PAE at the final concentration of 0.3125 mg/mL for 48 h. As shown in Figure 3(a), cells treated with PAE showed 2-fold migration efficiency compared with control ($p < 0.01$). Similar to

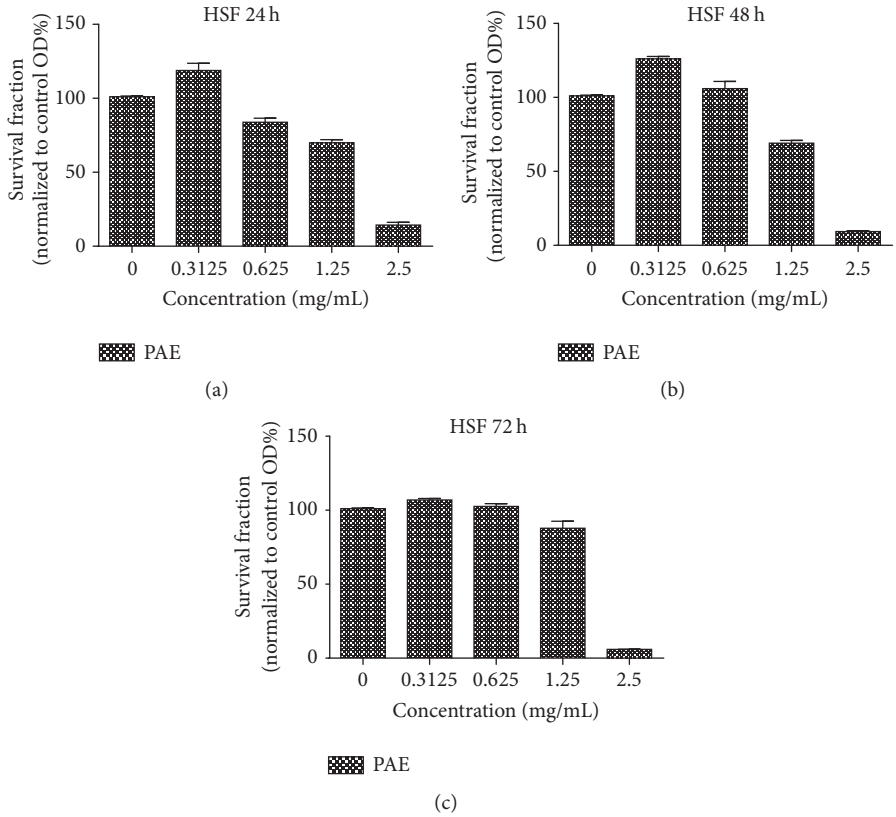

Figure 2: MTT assay using different doses of PAE on HSF at different time points. (a) The survival fraction of different doses of extract on HSF at 24 h (normalized to control group); (b) the survival fraction of different doses of extract on HSF at 48 h (normalized to control group); (c) the survival fraction of different doses of extract on HSF at 72 h (normalized to control group).

the transwell assay, the cell scratch test also significantly improved the migration of wound closure in the PAE-treated group of HSF cells (Figure 3(b), $p < 0.01$).

3.3. PAE Enhanced NF-κB Canonical Pathway and ERK Phosphorylation. Compared with the control, the expression of downstream RelA in the canonical NF- κB pathway was significantly higher in the PAE-treated cells. Interestingly, we found that the level of ERK phosphorylation was significantly improved while the level of ERK total protein scarcely changed ($p < 0.05$) (Figure 4(a)). These suggested that the PAE enhanced NF-κB canonical pathway and ERK pathway. Furthermore, we determined the molecular mechanism of PAE in the activation of NF-κB pathway using BAY 11-7082, a complete and specific NF-κB pathway inhibitor (Figure 4(b)) [13]. The results suggested that the expression of p-IκBα was gradually decreased depending on the dose of BAY 11-7082. Further, the activities of NF-κB pathway were suppressed. We added the PAE (0.3125 mg/mL final concentration) after the inhibition of NF-κB pathway using the BAY 11-7082. After treatment with PAE for 48 h, we found that the reintroduction of PAE failed to restore the expression of p-IκBα suggesting that NF-κB pathway was still suppressed (Figure 4(c)). Moreover, as shown in Figures 4(d) and 4(e), the PAE-induced cell growth and migration were prevented by pretreatment with BAY 11-7082 in HSF cells. The result confirmed that the PAE analogues promoted HSF migration and proliferation by activating the NF-κB pathway.

3.4. PAE Increases RelA and Phosphorylation of ERK Nuclear Translocation. As illustrated in Figure 5(a), the antibody against RelA showed green fluorescence whereas the nucleus was stained blue by DAPI. Areas of overlap in the merged images presented aquamarine color. The control group exhibited green fluorescence in the cytoplasm. During the PAE treatment, the green fluorescence was evenly distributed, and the aquamarine area in the merged image was increased suggesting translocation of RelA from the cytoplasm to the nucleus. Similar results were detected in the p-ERK protein (Figure 5(b)). However, ERK translocation occurred barely (Figure 5(c)). PAE increased the protein levels along with the nuclear translocation of RelA and p-ERK proteins.

3.5. PAE Promoted Wound Healing of Cutaneous Thermal Burn In Vivo. Based on the effect of PAE on migration and proliferation in vitro, we hypothesized that the PAE improves skin wound healing in vivo.

Briefly, we created a deep second-degree thermal burn in C57 mice, as described in Materials and Methods. Originally, we failed to distinguish the skin lesions until swelling and ulceration were detected during the following days. The burn

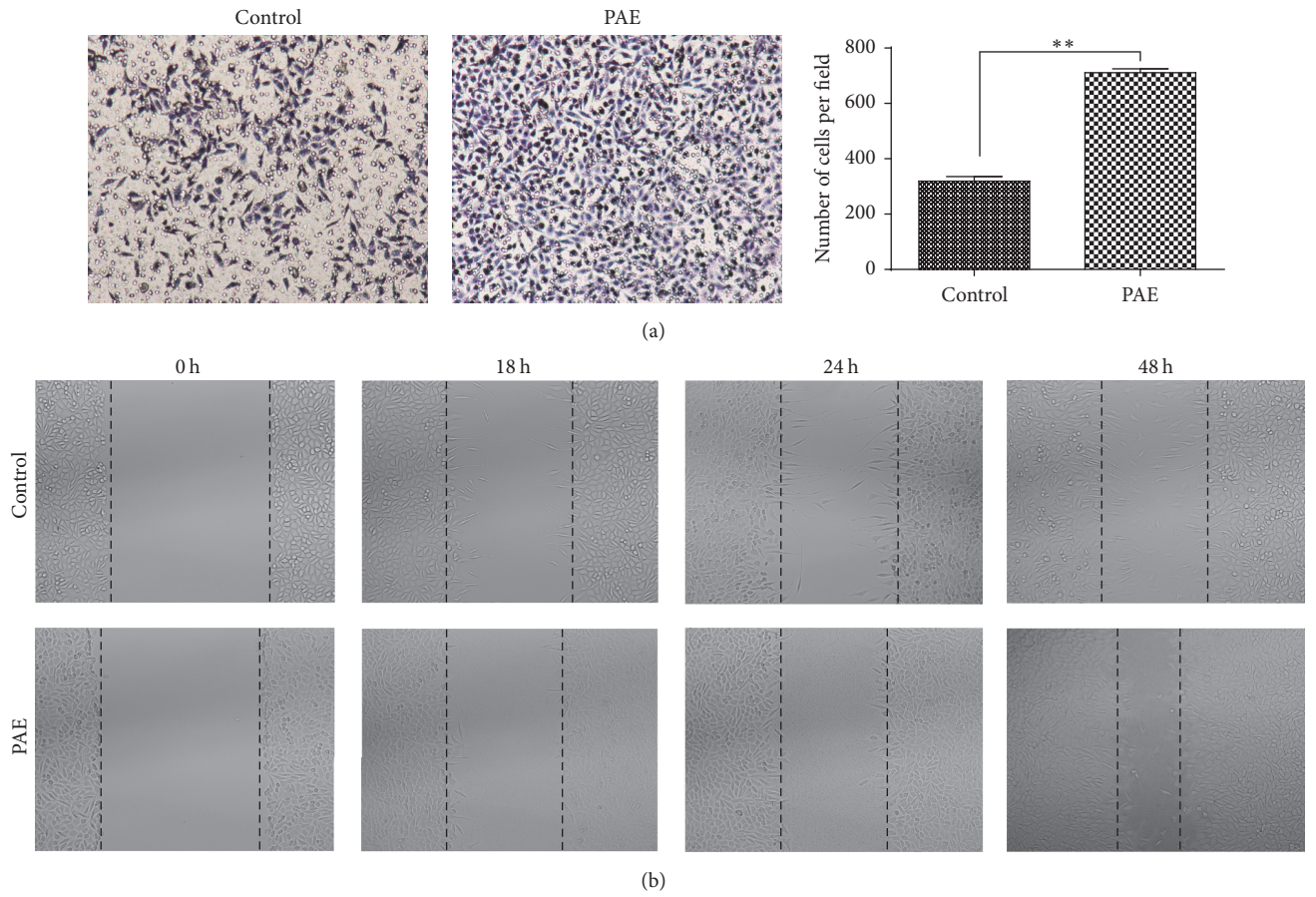

Figure 3: Effect of PAE on cell migration in HSF cells. The differentially cultured HSF (0.3125 mg/mL) for 48 h. (a) Transwell migration assay: images obtained at 24 h after HSF were incubated in Milicells 24 h (left); the migratory cells per visual field (100x) were counted and expressed as the average numbers. Data represent mean ± SD. $^{**}p < 0.01$ versus control group (right). (b) Cell scratch test: images obtained at 0, 18, 24, and 48 h after scratch formation.

Table 1: Healing rates at different time points after burn (%).

Group	7 d	14 d	21 d
Control	24.25 ± 4.68	59.22 ± 6.83	87.16 ± 2.65
Treatment	39.45 ± 8.11*	83.73 ± 5.11*	97.35 ± 1.29*

*The healing rate of the treatment group was compared with the control group at varied time points, $p < 0.05$.

was wiped with PAE. The treated wound showed significant healing.

Microscopic, immunohistochemical, and immunocytochemical staining indicated epithelial repair, follicular regeneration, and fibrous tissue formation following PAE treatment. The healing rate and healing phase showed significant differences between the PAE-treated wound and control wound. The healing rate of PAE-treated wound was higher than that of the control during the healing phase (Table 1 and Figure 6, $p < 0.05$). In general, the results demonstrated that PAE greatly accelerated the healing of burn wounds.

3.6. PAE Enhanced NF-κB Pathway and ERK Phosphorylation In Vivo. Tissue microarrays were constructed using the samples collected regularly from the wound margins with different treatments using the method described. Immunohistochemical staining (IHC) further confirmed the regulatory mechanism of NF-κB and ERK pathways underlying the PAE effect during the healing phase. Specifically, the level of RelA in NF-κB pathway was significantly improved in the treated group, and the p-ERK staining was increased while that of the ERK total protein was barely altered (Figure 7(a)). Simultaneously, the Western blot suggested the role of RelA in PAE-treated wound and the expression of upstream IKK β and IκBα showed no significant changes between the different groups. The expression of ERK phosphorylation was enhanced while that of total ERK showed no changes (Figure 7(b)). Thus, the PAE promoted wound healing by enhancing NF-κB and ERK pathway activities in vivo.

4. Discussion

The therapeutic role of PAE in wound healing has been demonstrated clinically [19–21]. However, due to the complex chemical composition, its potential molecular mechanisms are still unclear. In the current study, we extracted and purified the products from *P. americana* and analyzed the

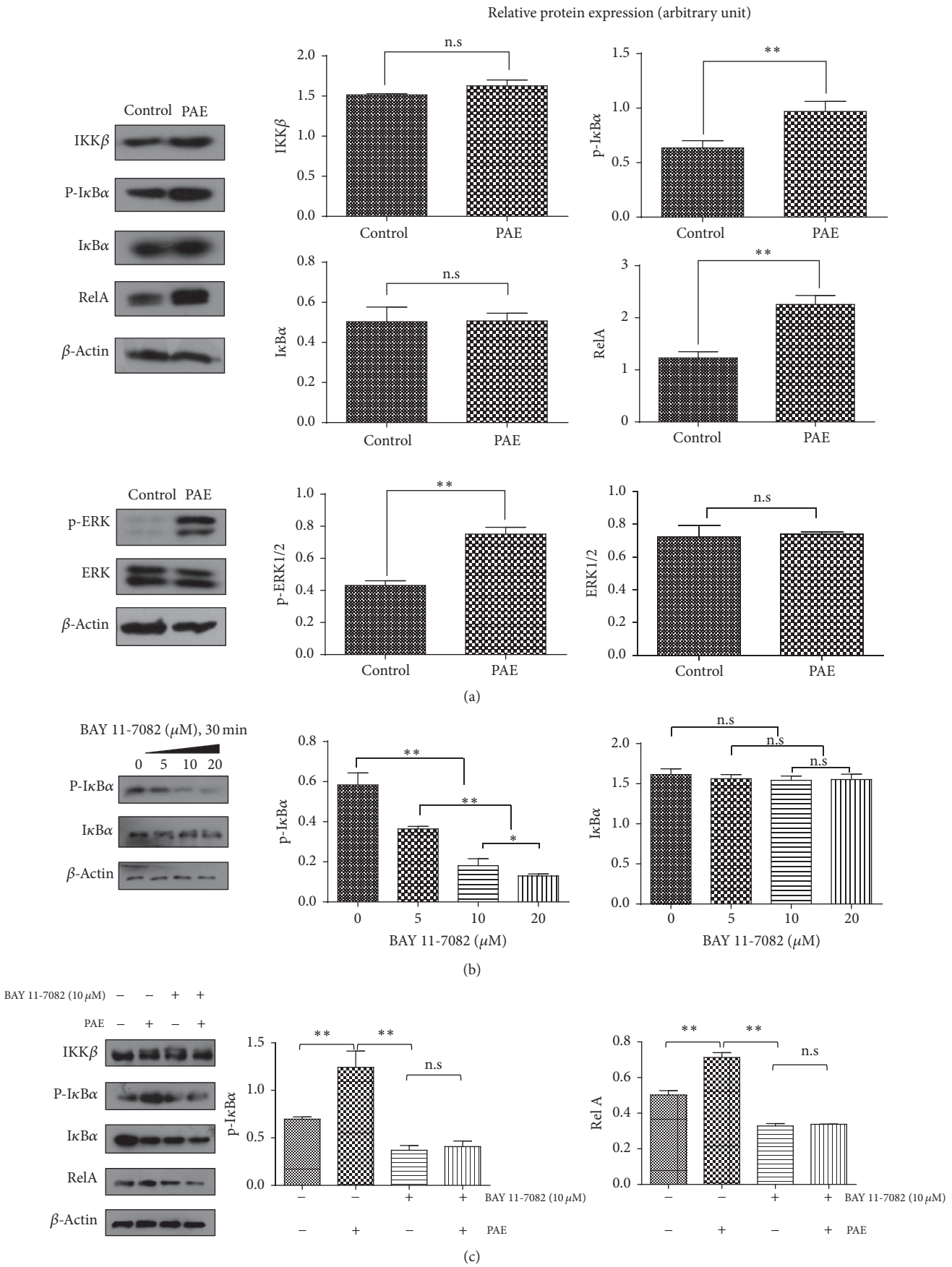

Figure 4: Continued.

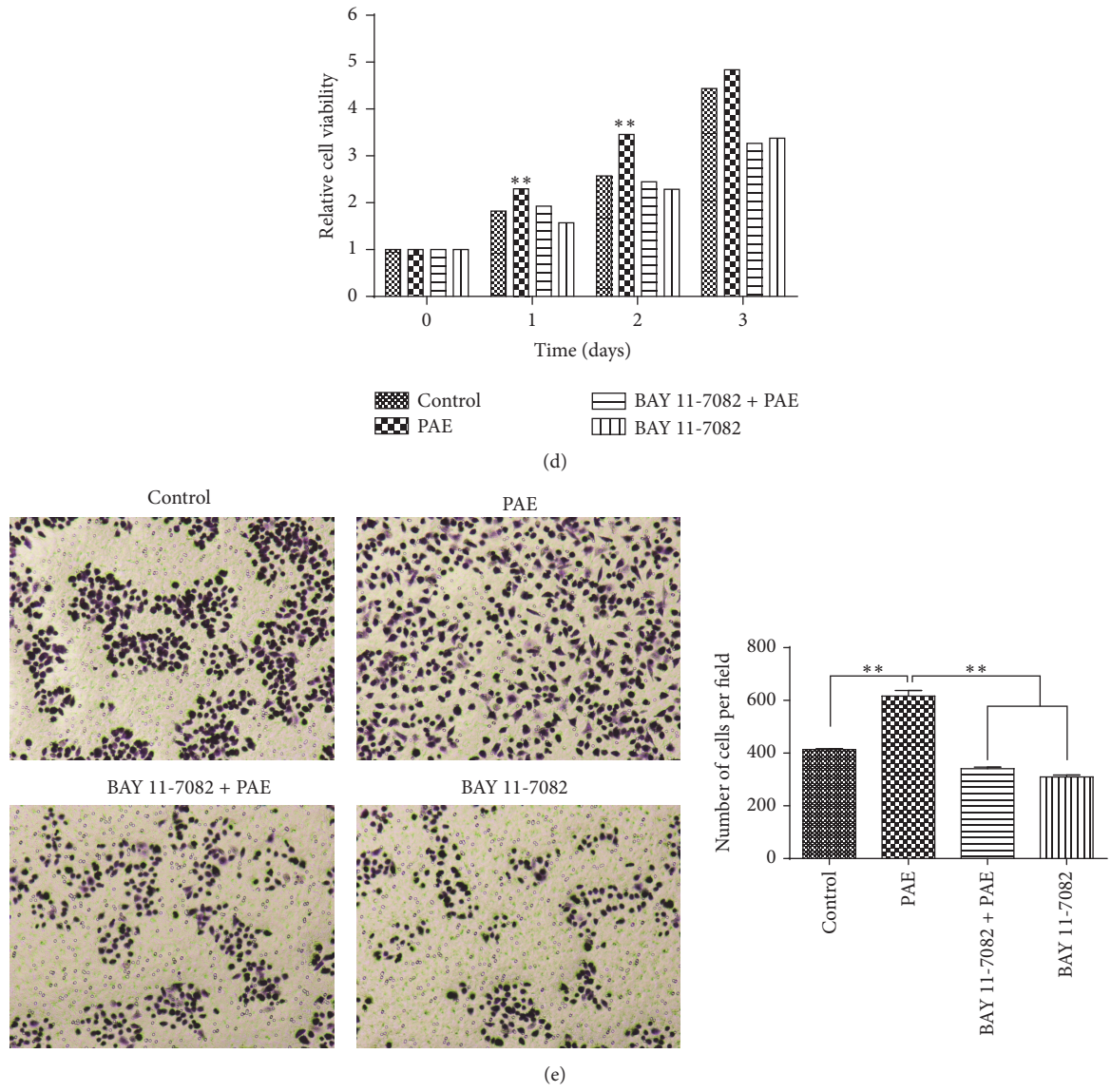

Figure 4: PAE affected NF-κB canonical and ERK pathways. HSF cells were differentially cultured for 48 h, and the protein expression of (a) NF-κB canonical pathway and ERK pathway varied; (b) NF-κB canonical pathway proteins in the presence of BAY 11-7082; (c) NF-κB pathway expression in the presence of BAY 11-7082 and PAE. Actin was used as a loading control. Cells were incubated with a medium containing PAE at the indicated concentrations for 48 h after pretreatment with BAY 11-7082 (10 μM) for 30 min. Cell proliferation (d) was determined by MTT and (e) migration was tested by transwell assay. Data represent mean ± SD. $^{*}p < 0.05$; $^{**}p < 0.01$ versus control group.

extract with greater efficacy for further study. We detected the effect of PAE on the proliferation and migration of human skin fibroblasts in vitro and in healing of thermal injury using the mouse model [4, 19]. Results indicate that PAE promoted wound healing via NF-KB signaling in vitro and in vivo.

Wound healing is a well-orchestrated biological event composed of three distinct but overlapping phases: inflammation, proliferation, and remodeling. Fibroblast is one of the major skin components and therefore regarded as the important determinants of wound healing efficiencies [22]. In our study, we found that PAE promoted proliferation and migration of HSF [23]. To establish the pharmacological effects of PAE and validate the optimal extraction process, the HSF were used in the in vitro wound healing model for evaluation of the cellular and molecular effects of PAE. The fibroblasts enhanced proliferation and migration after treatment with PAE (0.3125 mg/mL) for 48 h. In addition, PAE significantly increased the healing rates and reduced the healing time by enhancing epithelial repair, follicular regeneration, and fibrous tissue proliferation following cutaneous thermal injury in vivo [24–26].

The expression of growth mediators is modulated by NF-κB pathway. NF-κB plays a critical role in regulating the immune response to extracellular stimuli. It is normally sequestered in the cytoplasm by a family of inhibitory proteins known as inhibitors of NF-κB (IκBs) [16, 27]. Activation

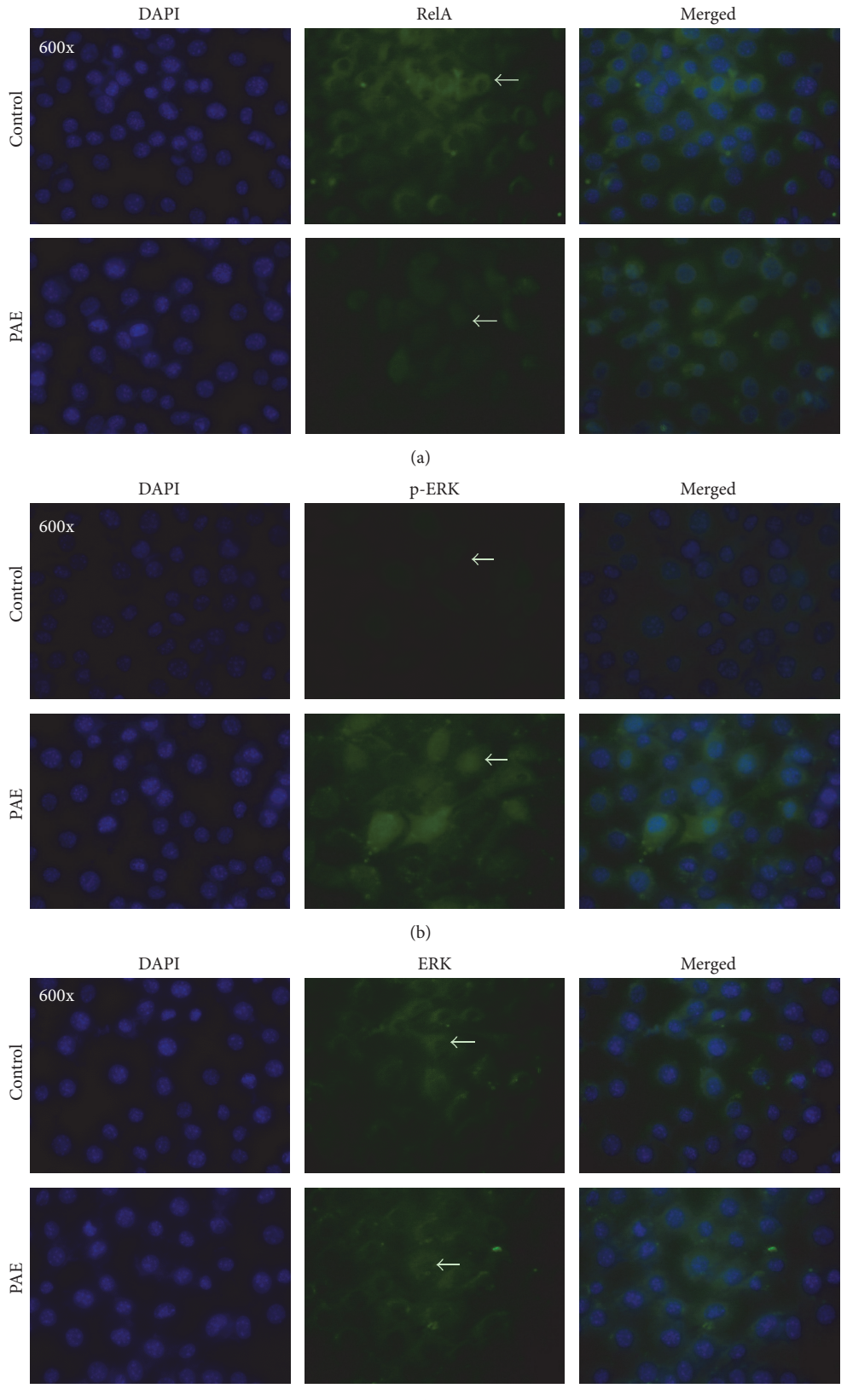

Figure 5: Immunofluorescence analysis of the spatial localization of the NF-κB canonical and ERK pathways. Cells were treated with PAE for 48 h, fixed, and incubated to determine the immunofluorescence. The antibodies against (a) RelA, (b) p-ERK, and (c) ERK presented green fluorescence, whereas a blue fluorescent signal was generated by DAPI staining of the cell nuclei. Areas of overlap between the green and the blue fluorescence appeared as merged images.

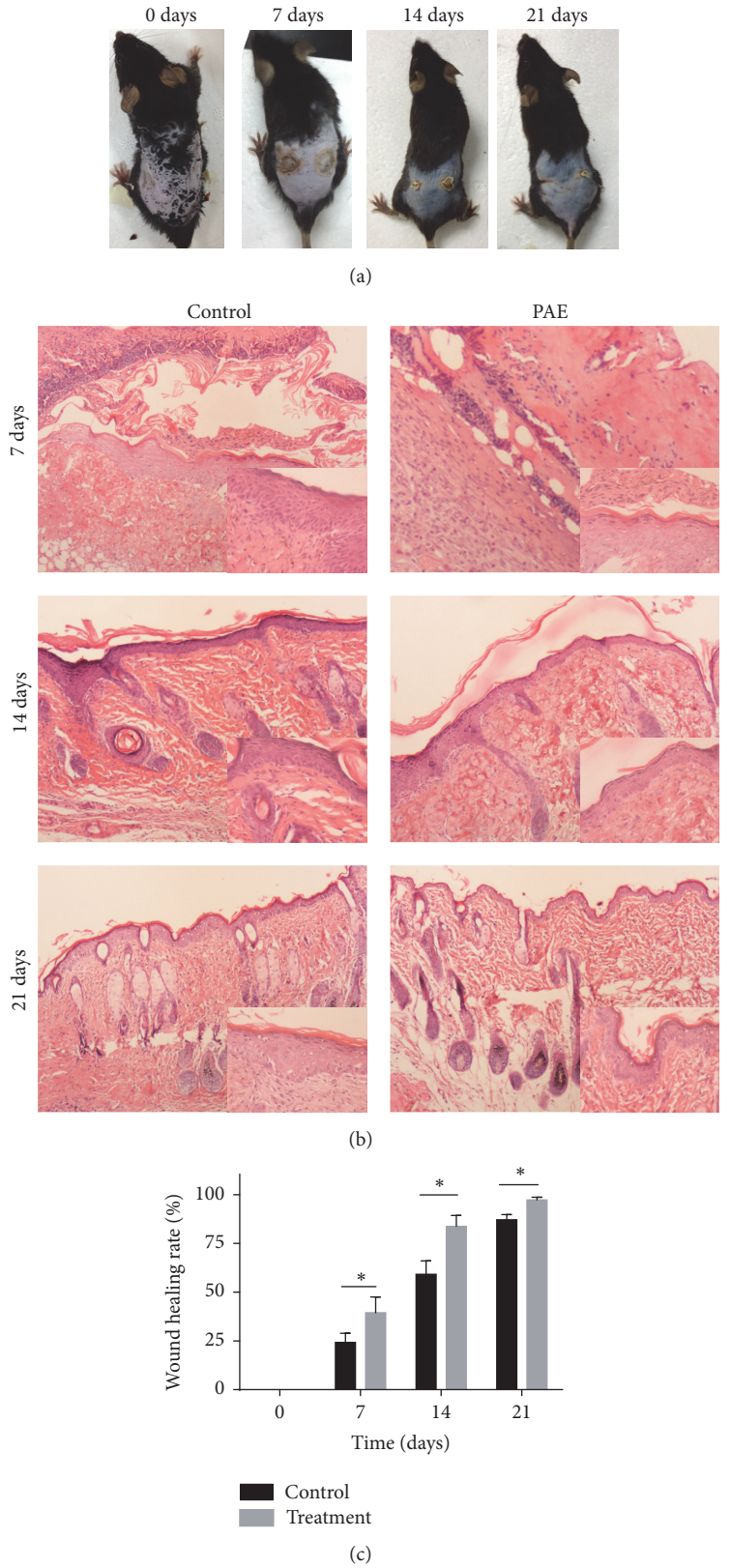

FIGURE 6: PAE affected wound healing in cutaneous thermal burns in vivo. In the C57 mouse model of thermal injury, the left wound of the dorsal flank was treated with PAE (5 mg/mL) while the right side treated with normal saline served as the daily control. (a) Representative images of thermal injury on days 0, 7, 14, and 21; (b) histological HE staining of differentially treated tissues on days 0, 7, 14, and 21; (c) healing rate of thermal wound. $^{*}P < 0.05$ versus control group.

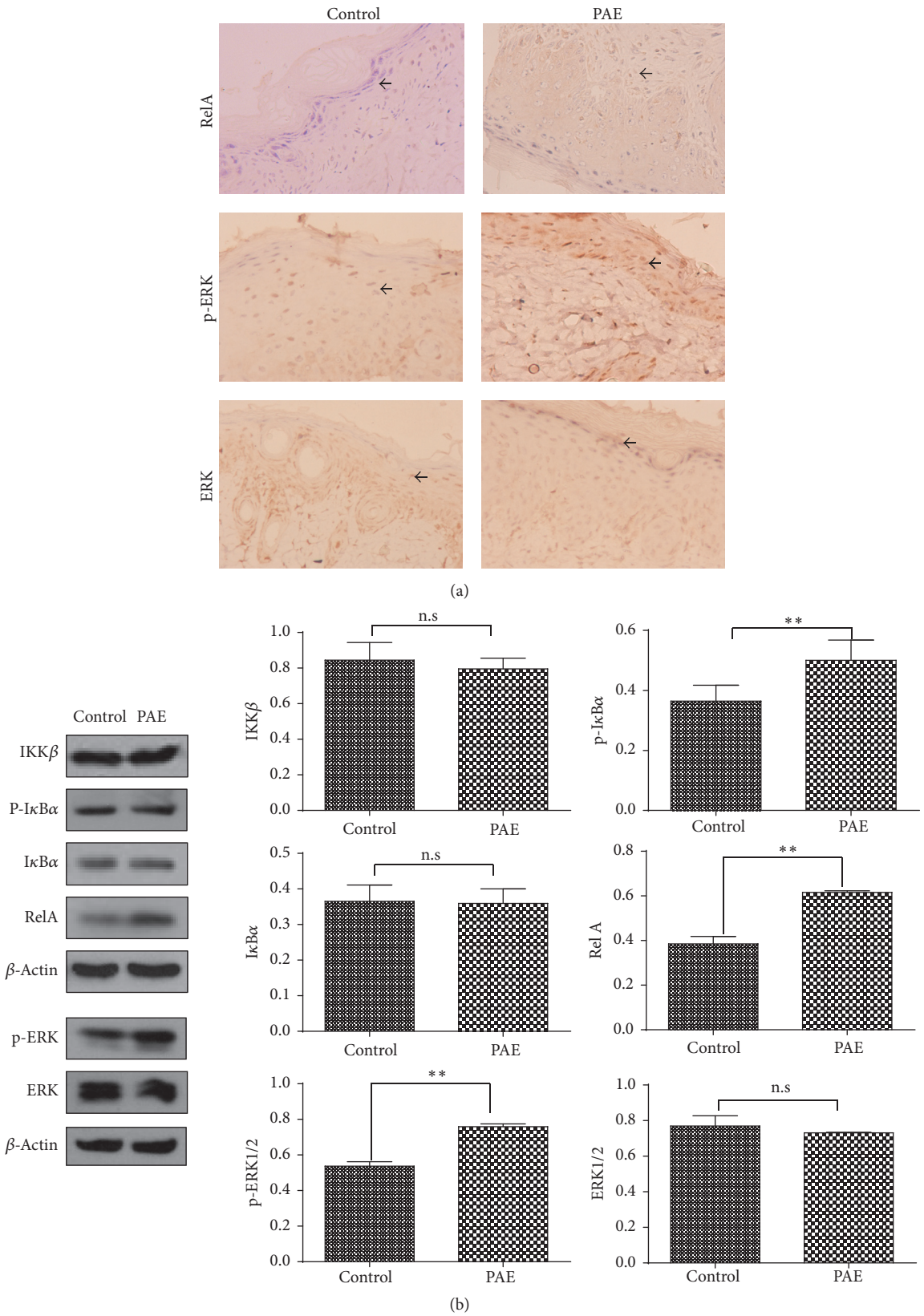

Figure 7: NF-κB canonical pathway and ERK pathway activities in vivo. (a) Molecular expression of NF-κB canonical pathway and ERK pathway in PAE-treated and control tissues was assayed by IHC, and the representative images are shown (400x). (b) Western blot of protein expression in NF-κB canonical and ERK pathways. Actin was used as a loading control. Data represent mean ± SD. $^{**}p < 0.01$ versus control group.

of NF-κB, releases RelA from its inhibitory protein IκB-α, followed by nuclear translocation to trigger the transcription of specific target genes such as TNF-α, IL-1β, and IL-6 [23, 28]. To determine the molecular mechanism of NF-κB activation, we tested the expression of upstream IKK β, P-IκBα, and IκBα and downstream RelA activation. The results showed that PAE stimulation dramatically increased the phosphorylation of IκBα and RelA proteins. However, PAE-induced IκBα and RelA activation was significantly blocked by pretreatment with BAY 11-7082. Meanwhile, we found similar results in the cutaneous thermal injury in vivo. Collectively, our results suggested that PAE promoted the migration and proliferation in vitro and wound healing in vivo via NF-κB activation.

Simultaneously, we hypothesized that PAE might activate more than one pathway resulting in HSF proliferation and migration. We found an increase in the phosphorylation and nuclear translocation of p-ERK despite stable levels of total ERK. Phosphorylation and nuclear translocation of ERK1 and ERK2 are critical for gene transcription and expression. Therefore, the kinetics and localization of ERK1/2 are intrinsically linked. ERK1 and ERK2 are the most thoroughly studied in the ERK family and involved in a wide range of physiological processes, including the regulation of cell meiosis, mitosis, and anaphase. A variety of stimuli such as growth factors and cytokines are associated with ERK1/2 pathway activation. ERK activation determines its cellular proliferation and migration [29]. In this study, PAE acts as a stimulus to phosphorylate ERK1/2, resulting in skin wound healing.

5. Conclusion

In summary, PAE promotes wound healing in vitro and in vivo in experimental models. These processes are closely correlated with the increased activation of NF-κB and ERK signaling pathways. Furthermore, the enhanced activities of NF-κB and ERK pathways may represent major molecular targets of PAE, which accelerate wound healing by upregulating the expression of a series of genes involved in cell proliferation, fibrogenesis, reepithelialization, and remodeling [2, 29, 30].

Conflicts of Interest

The authors declare that they have no conflicts of interest.

Acknowledgments

This study was supported by the National Natural Science Foundation of China (no. 81403194).

References

[1] H. X. Shi, C. Lin, B. B. Lin et al., "The anti-scar effects of basic fibroblast growth factor on the wound repair in vitro and in vivo," *PLoS ONE*, vol. 8, no. 4, Article ID e59966, 2013.

[2] M. Li, Y. Zhao, H. Hao et al., "Mesenchymal stem cell-conditioned medium improves the proliferation and migration of keratinocytes in a diabetes-like microenvironment," *The International Journal of Lower Extremity Wounds*, vol. 14, no. 1, pp. 73–86, 2015.

[3] X. Chen, X. Ran, R. Sun et al., "Protective effect of an extract from Periplaneta americana on hematopoiesis in irradiated rats," *International Journal of Radiation Biology*, vol. 85, no. 7, pp. 607–613, 2009.

[4] A. E. Brown, R. M. France, and S. H. Grossman, "Purification and characterization of arginine kinase from the American cockroach (*Periplaneta americana*)," *Archives of Insect Biochemistry and Physiology*, vol. 56, no. 2, pp. 51–60, 2004.

[5] K. Y. Jeong, H. Hwang, J. Lee et al., "Allergenic characterization of tropomyosin from the dusky brown cockroach, periplaneta fuliginosa," *Clinical and Vaccine Immunology*, vol. 11, no. 4, pp. 680–685, 2004.

[6] P.-N. Li, H. Li, L.-X. Zhong et al., "Molecular events underlying maggot extract promoted rat in vivo and human in vitro skin wound healing," *Wound Repair and Regeneration*, vol. 23, no. 1, pp. 65–73, 2015.

[7] S. Subramaniam and K. Unsicker, "Extracellular signal-regulated kinase as an inducer of non-apoptotic neuronal death," *Neuroscience*, vol. 138, no. 4, pp. 1055–1065, 2006.

[8] T. Wada and J. M. Penninger, "Mitogen-activated protein kinases in apoptosis regulation," *Oncogene*, vol. 23, no. 16, pp. 2838–2849, 2004.

[9] M. De Melo, M. W. Gerbase, J. Curran, and J.-C. Pache, "Phosphorylated extracellular signal-regulated kinases are significantly increased in malignant mesothelioma," *Journal of Histochemistry and Cytochemistry*, vol. 54, no. 8, pp. 855–861, 2006.

[10] U. Knauf, C. Tschopp, and H. Gram, "Negative regulation of protein translation by mitogen-activated protein kinase-interacting kinases 1 and 2," *Molecular and Cellular Biology*, vol. 21, no. 16, pp. 5500–5511, 2001.

[11] J. A. Sheridan, M. Zago, P. Nair et al., "Decreased expression of the NF-KB family member RelB in lung fibroblasts from Smokers with and without COPD potentiates cigarette smoke-induced COX-2 expression," *Respiratory Research*, vol. 16, no. 1, article 54, 2015.

[12] L. Fengyang, F. Yunhe, L. Bo et al., "Stevioside suppressed inflammatory cytokine secretion by downregulation of NF-kB and MAPK signaling pathways in LPS-Stimulated RAW264.7 cells," *Inflammation*, vol. 35, no. 5, pp. 1669–1675, 2012.

[13] K.-C. Chan, H.-H. Ho, C.-N. Huang, M.-C. Lin, H.-M. Chen, and C.-J. Wang, "Mulberry leaf extract inhibits vascular smooth muscle cell migration involving a block of small GTPase and Akt/NF-kB signals," *Journal of Agricultural and Food Chemistry*, vol. 57, no. 19, pp. 9147–9153, 2009.

[14] Y. Fu, B. Liu, X. Feng et al., "Lipopolysaccharide increases Toll-like receptor 4 and downstream Toll-like receptor signaling molecules expression in bovine endometrial epithelial cells," *Veterinary Immunology and Immunopathology*, vol. 151, no. 1-2, pp. 20–27, 2013.

[15] C. F. Rizzi, J. L. Mauriz, D. S. F. Corrêa et al., "Effects of low-level laser therapy (LLLT) on the nuclear factor (NF)-κB signaling pathway in traumatized muscle," *Lasers in Surgery and Medicine*, vol. 38, no. 7, pp. 704–713, 2006.

[16] K. F. Benson, R. A. Newman, and G. S. Jensen, "Antioxidant, anti-inflammatory, anti-apoptotic, and skin regenerative properties of an Aloe vera-based extract of Nerium oleander leaves (NAE-8®)," *Clinical, Cosmetic and Investigational Dermatology*, vol. 8, pp. 239–248, 2015.

[17] D. D. S. Tavares Pereira, M. H. M. Lima-Ribeiro, N. T. De Pontes-Filho, A. M. D. A. Carneiro-Leão, and M. T. D. S. Correia, "Development of animal model for studying deep second-degree thermal burns," *Journal of Biomedicine and Biotechnology*, vol. 2012, Article ID 460841, 7 pages, 2012.

[18] S. Ebeling, K. Naumann, S. Pollok et al., "From a traditional medicinal plant to a rational drug: Understanding the clinically proven wound healing efficacy of birch bark extract," *PLoS ONE*, vol. 9, no. 1, Article ID e86147, 2014.

[19] M. D. Moreira, M. C. Picanço, L. C. A. Barbosa, R. N. C. Guedes, E. C. Barros, and M. R. Campos, "Compounds from Ageratum conyzoides: isolation, structural elucidation and insecticidal activity," *Pest Management Science*, vol. 63, no. 6, pp. 615–621, 2007.

[20] V. Thangam Sudha, N. Arora, S. Sridhara, S. N. Gaur, and B. P. Singh, "Biopotency and identification of allergenic proteins in Periplaneta americana extract for clinical applications," *Biologicals*, vol. 35, no. 2, pp. 131–137, 2007.

[21] X.-Y. Wang, Z. C. He, L.-Y. Song et al., "Chemotherapeutic effects of bioassay-guided extracts of the American cockroach, Periplaneta americana," *Integrative Cancer Therapies*, vol. 10, no. 3, pp. NP12-NP23, 2011.

[22] G. Dieamant, M. D. C. V. Pereda, C. Nogueira et al., "Antiageing mechanisms of a standardized supercritical CO2 preparation of black jack (Bidens pilosa L.) in human fibroblasts and skin fragments," *Evidence-Based Complementary and Alternative Medicine*, vol. 2015, Article ID 280529, 11 pages, 2015.

[23] J. P. Dai, D. X. Zhu, J. T. Sheng et al., "Inhibition of tanshinone IIA, salvianolic acid A and salvianolic acid B on areca nut extract-induced oral submucous fibrosis in vitro," *Molecules*, vol. 20, no. 4, pp. 6794–6807, 2015.

[24] M. Harishkumar, Y. Masatoshi, S. Hiroshi, I. Tsuyomu, and M. Masugi, "Revealing the mechanism of in vitro wound healing properties of citrus tamurana extract," *BioMed Research International*, vol. 2013, Article ID 963457, 8 pages, 2013.

[25] S. Huang, Y. Wu, D. Gao, and X. Fu, "Paracrine action of mesenchymal stromal cells delivered by microspheres contributes to cutaneous wound healing and prevents scar formation in mice," *Cytotherapy*, vol. 17, no. 7, pp. 922–931, 2015.

[26] Y. Ponnusamy, N. J.-Y. Chear, S. Ramanathan, and C.-S. Lai, "Polyphenols rich fraction of *Dicranopteris linearis* promotes fibroblast cell migration and proliferation in vitro," *Journal of Ethnopharmacology*, vol. 168, pp. 305–314, 2015.

[27] Y. Xie, Y. Li, X. Peng, F. Henderson Jr., L. Deng, and N. Chen, "Ikappa B kinase alpha involvement in the development of nasopharyngeal carcinoma through a NF-κB-independent and ERK-dependent pathway," *Oral Oncology*, vol. 49, no. 12, pp. 1113–1120, 2013.

[28] D. Li, Y. Fu, W. Zhang et al., "Salidroside attenuates inflammatory responses by suppressing nuclear factor-κB and mitogen activated protein kinases activation in lipopolysaccharide-induced mastitis in mice," *Inflammation Research*, vol. 62, no. 1, pp. 9–15, 2013.

[29] D. Ti, M. Li, X. Fu, and W. Han, "Causes and consequences of epigenetic regulation in wound healing," *Wound Repair and Regeneration*, vol. 22, no. 3, pp. 305–312, 2014.

[30] W. S. Pessoa, L. R. De Moura Estevão, R. S. Simões et al., "Fibrogenesis and epithelial coating of skin wounds in rats treated with angico extract (Anadenanthera colubrina var. cebil)," *Acta Cirurgica Brasileira*, vol. 30, no. 5, pp. 353–358, 2015.

Hindawi
Evidence-Based Complementary and Alternative Medicine
Volume 2017, Article ID 7812598, 7 pages
https://doi.org/10.1155/2017/7812598

Research Article

Wound Healing Effects of *Prunus yedoensis* Matsumura Bark in Scalded Rats

Jin-Ho Lee,[1] Kyungjin Lee,[2] Mi-Hwa Lee,[1] Bumjung Kim,[1] Khanita Suman Chinannai,[1] Heseung Hur,[1] Inhye Ham,[2] and Ho-Young Choi[2]

[1]*Department of Science in Korean Medicine, Graduate School, Kyung Hee University, Seoul 02447, Republic of Korea*
[2]*Department of Herbology, College of Korean Medicine, Kyung Hee University, Seoul 02447, Republic of Korea*

Correspondence should be addressed to Ho-Young Choi; hychoi@khu.ac.kr

Received 29 December 2016; Accepted 9 March 2017; Published 19 March 2017

Academic Editor: Ipek Suntar

Pruni Cortex has been used to treat asthma, measles, cough, urticaria, pruritus, and dermatitis in traditional Korean medicine. The objective of this study was to investigate the effects of *Prunus yedoensis* Matsumura bark methanol extract (PYE) on scald-induced dorsal skin wounds in rats. Scalds were produced in Sprague-Dawley rats with 100°C water and treated with 5% and 20% PYE (using Vaseline as a base), silver sulfadiazine (SSD), and Vaseline once a day for 21 days, beginning 24 hours after scald by treatment group allocation. The PYE-treated groups showed accelerated healing from 12 days after scald, demonstrated by rapid eschar exfoliation compared to the control and SSD groups. PYE-treated groups showed higher wound contraction rates and better tissue regeneration in comparison with the control group. Serum analysis showed that transforming growth factor beta 1 and vascular endothelial growth factor levels remained high or gradually increased up to day 14 in both PYE groups and then showed a sharp decline by day 21, implying successful completion of the inflammatory phase and initiation of tissue regeneration. These findings suggested that PYE is effective in promoting scald wound healing in the inflammation and tissue proliferation stages.

1. Introduction

Burn injuries cause considerable morbidity, mortality, and socioeconomic losses. Scalds, burns caused by hot liquids, are one of the most frequently reported forms of burn. In particular, more than 50% of preschool pediatric burn patients are scald injury patients [1]. Burn injuries, including scalds, result in mild-to-severe scars on the skin. Thus, patients continuously experience serious psychological distress as well as physical pain. Therefore, better acute care and therapeutics are needed in burn management.

Many researchers around the world are investigating the pathophysiology of burns and determining the effects of new and old treatments [2]. Traditional treatment using herbal medicine could also be an effective therapy for burns. *Aloe vera* and potato are typical herbal medicines used to treat thermal burns [3, 4].

Prunus yedoensis Matsumura (PY) is one of the useful medicinal plants native to Jeju Island in Korea. The bark of this plant has been used to treat asthma, measles, cough, urticaria, pruritus, and dermatitis in traditional Korean medicine [5]. Recently, it was discovered to have a vasorelaxant effect. This effect is exerted via activation of the nitric oxide- (NO-) cGMP pathway and NO formation from L-arginine, which blocks the entry of extracellular Ca^{2+} into cells via receptor-operated and voltage-dependent Ca^{2+} channels, as demonstrated in rat isolated thoracic aorta [5]. In addition, the bark has an anti-inflammatory effect via the inhibition of nuclear factor-kappa B in lipopolysaccharide- (LPS-) induced RAW 264.7 macrophage cells [6] and the inhibition of LPS-induced inflammatory cytokine synthesis via IκBα degradation and MAPK activation in macrophages [7].

As described above, the bark of PY (BPY) has been used to treat inflammatory skin diseases in traditional medicine, and recent studies have demonstrated the anti-inflammatory effects of BPY. Thus, we hypothesized that BPY might be useful to treat skin damage caused by scalds.

Therefore, the purpose of this study was to determine the effects of *P. yedoensis* Matsumura bark methanol extract

(PYE) on scald wound healing through investigating the histopathological characteristics of the wounded area and serum levels of inflammatory cytokines and angiogenesis factors.

2. Materials and Methods

2.1. Preparation of PYE. Dried BPY was purchased from a herbal drug company (DongWooDang Pharmacy Co., Ltd., Korea). A voucher specimen (number PY 002) of BPY was deposited at the laboratory of herbology, College of Korean Medicine, Kyung Hee University, Seoul, Korea.

A crude extract was prepared by a decoction of dried BPY (3 kg) in 100% methanol three times (3 h per time) using a heating mantle-reflux. After filtering with filter paper, the extract was evaporated using a rotary vacuum evaporator (N-N series, Eyela Co., Ltd., Japan) and lyophilized using a freeze-dryer (OPR-FD4-8612 model, Operon Co., Ltd., Korea). The yield of crude extract was 27%.

2.2. Animals. Male Sprague-Dawley (SD) rats (6 weeks old, weight 180–220 g; Samtaco Co., Ltd., Korea) were housed under controlled conditions (22 ± 2°C; lighting, 07:00–19:00) with food and water available ad libitum.

2.3. Induction and Treatment of Scald Wounds. All experiments were performed according to the animal welfare guidelines issued by the Kyung Hee University Institutional Animal Care and Use Committee (protocol approval number KHUASP (SE)-13-003). Scald wounds were induced on the backs of the SD rats using previously described methods [8]. After scalding, rats were randomly divided into 5 groups (control, silver sulfadiazine, Vaseline, 5% PYE, and 20% PYE, $n = 8$, resp.) and, after 24 hours, 0.5 g of the experimental substances was applied to the scalded area once a day for 3 weeks. The control (CON) group was not treated after scald. The silver sulfadiazine (SSD) group was treated with the reference standard of a 1% (w/w) SSD cream, the Vaseline group was treated with Vaseline, and the 5% and 20% PYE groups were treated with Vaseline-based 5% and 20% (w/w) PYE ointments, respectively.

2.4. Evaluation of Wound Healing Potential. The wound area was photographed every 3 days and analyzed using ImageJ (Broken Symmetry Software). The percentage of the wound contracture rate was calculated using the following formula: % contracture = specific day wound size/initial wound size × 100.

IL-10, transforming growth factor-β1 (TGF-β1), and vascular endothelial growth factor (VEGF) levels in rat serum were measured using the same methods as in our previous study [8].

For histopathological examinations, rats were euthanized at days 2, 14, and 21 ($n = 1$, 1, and 4, resp.) after scald using ether, and skin samples were taken. After fixation using a 10% formalin solution, the tissue was washed in running tap water, dehydrated in ascending grades of ethyl alcohol, and cleared in xylene. The tissue was placed in paraffin, cut into 6 μm thick slices using a microtome and stained with hematoxylin and eosin (H&E). Masson-Goldner trichrome was utilized for histological studies, including evaluation of the extent of reepithelialization, maturation, and organization of the epidermis, granulation tissue formation, collagenization, and inflammatory cells and scar formation in the dermis.

In the current study, the same CON, SSD, and Vaseline treated data as the data described in the previous study [8] were used.

2.5. Statistical Analysis. Data were expressed as the mean ± standard error of the mean. Statistical comparisons were made using one-way analysis of variance followed by Tukey's post hoc test using SPSS (version 13.0) statistical analysis software (IBM Inc., IL, USA). P values less than 0.05 were considered to be statistically significant.

3. Results and Discussion

3.1. Clinical Assessment. From day 3 to day 9, all groups exhibited thick scabs with red rims along the margins. On day 12, the scabs were falling off from the wound surface and wound sizes were decreased in Vaseline and PYE groups but thick and dark brown scabs still remained in SSD and control groups. On days 18 and 21, the wound surfaces were almost closed and wound sizes were smallest in PYE groups. During the experiment periods, all groups that had received some form of ointment treatment showed significantly faster-wound healing process than the control group. In particular, PYE groups showed the fastest wound healing processes (Figures 1 and 2).

3.2. Histopathological Results. No epidermal regeneration was observed on day 2 (Figures 3(a)–3(e) and Figures 4(a)–4(e)). On day 14, the Vaseline group and PYE groups showed significantly better epithelialization than the control group (Figures 3(h)–3(j); Figures 4(h)–4(j)).

On day 2, all rats exhibited damage to the epidermis, dermis, and subcutaneous tissue. On day 14, a remarkably significant increase in the quantity of granulation tissue was observed in both PYE groups compared to the control group and the Vaseline group (Figures 3(f)–3(j)). The 20% PYE group showed the thickest granulation tissue (Figure 3(j)). In contrast, the granulation tissue observed in the control group was uneven and patchy (Figure 3(f)). And significant masses of granulation tissue were observed in the PYE-treated groups on day 21 (Figures 3(n) and 3(o)). Granulation tissue can be found in secondary intention healing and is dense with blood vessels, macrophages, and fibroblasts embedded in a loose matrix of collagen and fibronectin [9]. Thus, granulation tissue is one of the important factors in the wound healing processes. These results suggest that the wound healing effect of PYE application is related to the activation of granulation tissue formation.

On day 2, all groups showed noticeably increased inflammatory cell infiltration. On day 14, the control group exhibited wide ulcerations containing inflammatory cells, a sign of mild inflammation (Figure 3(f)). On day 21, inflammatory

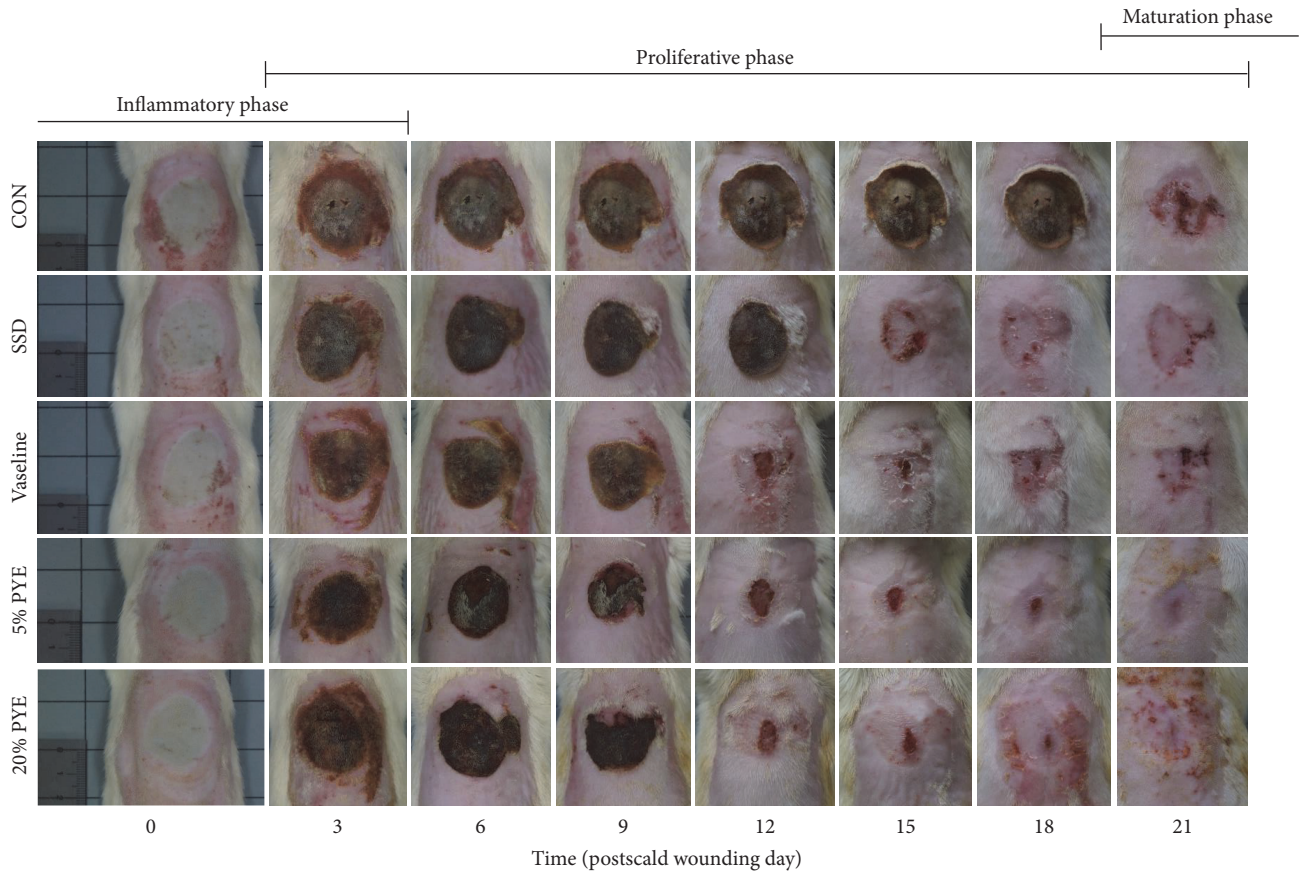

Figure 1: Gross appearance of the scald wounds on days 0, 3, 6, 9, 12, 15, 18, and 21. CON, control; SSD, silver sulfadiazine; PYE, *Prunus yedoensis* Matsumura bark methanol extract.

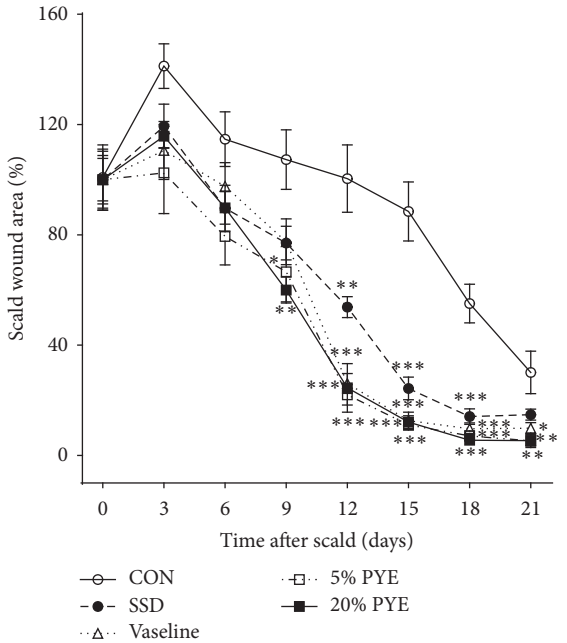

Figure 2: Changes in scald wound sizes. The percentage of wound contracture rate was calculated using the following formula: % contracture = specific day wound size/initial wound size × 100. CON, control; SSD, silver sulfadiazine; PYE, *Prunus yedoensis* Matsumura bark methanol extract. Values were expressed as the mean ± standard error of the mean ($n = 6$). $^{*}P < 0.05$, $^{**}P < 0.01$, and $^{***}P < 0.001$ versus control.

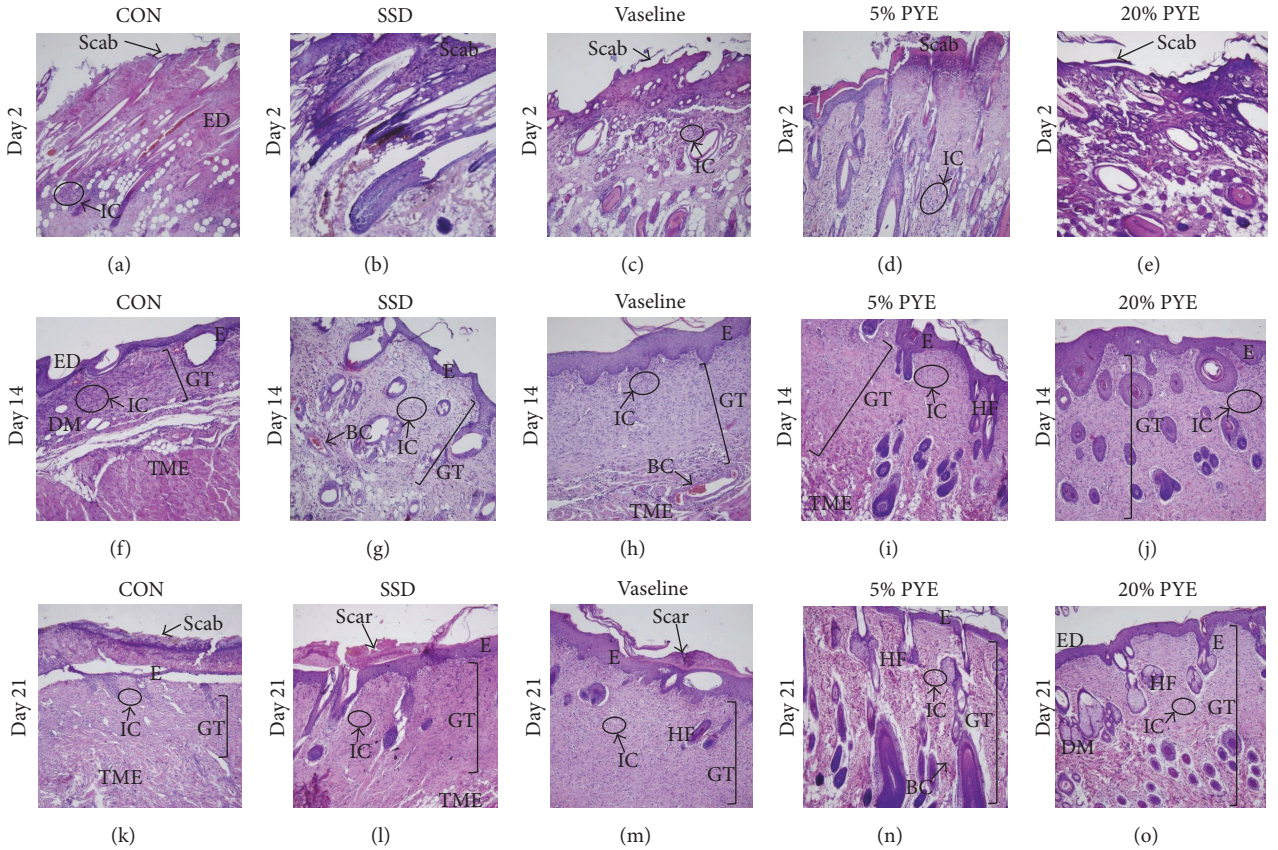

Figure 3: Histological appearance of scald wounds stained with hematoxylin and eosin on days 2, 14, and 21. Magnification: ×100. CON, control; SSD, silver sulfadiazine; PYE, *Prunus yedoensis* Matsumura bark methanol extract; ED, epidermis; IC, inflammatory cells; GT, granulation tissue; DM, dermis; E, epithelialization; TME, tunica muscularis externa; HF, hair follicle; BC, blood capillaries.

cells were observed with little quantity in PYE groups (Figures 3(n) and 3(o)).

Collagen deposition was observed on day 2. On day 14, abundant masses of newly formed collagen had formed on the dermis (Figures 4(f)–4(j)). On day 21, collagen was observed in the dermis in the PYE groups (Figures 4(n) and 4(o)), while collagen fibers filled the dermis in the control group (Figure 4(k)). Collagen content in the PYE groups had significantly increased during the early phases of healing. Day 14 observations suggest that collagen regeneration occurred more efficiently in the PYE groups than in the Vaseline group (Figures 4(h)–4(j)).

3.3. Quantification of Interleukin-10 (IL-10). The wound healing process involves a complex series of overlapping phases that include inflammation, heightened proliferation, and tissue reconstruction [10, 11]. These phases rely on precisely orchestrated interactions between various cells [12]. The inflammatory phase plays an adjunctive role in wound repair by supplying growth factors, cytokines, and chemokines that organize tissue infiltration of peripheral immune cells, such as neutrophils and macrophages, which are required for wound repair. The proliferative phase involves angiogenesis, collagen deposition, connective tissue formation, and wound contraction. Complications that occur during the inflammatory and proliferative phases may disrupt healing after burn injuries, possibly leading to infections and increased morbidity [13].

Serum samples were collected on days 2, 7, 14, and 21 to determine the impact of the scald wound on the anti-inflammatory response. After 7 days, the IL-10 levels were increased in PYE groups. On day 14, IL-10 level was significantly increased in the PYE groups compared to control group (Figure 5). On day 21, IL-10 levels in all treatment groups were higher than in the control group. IL-10 possesses potent anti-inflammatory properties, inhibiting proinflammatory cytokine production by activated macrophages [14]. In the present study, IL-10 levels were significantly increased on day 14 in the 5% PYE-treated group. This result suggests that PYE could cease or shorten the inflammatory phase at the wound site.

3.4. Quantification of Transforming TGF-β1. An increase in TGF-β1 was observed between day 7 and day 14 in both of the 5% and 20% PYE groups (90.7 ± 1.7 ng/mL % to 110.1 ± 6.1 ng/mL and 85.8 ± 1.5 ng/mL to 102.4 ± 5.4 ng/mL, resp.), followed by a significant decrease in the levels (to 58.9 ± 2.5 ng/mL and 57.2 ± 4.5 ng/mL, resp.) on day 21 (Figure 6). TGF-β1, an important transforming growth factor, is involved in the whole wound healing processes including

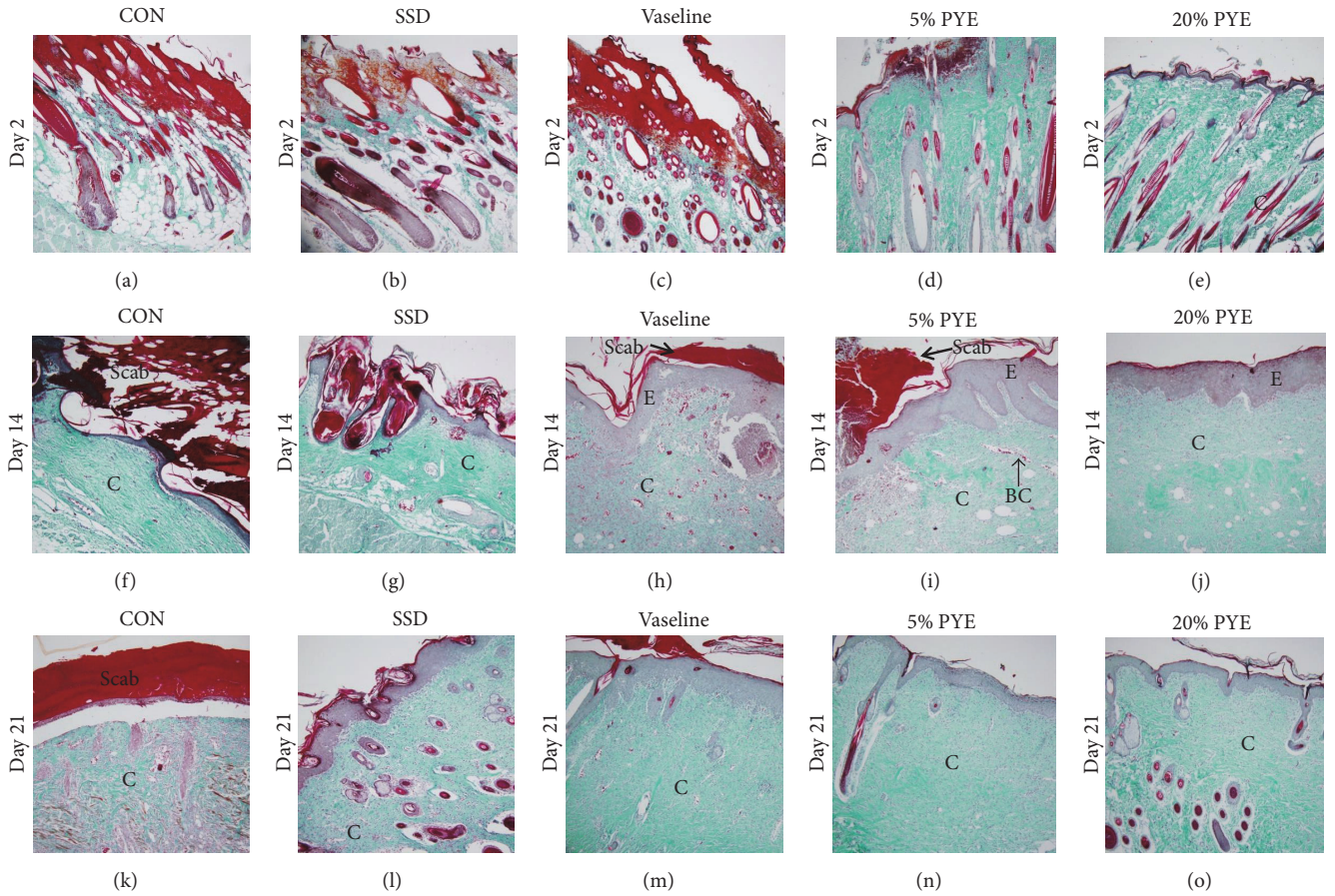

FIGURE 4: Histological appearance of scald wounds stained with Masson-Goldner trichrome stain on days 2, 14, and 21. Magnification: ×100. CON, control; SSD, silver sulfadiazine; PYE, *Prunus yedoensis* Matsumura bark methanol extract; C, collagen; E, epithelialization; BC, blood capillaries.

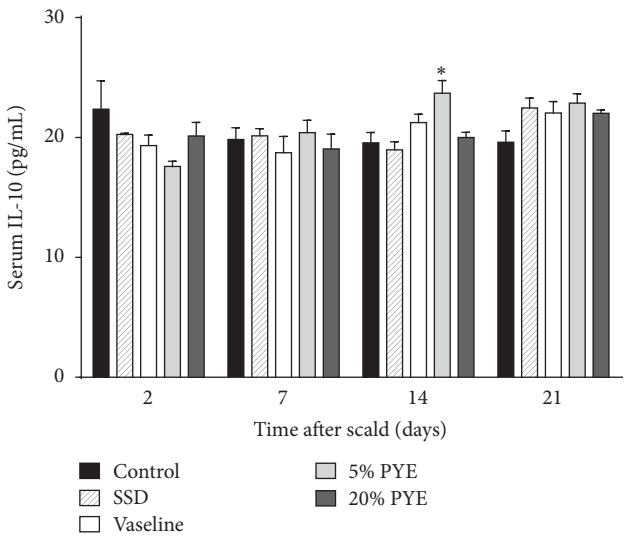

FIGURE 5: Interleukin-10 (IL-10) levels in cutaneous scalded rat serum. SSD, silver sulfadiazine; PYE, *Prunus yedoensis* Matsumura bark methanol extract. Values were expressed as the mean ± standard error of the mean (n = 4–6). $^{*}P < 0.05$ versus control.

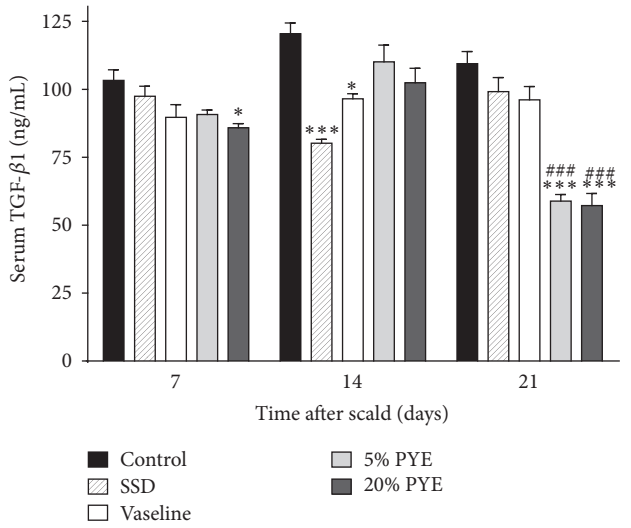

FIGURE 6: Transforming growth factor beta 1 (TGF-β1) levels in cutaneous scalded rat serum. SSD, silver sulfadiazine; PYE, *Prunus yedoensis* Matsumura bark methanol extract. Values were expressed as mean ± standard error of the mean (n = 4-5). $^{*}P < 0.05$ and $^{***}P < 0.05$ versus control. $^{###}P < 0.001$ versus Vaseline.

inflammation, angiogenesis, collagen synthesis, fibroblast proliferation, and remodeling of the new extracellular matrix [15, 16]. It is a proponent of dermal fibrosis and a promoting factor in wound healing processes, and it can improve the rate of healing and wound strength [17, 18]. However, an excess of TGF-β1 leads to hypertrophic scarring and keloid formation [17]. Thus, TGF-β1 should be increased in the early and interim stages of wound healing process and should be decreased in later stages of the wound healing process. In the present study, TGF-β1 levels in both of the 5% and 20% PYE-treated groups increased on day 14 compared to day 7 and then significantly decreased on day 21 in comparison to the other groups. These results, general evaluations (Figures 1 and 2), and histopathological observations (Figures 3 and 4) suggested that PYE could promote wound healing and almost heal scald wounds by day 21 via regulation of TGF-β1.

3.5. Quantification of VEGF. Angiogenesis is one of the essential elements of the wound healing process, and VEGF is the most important proangiogenic mediator [19]. VEGF contributes to vascular permeability, affects the interactions between endothelial cells and circulating inflammatory cells, increases the number of dermal mast cells, and plays a role in recruiting macrophages to damaged skin at early stages of healing [19]. In addition, VEGF contributes to wound closure and epidermal repair in the proliferative phase of wound healing. In the final stages of the wound healing process, VEGF promotes scar tissue formation by multiple mechanisms [19]. Thus, VEGF levels should be reduced to reduce scarring. In the present study, on day 7, VEGF levels were significantly higher in both the 5% PYE and 20% PYE groups than in the other groups. As the experiment progressed to day 14 and day 21, the VEGF levels in PYE groups continually dropped. This was a distinctive pattern; other groups showed relatively low VEGF levels until day 7, which increased on day 14 but decreased again on day 21. On day 21, the VEGF levels in PYE groups were significantly lower than in the control group, and the VEGF level in 20% PYE group was significantly lower than in the Vaseline group (Figure 7). These results suggest that PYE could heal scald wounds faster and result in less scarring compared to other treatments, by regulating VEGF in the whole wound healing process.

The TGF-β1 and VEGF results from our study suggest that PYE assists and enables unmitigated completion of angiogenesis, reepithelialization, and connective tissue regeneration processes. These findings were further supported by histopathological observations and general evaluation.

Vaseline is a well-known ointment base for burns, wounds, lesions, and other skin conditions [20]. SSD 1% cream is the most widespread topical treatment used in burn injuries due to its antimicrobial efficacy [21]. However, it also has some potential side effects that can lead to delays in the wound healing process and induce serious cytotoxic activity in host cells [22–24]. In the present study, PYE showed better-wound healing effects than Vaseline and SSD in scald wounds.

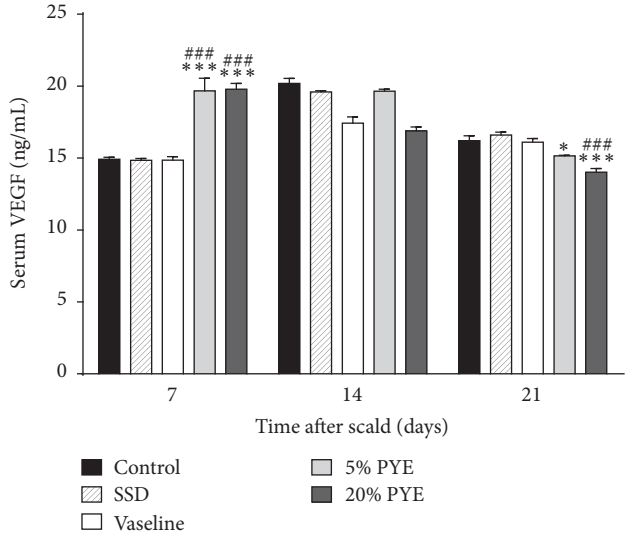

Figure 7: Vascular endothelial growth factor (VEGF) levels in cutaneous scalded rat serum. SSD, silver sulfadiazine; PYE, *Prunus yedoensis* Matsumura bark methanol extract. Values were expressed as mean ± standard error of the mean (n = 4–6). $^{*}P < 0.05$ and $^{***}P < 0.05$ versus control. $^{###}P < 0.001$ versus Vaseline.

4. Conclusions

PYE showed faster and more effective wound healing activities than SSD and Vaseline in the skin of experimentally scalded rats. Histopathological evaluation results showed better reepithelialization, vascularization, granulation tissue formation, and collagen deposition in the PYE groups than the other groups. PYE application to scald wounds resulted in less scarring than the other treatments. These effects were due to the appropriate regulation of IL-10, TGF-β1, and VEGF.

Conflicts of Interest

The authors have declared that there are no conflicts of interest.

Authors' Contributions

Jin-Ho Lee and Kyungjin Lee participated in the data analysis and drafted this paper. Mi-Hwa Lee, Bumjung Kim, Khanita Suman Chinannai, Heseung Hur, and Inhye Ham carried out the animal experiment. Ho-Young Choi was the general supervisor for this research and participated in both the study design and critical revision of the paper and all authors agreed to accept equal responsibility for the accuracy of the content of the paper. Jin-Ho Lee and Kyungjin Lee contributed equally to current manuscript.

Acknowledgments

This study was supported by a grant from the High Value-Added Food Technology Development Program, Korea Institute of Planning & Evolution for Technology in Food, Agriculture, Forestry & Fisheries (314071-03-1-HD020).

References

[1] M. Peden, "World report on child injury prevention calls for evidence-based interventions," *International Journal of Injury Control and Safety Promotion*, vol. 16, no. 1, pp. 57–58, 2009.

[2] S. E. Wolf, H. A. Phelan, and B. D. Arnoldo, "The year in burns 2013," *Burns*, vol. 40, no. 8, pp. 1421–1432, 2014.

[3] J. Somboonwong and N. Duansak, "The therapeutic efficacy and properties of topical *Aloe vera* in thermal burns," *Journal of the Medical Association of Thailand*, vol. 87, supplement 4, pp. S69–S78, 2004.

[4] S. Van De Velde, E. De Buck, T. Dieltjens, and B. Aertgeerts, "Medicinal use of potato-derived products: conclusions of a rapid versus full systematic review," *Phytotherapy Research*, vol. 25, no. 5, pp. 787–788, 2011.

[5] K. Lee, I. Ham, G. Yang et al., "Vasorelaxant effect of *Prunus yedoensis* bark," *BMC Complementary and Alternative Medicine*, vol. 13, article 31, 2013.

[6] J. Lee, G. Yang, K. Lee et al., "Anti-inflammatory effect of *Prunus yedoensis* through inhibition of nuclear factor-kappaB in macrophages," *BMC Complementary and Alternative Medicine*, vol. 13, article 92, 2013.

[7] J.-M. Yun, S.-B. Im, M.-K. Roh et al., "*Prunus yedoensis* bark inhibits lipopolysaccharide-induced inflammatory cytokine synthesis by IκBα degradation and MAPK activation in macrophages," *Journal of Medicinal Food*, vol. 17, no. 4, pp. 407–413, 2014.

[8] K. Lee, B. Lee, M.-H. Lee et al., "Effect of Ampelopsis Radix on wound healing in scalded rats," *BMC Complementary and Alternative Medicine*, vol. 15, no. 1, article 213, 2015.

[9] H. P. Lorenz and M. T. Longaker, *Wounds: Biology, Pathology and Management*, Stanford University Medical Center, Stanford, Calif, USA, 2003.

[10] A. Gosain and L. A. DiPietro, "Aging and wound healing," *World Journal of Surgery*, vol. 28, no. 3, pp. 321–326, 2004.

[11] D. G. Greenhalgh, "The role of apoptosis in wound healing," *The International Journal of Biochemistry & Cell Biology*, vol. 30, no. 9, pp. 1019–1030, 1998.

[12] A. J. Singer and R. A. F. Clark, "Cutaneous wound healing," *The New England Journal of Medicine*, vol. 341, no. 10, pp. 738–746, 1999.

[13] M. G. Schwacha, E. Nickel, and T. Daniel, "Burn injury-induced alterations in wound inflammation and healing are associated with suppressed hypoxia inducible factor-1α expression," *Molecular Medicine*, vol. 14, no. 9-10, pp. 628–633, 2008.

[14] K. W. Moore, R. De Waal Malefyt, R. L. Coffman, and A. O'Garra, "Interleukin-10 and the interleukin-10 receptor," *Annual Review of Immunology*, vol. 19, pp. 683–765, 2001.

[15] A. B. Roberts, M. B. Sporn, R. K. Assoian et al., "Transforming growth factor type β: rapid induction of fibrosis and angiogenesis in vivo and stimulation of collagen formation in vitro," *Proceedings of the National Academy of Sciences of the United States of America*, vol. 83, no. 12, pp. 4167–4171, 1986.

[16] A. V. Nall, R. E. Brownlee, C. P. Colvin et al., "Transforming growth factor β1 improves wound healing and random flap survival in normal and irradiated rats," *Archives of Otolaryngology—Head and Neck Surgery*, vol. 122, no. 2, pp. 171–177, 1996.

[17] M. Pakyari, A. Farrokhi, M. K. Maharlooei, and A. Ghahary, "Critical role of transforming growth factor beta in different phases of wound healing," *Advances in Wound Care*, vol. 2, no. 5, pp. 215–224, 2013.

[18] K. C. Flanders and J. K. Burmester, "Medical applications of transforming growth factor-beta," *Clinical Medicine & Research*, vol. 1, no. 1, pp. 13–20, 2003.

[19] N. N. Nissen, P. J. Polverini, R. L. Gamelli, and L. A. DiPietro, "Basic fibroblast growth factor mediates angiogenic activity in early surgical wounds," *Surgery*, vol. 119, no. 4, pp. 457–465, 1996.

[20] H.-Q. Zhang, T.-P. Yip, I. Hui, V. Lai, and A. Wong, "Efficacy of moist exposed burn ointment on burns," *The Journal of Burn Care & Rehabilitation*, vol. 26, no. 3, pp. 247–251, 2005.

[21] A. F. P. M. Vloemans, A. M. Soesman, M. Suijker, R. W. Kreis, and E. Middelkoop, "A randomised clinical trial comparing a hydrocolloid-derived dressing and glycerol preserved allograft skin in the management of partial thickness burns," *Burns*, vol. 29, no. 7, pp. 702–710, 2003.

[22] L. Braydich-Stolle, S. Hussain, J. J. Schlager, and M.-C. Hofmann, "In vitro cytotoxicity of nanoparticles in mammalian germline stem cells," *Toxicological Sciences*, vol. 88, no. 2, pp. 412–419, 2005.

[23] A.-R. C. Lee, H. Leem, J. Lee, and K. C. Park, "Reversal of silver sulfadiazine-impaired wound healing by epidermal growth factor," *Biomaterials*, vol. 26, no. 22, pp. 4670–4676, 2005.

[24] S. M. Hussain, K. L. Hess, J. M. Gearhart, K. T. Geiss, and J. J. Schlager, "In vitro toxicity of nanoparticles in BRL 3A rat liver cells," *Toxicology in Vitro*, vol. 19, no. 7, pp. 975–983, 2005.

Hindawi
Evidence-Based Complementary and Alternative Medicine
Volume 2017, Article ID 5820405, 8 pages
https://doi.org/10.1155/2017/5820405

Research Article

Bletilla striata Micron Particles Function as a Hemostatic Agent by Promoting Rapid Blood Aggregation

Chen Zhang,[1] Rui Zeng,[2] Zhencheng Liao,[1] Chaomei Fu,[1] Hui Luo,[3] Hanshuo Yang,[3] and Yan Qu[1]

[1] *The Ministry of Education Key Laboratory of Standardization of Chinese Herbal Medicine, Key Laboratory of Systematic Research, Development and Utilization of Chinese Medicine Resources in Sichuan Province-Key Laboratory Breeding Base Co-Founded by Sichuan Province and MOST, Pharmacy College, Chengdu University of Traditional Chinese Medicine, Chengdu 611137, China*
[2] *College of Pharmacy, Southwest University for Nationalities, Chengdu 610041, China*
[3] *State Key Laboratory of Biotherapy and Cancer Center, West China Hospital, Sichuan University and Collaborative Innovation Center for Biotherapy, Chengdu, 610041, China*

Correspondence should be addressed to Hanshuo Yang; yhansh@126.com and Yan Qu; quyan@cdutcm.edu.cn

Received 20 December 2016; Accepted 21 February 2017; Published 12 March 2017

Academic Editor: Ipek Suntar

The human body cannot control blood loss without treatment. Available hemostatic agents are ineffective at treating cases of severe bleeding and are expensive or raise safety concerns. *Bletilla striata* serve as an inexpensive, natural, and promising alternative. However, no detailed studies on its hemostatic approach have been performed. The aim of this study was to examine the hemostatic effects of *B. striata* Micron Particles (BSMPs) and their hemostatic mechanisms. We prepared and characterized BSMPs of different size ranges and investigated their use as hemostatic agent. BSMPs of different size ranges were characterized by scanning electron microscope. In vitro coagulation studies revealed BSMP-blood aggregate formation via stereoscope and texture analyzers. In vivo studies based on rat injury model illustrated the BSMP capabilities under conditions of hemostasis. Compared to other BSMPs of different size ranges, BSMPs of 350–250 μm are most efficient in hemostasis. As powder sizes decrease, the degree of aggregation between particles and hemostatic BSMP effects declines. The BSMP in contact with a bleeding surface locally forms a visible particle/blood aggregate as a physical barrier that facilitates hemostasis. Considering the facile preparation, low cost, and long shelf life of *B. striata*, BSMPs offer great potential as mechanisms of trauma treatment.

1. Introduction

Uncontrolled bleeding is a major cause of trauma-related death [1]. The human body's physiological response to injury involves three stages: plate plug formation and enzymatic cascade formation resulting in fibrin generation and clot dissolution and wound site healing [2, 3]. The human body's natural mechanisms cannot control massive amounts of blood loss resulting from major traumas [4]. Sustaining hemostasis in cases of clinical hemorrhaging is a challenging task that involves applying extensive efforts to stabilize medically difficult-to-treat traumatic injuries [5].

In general, an ideal hemostatic agent should be highly efficacious, easy to use and sterilize, nonantigenic, stable, and inexpensive [6]. *B. striata* (Thunb.) Reichb. f. (Orchidaceae) known as Hyacinth Orchid, Common Bletilla Tuber, Japanorchidee (German), Shiran (Japanese), Jaran (Korean), and Baiji (baiji) is not only an ornamental garden in Europe and United States but an important astringent hemostatic medicinal plant native to East Asia [7, 8]. Traditional Chinese Medicine (TCM) holds that it is capable of restraining leakage of blood and stopping bleeding, dispersing swelling, and promoting tissue regeneration [9]. Thus, it could be effectively applied in the treatment of hematemesis, traumatic bleeding, and ulcerative carbuncle [10, 11].

These findings from traditional applications suggest that *Bletilla striata* particles can be used as hemostatic agents to treat traumatic bleeding. However, no detailed studies

on their hemostatic modes of action have been performed. In a previous study, we found that particle size ranges are the main factor affecting hemostatic outcomes. To improve the hemostatic efficiency of BSMPs, explore its hemostatic mechanism, and determine the best size range for hemostasis, we characterized BSMPs into different size ranges (350–250, 250–180, 180–125, 125–75, and <75 μm), by means of scanning electron microscope and Fourier transform infrared (FTIR) spectroscopy in conjunction with physical characterization measurements. We conducted in vivo efficacy studies on rats. Through in vitro blood/BSMP coagulation studies, internal characterizations of blood/BSMP aggregation based on texture analyzer stereoscope and physical property analyses were then used to assess the bioactivity and efficacy of BSMPs of different size ranges.

2. Materials and Methods

2.1. Materials. Tubers of *B. striata* were purchased from Sichuan Chinese Medicine Yinpian Co. Ltd. Sprague-Dawley (SD) rats were obtained from the Chengdu Dossy Experimental Animal Co. Ltd., China. All other chemicals were of analytical grade.

2.2. BSMP Preparation and Characterization. The plant material was oven-dried at 60°C for 24 h and finely pulverized using QE-300 g Omnipotent Disintegrator (Zhejiang Yili Garment Co., Ltd.) and Micronizing Pharmaceutical Vibrating Mill (Jinan Beili Co., Ltd.). Particles of different particle size ranges (350–250, 250–180, 180–125, 125–75, and <75 μm) were strained through matched sieves. Morphological characterizations of BSMPs were performed on ZEISS SUPRA 40 (Germany) SEM at an accelerated voltage of 150 KV and at a working distance of 10–15 mm. The samples were coated with 10 nm thick platinum pieces to make the samples conductive. The specific surface area (m^2/g) of BSMP was determined by measuring the adsorption of nitrogen according to the Brunauer-Emmett-Teller (BET) principle and using the ASAP 2010 instrument (Micromeritics instrument Co., USA). Measurements were repeated three times after degassing each sample for 24 h at 40°C. FTIR spectrum was obtained using a Spectrum One FTIR (PerkinElmer Co., USA). In brief, the BSMP samples were formed into pellets with KBr and then scanned under 4,000 to 400 cm^{-1} wavelengths. Five replicated spectra were collected for every sample pressed on the ATR crystal. The background spectrum was obtained against the air.

2.3. Blood/BSMP Aggregation. The dry BSMP was added in 1.5 ml EP tubes. Blood was collected via the abdominal aortic method from SD rats through vacuum pick blood vessels containing 10% (w/v) sodium citrate anticoagulant to prevent blood clotting. We then added 0.5 ml of anticoagulant blood to EP tube vials containing BSMPs. Vials were then rotated for 30 s and set vertically on the lab bench. The vials were inverted every 30 s until the blood/BSMPs completely ceased to flow, and the time period of this stage was recorded. All experimental groups were run in triplicate ($n = 3$).

2.4. Internal Structure of Blood/BSMP Aggregation. We covered 5 g of BSMP in glass garden (5 × 5 cm). Anticoagulant blood was added through a pipetting gun to the surfaces of the BSMPs to ensure blood scattering. After 5 minutes, surface characterizations of BSMP anticoagulant blood absorption were performed using images acquired from a Discovery.V20 from Zeiss stereoscope (Germany). BSMPs that absorbed the anticoagulant blood formed an aggregation. The blood/BSMP aggregation was embedded into Tissue Freezing Medium. A 10 μm thick frozen section was then cut using a CM1520 from Leica Freezing Microtome (USA). The internal characterization of the frozen section was imaged using a Discovery.V20 from Zeiss stereoscope (Germany).

2.5. Texture Analysis of Blood/BSMP Aggregation. The blood/BSMP aggregations were then collected. We then conducted a texture analysis of the blood/BSMP aggregations using a Food Technology Corporation TMS-Pro Texture Analyzer (USA) fitted with a 250 N Intelligent Loadcell and a 6 mm diameter cylinder probe and programed to test a series of blood/BSMP aggregations. The test program moved the probe at 50 mm/min to meet the aggregation and then moved it an additional 2 mm to break it before returning to the starting position. The TMS-Pro software program was then used to analyze the data and to calculate the peak force achieved upon breaking each sample. The patterns of each breakage event were also assessed visually. A TMS-Pro graphical representation of the sample test results is shown here (force applied against cumulative displacement). All experimental groups were run in triplicate ($n = 3$).

2.6. Rat Tail Amputation. Hemostatic effects of BSMP in terms of stopping bleeding were evaluated using a tail amputation model and healthy male Sprague-Dawley (SD) rats (250 ± 20 g, 7 weeks of age). Rats were divided into six groups of five treated with cotton gauze and BSMPs (350–250, 250–180, 180–125, 125–75, and <75 μm), respectively. Animal procedures were carried out under an institutionally approved protocol in accordance with ethical principles and standards of the Federation of European Animal Science Associations and were approved by the Ethical Committee at the Chengdu University of Traditional Chinese Medicine. All rats were anesthetized with 1.25 ml 10% chloral hydrate (0.5 ml per 100 g) prior to surgery. BSMP samples were dried at 60°C in a vacuum for 5 hours and sterilized by UV irradiation for 3 hours and were then placed into transparent glass bottles. Each rat tail measuring 16 cm in length was cut 6 cm from the tip using surgical scissors. Each wound section was covered with BSMPs directly to control bleeding with slight pressure. The cessation of blood flow was timed. A gauze sponge served as a control condition in this study. At the end of the experiment, the rats were euthanized using an overdose of anesthesia.

2.7. Statistical Analysis. Data points are expressed as the means ± standard deviations. Where suitable, data were analyzed using ANOVA single factor analyses to demonstrate

Table 1: Major absorptions in IR spectra of BSMPs of different sizes.

BSMP (μm)					Assignment
>250	250–180	180–125	125–75	<75	
		Frequency (cm^{-1})			
3399	3399	3399	3387	3387	O–H and N–H group stretching
2890	2890	2890	2890	2890	C–H stretching
1735	1736	1736	1736	1736	C=O stretching
1647	1647	1647	1650	1648	COO– stretching and C=C aromatic skeletal vibration
1514	1514	1514	1514	1514	Aromatic skeletal stretching
1431	1431	1429	1431	1429	CH3 and CH symmetric bending
1377	1379	1379	1379	1379	CH3 and CH symmetric bending
1319	1317	1315	1315	1316	C–N stretching
1239	1243	1244	1243	1242	C–O stretching
1151	1150	1150	1150	1150	C–O stretching
1078	1075	1065	1075	1075	C–O stretching
1031	1030	1030	1031	1031	C–O stretching
896	895	895	895	895	C–H stretching out of plane of aromatic ring
811	811	811	811	811	C–H stretching out of plane of aromatic ring
614	614	614	614	614	O–H bending

differences between groups. Differences were considered statistically significant at $p < 0.05$.

3. Results

3.1. BSMP Characterization. The SEM images shown in Figure 1(a) present morphological characteristics of the BSMPs (350–250, 250–180, 180–125, and <75 μm). As particle sizes decreased, surface features of the BSMPs became smoother. The specific surface areas of BSMPs of different sizes are shown in Figure 1(b). Surface areas ranged from 102.602 to 366.878 m^2/g. As particle sizes decreased, surface areas increased. The specific surface of BSMPs with a particle size of <75 μm was higher than that of other BSMPs. The FTIR spectrum of the BSMP samples from 400 to 4000 cm^{-1} is shown in Figure 1(c), and the results show that no new chemical bonds formed in the BSMPs. The wavenumbers of functional groups of the BSMP samples are given in Table 1. In the "fingerprint" region, the spectra are very complex. As Figure 1(c) and Table 1 show, the overall spectral profiles of BSMPs of different sizes were almost uniform.

3.2. Blood/BSMP Aggregation. Coagulation time was evaluated from plastic vials to elucidate any direct effects on coagulation in vitro. When anticoagulant blood was added to the BSMPs, a coagulum formed significantly faster in the BSMPs (350–250 μm) than in the other groups (Figure 2). As particle sizes decreased, BSMP capacities to absorb blood weakened. A delay in blood coagulation was observed with a decrease in BSMP particle size. Even in cases of delay, an aggregation quickly formed between a fraction of the blood and particles.

3.3. The Internal Structure of Blood/BSMP Aggregation. To further study the hemostatic mechanisms of BSMPs, we observed blood/BSMP aggregation formation under a stereoscope (Figures 3(a) and 3(b)). BSMPs (350–250, 250–180, and 180–125 μm) in contact with anticoagulant blood formed visible aggregations, but BSMPs (125–75 and <75 μm) did not form blood/BSMP aggregations after being in contact with anticoagulant blood, and anticoagulant blood even gathered on surfaces of the BSMPs (<75 μm) (Figure 3(b)). Thus, BSMP particle sizes had a crucial influence on blood/BSMP aggregation formation. The internal structure of the blood/BSMPs (350–250, 250–180, and 180–125 μm) is shown in Figures 3(c) and 3(d). BSMP particles gathered via anticoagulant blood (Figures 3(c) and 3(d)). As BSMP particle sizes decreased, the degree of aggregation between BSMP particles declined. Blood indeed gathered on the surfaces of the BSMPs (125–75 and <75 μm) (Figures 3(b), 3(c), and 3(d)).

3.4. Texture Analysis of Blood/BSMP Aggregations. A texture analysis of the blood/BSMP (350–250, 250–180, 180–125 125–75, and <75 μm) aggregations is shown in Figure 5. Hardness values of the blood/BSMP (180–15 and <75 μm) aggregations were similar at roughly 10 N with no obvious signs of brittleness. Compared to blood/BSMP (125–75 and <75 μm) aggregations, the stress curve of blood/BSMP (250–180 and 180–125 μm) aggregations was found to be analogous, and the hardness of blood/BSMP (250–180 and 180–125 μm) aggregations reached a maximum value. As is shown in Figure 4, while the fragmentation of blood/BSMP (350–250) aggregation required constant force, squeeze forces did not increase rapidly. Compared to the other groups, measurements of the blood/BSMP (350–250) aggregation showed apparent toughness owing to its internal structure.

3.5. Rat Tail Amputation. Initial efficacy studies were performed on tail amputation rat models (Figure 5(a)). As particle sizes decreased, hemostatic effects of BSMPs were

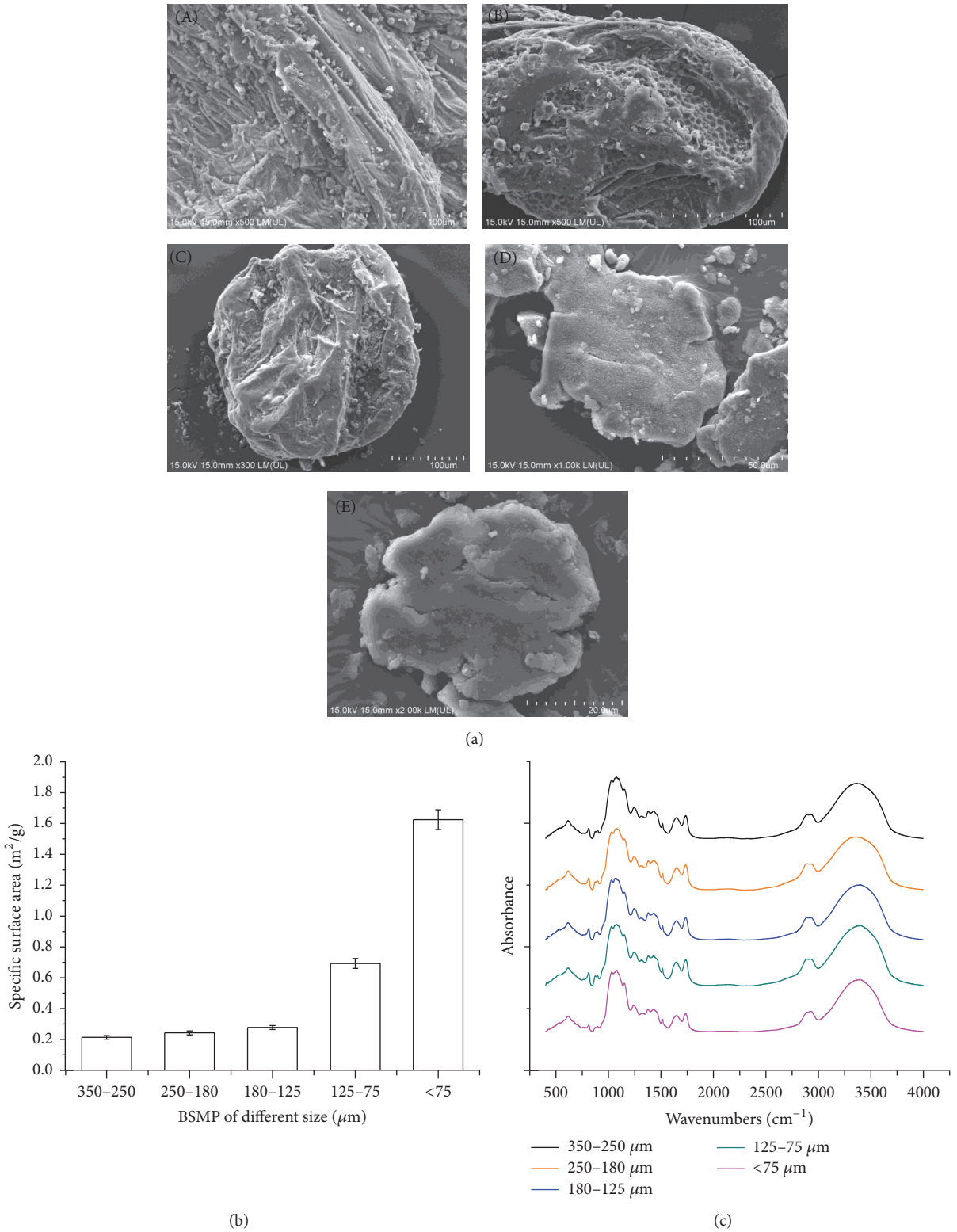

Figure 1: (a) SEM images of surface structures of BSMPs of various sizes ((A) 350–250 μm; (B) 250–180 μm; (C) 180–125 μm; (D) 125–75 μm; (E) <75 μm;). (b) Effects of particle size on specific surface area. (c) The FTIR of BSMPs of different sizes.

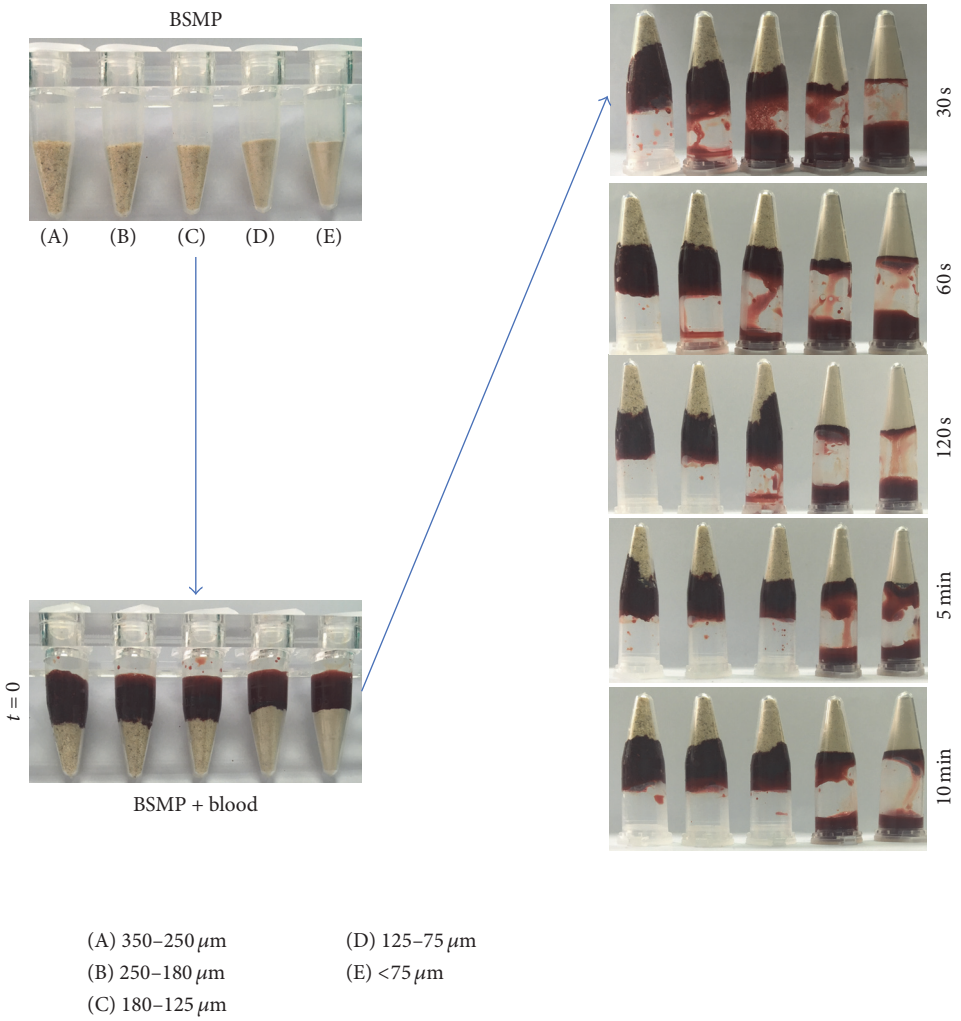

Figure 2: Macroscopic view of BSMP (350–250, 250–180, 180–125, and <75 μm) Stopper-induced formation of blood/BSMP aggregates in the anticoagulant blood.

attenuated as shown in Figures 5(b) and 5(c). After ruling out individual differences, BSMPs (350–250 μm) rapidly controlled bleeding after 60 s and wounds clotted after applying only a small number of BSMPs (350–250 μm) whereas the gauze control stopped bleeding but did not promote coagulation even after 10 min. The value for the gauze sponge conditions is therefore not represented in Figure 5(c). BSMPs in contact with a bleeding wound formed a visible aggregate and a rapid sealant at the surface of each wound, allowing for hemostasis to be reached quickly as shown in Figure 5(b).

4. Discussion

B. striata is a folkloric herb of the Orchid family that has been widely used in Traditional Chinese Medicine (TCM) as natural styptic powder for treating lung and stomach bleeding [10]. Our study results show that *B. striata* Micron Particles (BSMPs) spur hemostatic modes of action by forming a visible particle/blood aggregate as a physical barrier that gives rise to homeostasis. Compared to other hemostatic materials, BSMPs serve as an inexpensive, natural, and promising alternative.

The present study shows that BSMP size ranges are likely a key factor affecting hemostatic outcomes. With BSMP preparation, as particle sizes decreased, the surface structures of BSMPs (125–75 and <75 μm) changed, resulting in hemostatic inefficiency (Figure 1(b)). Compared to other groups, the special surface structures of BSMPs (350–250 μm) enable them to promote blood/particle aggregation and to form rapid sealants on wound surfaces to achieve rapid hemostasis. Recent studies have shown that *B. striata* contains numerous polysaccharides that have been identified as major active components responsible for the various biological effects [12]. Furthermore, bioactivity evaluations have revealed hemostatic activities of *B. striata* polysaccharides [13]. Polysaccharides on BSMP surfaces are a key factor affecting the hemostatic efficiency of BSMPs. We hypothesized that when BSMPs come into contact with blood, red blood

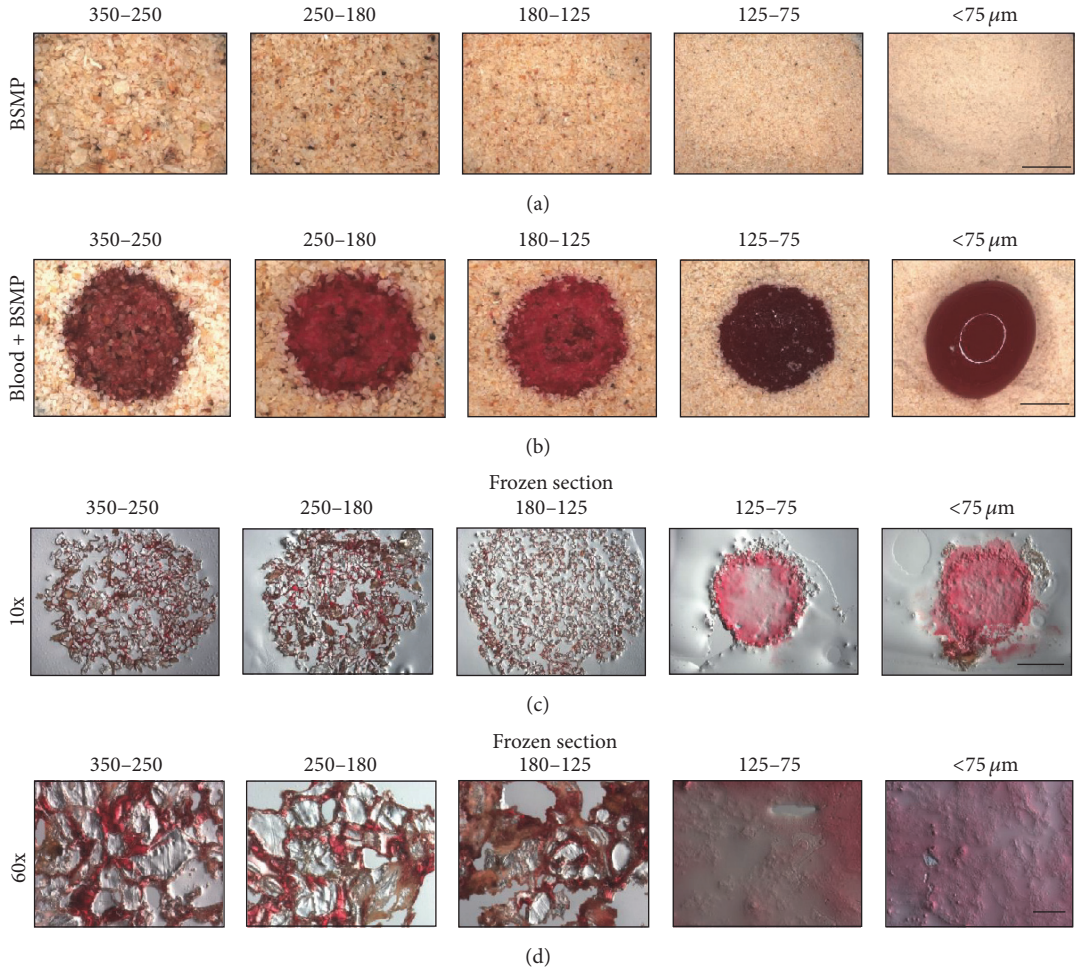

Figure 3: The internal structure of blood/BSMP aggregation. (a) Photographs of the BSMPs under a stereoscope (Scale Bar = 2 mm). (b) Photographs of the BSMPs and anticoagulant blood under a stereoscope (Scale Bar = 2 mm). (c) Photographs of frozen sections of the blood/BSMP aggregation (Scale Bar = 2 mm). (d) Photographs of frozen sections of the blood/BSMP aggregation (Scale Bar = 100 μm).

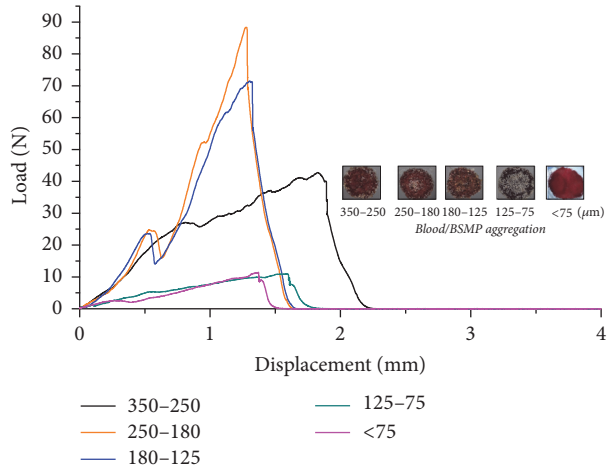

Figure 4: Texture analysis diagram of the blood/BSMP (350–250, 250–180, 180–125, and <75 μm) aggregations.

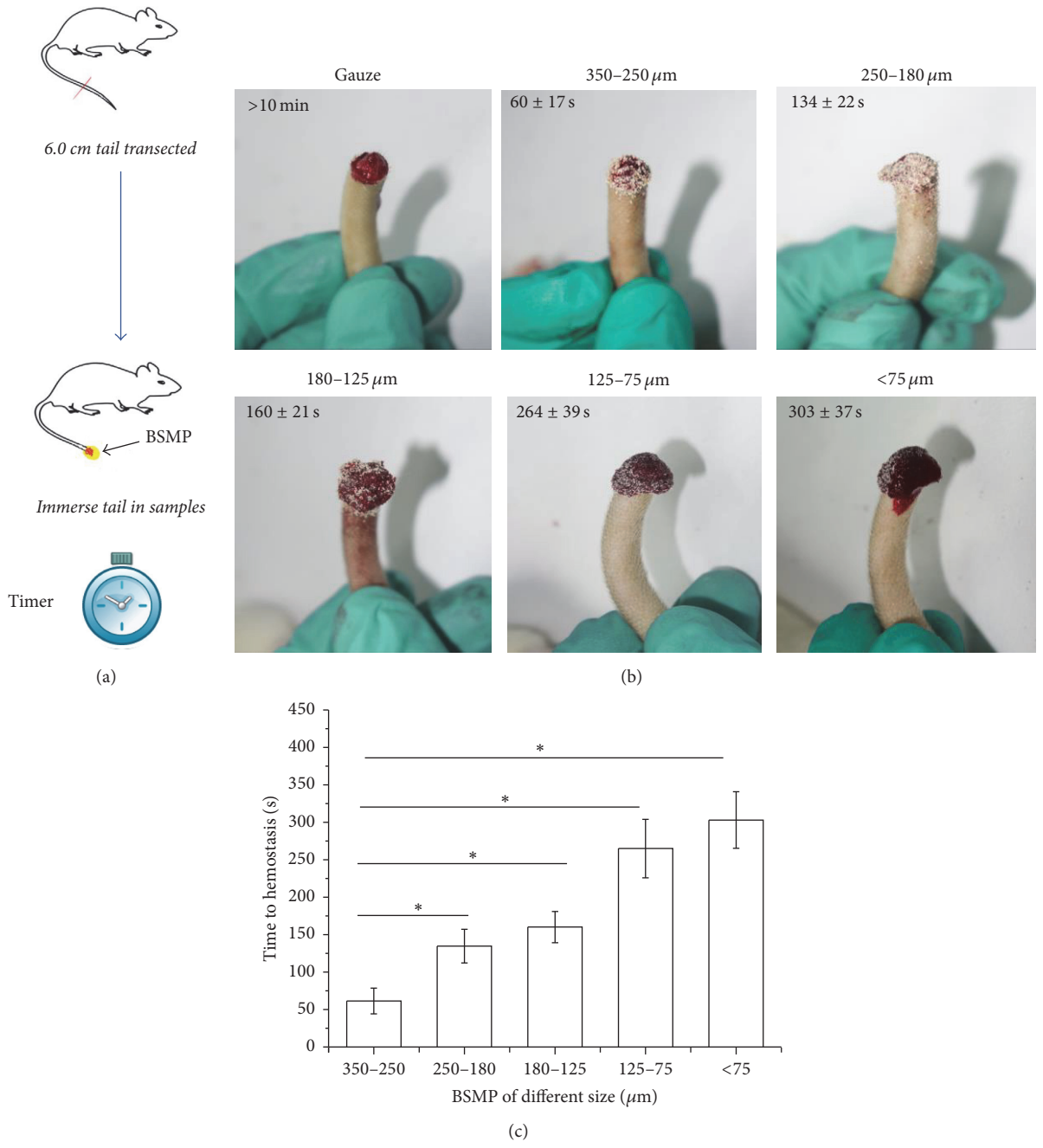

FIGURE 5: The hemostatic effect of the BSMPs evaluated by the rat tail amputation model. (a) A segment of each rat tail was amputated transversely, and the cut ends were immediately immersed in the BSMPs. (b) Photograph of tail amputation after short-term BSMP application (350–250, 250–180, 180–125, 125–75, and <75 μm) showing that bleeding has stopped and 10 min application of gauze showing continued bleeding. (c) Time to hemostasis for the same injury models ($n = 5$ for each group, $^{*}P < 0.05$).

cell aggregation and adhesion on polysaccharide surfaces form blood/BSMP aggregations that spur rapid hemostasis (Figure 3(d)).

The *Bletilla striata* polysaccharide is also known to protect against *Staphylococcus aureus* [14], to control inflammatory responses, and to accelerate wound closure, presenting potential applications for wound healing [15]. A novel water-soluble polysaccharide, *Bletilla striata* polysaccharide b (BSPb), has been isolated from *Bletilla striata*. BSPb was found to possess antioxidative stress and to offer anti-inflammatory functions against Ang II-induced ROS generation and proinflammatory cytokines activation [16]. BSMPs, in addition to stopping bleeding, offer anti-inflammatory properties and promote wound healing.

To improve the hemostasis efficiency of *Bletilla striata*, future studies will involve preparing *Bletilla striata*

polysaccharide hydrogel particles via blood aggregation as a hemostatic agent and comprehensive investigations of their hemostasis mechanisms [17]. For single injury models, hydrogel aggregate formation at the injury site can control bleeding.

5. Conclusion

The present study demonstrates that the facile production of BSMPs can show promise as an effective hemostatic agent. Anticoagulant blood/particle aggregations, internal structures of blood/BSMP aggregations examined under a stereoscope and texture analyses of blood/BSMP aggregations were used to predict the in vivo behaviors of BSMPs of different sizes. In vitro, an aggregate was formed in a fraction of the blood and BSMPs, forming a physical barrier to further blood loss. As the particle sizes of BSMPs decreased, the degree of aggregation declined. In vivo, hemostatic capacities of BSMPs of different sizes showed a decrease in the time to hemostasis in animal injury model. The hemostasis results of 350–250 μm BSMPs were found to be the most efficient of the five different sizes of BSMPs tested. To our knowledge, this is the first report on hemostatic mechanisms of BSMPs and the first efficacy study on BSMPs, which upon coming into contact with a bleeding surface form aggregations or sealants at wound surfaces that quickly spur hemostasis. This physical mechanism is not dependent on the body's physiological mechanisms and is therefore effective even for patients with coagulation disorders. Compared to other hemostatic materials such as chitosan hemostatic materials, zeolite, and mesoporous silica, BSMPs present many advantages (ease of preparation, low cost, long shelf life, and nontoxicity). BSMPs can be used as hemostatic with practical hemostatic mechanisms for treating trauma-related bleeding.

Conflicts of Interest

The authors declare that there are no conflicts of interest regarding the publication of this paper.

Acknowledgments

The project was supported by the National Natural Science Foundation of China (81603309) and the Program of Study Abroad for Young Scholar Sponsored by China Scholarship Council (CSC201500850007).

References

[1] H. R. Champion, R. F. Bellamy, C. P. Roberts, and A. Leppaniemi, "A profile of combat injury," *Journal of Trauma—Injury, Infection and Critical Care*, vol. 54, supplement 5, pp. S13–S19, 2003.

[2] D. Collen, "On the regulation and control of fibrinolysis. Edward Kowalski Memorial Lecture," *Thrombosis and Haemostasis*, vol. 43, no. 2, pp. 77–89, 1980.

[3] G. de Gaetano, "Historical overview of the role of platelets in hemostasis and thrombosis," *Haematologica*, vol. 86, no. 4, pp. 349–356, 2001.

[4] K. R. Ward, M. H. Tiba, W. H. Holbert et al., "Comparison of a new hemostatic agent to current combat hemostatic agents in a swine model of lethal extremity arterial hemorrhage," *Journal of Trauma - Injury, Infection and Critical Care*, vol. 63, no. 2, pp. 276–283, 2007.

[5] M. Gabay and B. A. Boucher, "An essential primer for understanding the role of topical hemostats, surgical sealants, and adhesives for maintaining hemostasis," *Pharmacotherapy*, vol. 33, no. 9, pp. 935–955, 2013.

[6] H. E. Achneck, B. Sileshi, R. M. Jamiolkowski, D. M. Albala, M. L. Shapiro, and J. H. Lawson, "A comprehensive review of topical hemostatic agents: efficacy and recommendations for use," *Annals of Surgery*, vol. 251, no. 2, pp. 217–228, 2010.

[7] X. He, X. Wang, J. Fang et al., "Bletilla striata: medicinal uses, phytochemistry and pharmacological activities," *Journal of Ethnopharmacology*, vol. 195, pp. 20–38, 2017.

[8] J.-M. Kong, N.-K. Goh, L.-S. Chia, and T.-F. Chia, "Recent advances in traditional plant drugs and orchids," *Acta Pharmacologica Sinica*, vol. 24, no. 1, pp. 7–21, 2003.

[9] C. Zheng, G. Feng, and H. Liang, "Bletilla striata as a vascular embolizing agent in interventional treatment of primary hepatic carcinoma," *Chinese Medical Journal*, vol. 111, no. 12, pp. 1060–1063, 1998.

[10] H.-Y. Hung and T.-S. Wu, "Recent progress on the traditional Chinese medicines that regulate the blood," *Journal of Food and Drug Analysis*, vol. 24, no. 2, pp. 221–238, 2016.

[11] L. Yu, X. Nie, H. Pan, S. Ling, D. Zhang, and K. Bian, "Diabetes mellitus ulcers treatment with Bletilla striata polysaccharide," *Zhongguo Zhongyao Zazhi*, vol. 36, no. 11, pp. 1487–1491, 2011.

[12] Y. Wang, J. Liu, Q. Li, Y. Wang, and C. Wang, "Two natural glucomannan polymers, from Konjac and Bletilla, as bioactive materials for pharmaceutical applications," *Biotechnology Letters*, vol. 37, no. 1, pp. 1–8, 2015.

[13] X. Cui, X. Zhang, Y. Yang, C. Wang, C. Zhang, and G. Peng, "Preparation and evaluation of novel hydrogel based on polysaccharide isolated from *Bletilla striata*," *Pharmaceutical Development and Technology*, 2016.

[14] Q. Li, K. Li, S.-S. Huang, H.-L. Zhang, and Y.-P. Diao, "Optimization of extraction process and antibacterial activity of bletilla striata polysaccharides," *Asian Journal of Chemistry*, vol. 26, no. 12, pp. 3574–3580, 2014.

[15] Y. Luo, H. Diao, S. Xia, L. Dong, J. Chen, and J. Zhang, "A physiologically active polysaccharide hydrogel promotes wound healing," *Journal of Biomedical Materials Research. A*, vol. 94, no. 1, pp. 193–204, 2010.

[16] L. Yue, W. Wang, Y. Wang et al., "Bletilla striata polysaccharide inhibits angiotensin II-induced ROS and inflammation via NOX4 and TLR2 pathways," *International Journal of Biological Macromolecules*, vol. 89, pp. 376–388, 2016.

[17] A. M. Behrens, M. J. Sikorski, T. Li, Z. J. Wu, B. P. Griffith, and P. Kofinas, "Blood-aggregating hydrogel particles for use as a hemostatic agent," *Acta Biomaterialia*, vol. 10, no. 2, pp. 701–708, 2014.

Hindawi
Evidence-Based Complementary and Alternative Medicine
Volume 2017, Article ID 9480791, 6 pages
https://doi.org/10.1155/2017/9480791

Research Article

Determination of the Wound Healing Potentials of Medicinal Plants Historically Used in Ghana

Sara H. Freiesleben,[1] Jens Soelberg,[1,2] Nils T. Nyberg,[1] and Anna K. Jäger[1]

[1]*Department of Drug Design and Pharmacology, Universitetsparken 2, 2100 Copenhagen, Denmark*
[2]*Museum of Natural Medicine, University of Copenhagen, Universitetsparken 2, 2100 Copenhagen, Denmark*

Correspondence should be addressed to Anna K. Jäger; anna.jager@sund.ku.dk

Received 12 December 2016; Accepted 16 January 2017; Published 23 February 2017

Academic Editor: Ipek Suntar

The present study was carried out to investigate the wound healing potentials of 17 medicinal plants historically used in Ghana for wound healing. Warm and cold water extracts were prepared from the 17 dried plant species and tested in vitro in the scratch assay with NIH 3T3 fibroblasts from mice. The wound healing scratch assay was used to evaluate the effect of the plants on cell proliferation and/or migration in vitro, as a test for potential wound healing properties. After 21 hours of incubation increased proliferation and/or migration of fibroblasts in the scratch assay was obtained for 5 out of the 17 plant species. HPLC separation of the most active plant extract, which was a warm water extract of *Philenoptera cyanescens*, revealed the wound healing activity to be attributed to rutin and a triglycoside of quercetin. The present study suggests that *Allophylus spicatus*, *Philenoptera cyanescens*, *Melanthera scandens*, *Ocimum gratissimum*, and *Jasminum dichotomum* have wound healing activity in vitro.

1. Introduction

Treatment of wounds is a frequent indication recorded in ethnopharmacological studies. Many traditional medicines are used for cleaning or treating wounds, but only a few have been tested pharmacologically for their wound healing potentials.

Early historical descriptions of Ghanaian medicinal plants from 1695–97, 1799–1803, and 1817 among the Fante, Ga, and Ashanti, respectively [1–3], include plants used for wound healing. The term "old leg injury" features prominently in the historical documents. This term is interpreted to refer to chronical wounds especially after a guinea worm infection [4]. Guinea worm disease is caused by the parasitic guinea worm, *Dracunculus medinensis*. After approximately one year of infection the female worm emerges through the skin, often in the legs or feet. The escape of the worm from the body is often accompanied by an ulceration of the area from which the worm has emerged [5]. Since the traditional way to remove the worm by winding it around a small stick can be conducted with only a few centimeters of the worm every day, this process can take a very long time, thereby leaving a serious wound [6]. The guinea worm is nearly extinct [7], so the use of medicinal plants for this special condition is not of much relevance today, but chronical wounds still appear as, for example, chronic venous leg ulcers or diabetic foot ulcers.

An extensive ethnopharmacological study of Ghanaian plants for wound healing recorded 104 plant species as being used for wound healing [8]; however only three species (*Aframomum melegueta, Melanthera scandens,* and *Ocimum gratissimum*) were the same as those recorded in previous centuries. This could be a reflection on the study areas not being at the same geographical and cultural areas of Ghana. None of the three species used historically was included in the subsequent in vitro testing of selected plant species [9].

The wound healing process for acute wounds consists of four phases: hemostasis, inflammation, proliferation and migration of cells, and tissue remodeling or resolution [10].

Hemostasis begins immediately after the injury and involves vascular constriction and aggregation of platelets to form a fibrin clot, from where proinflammatory cytokines and growth factors such as transforming growth factor, epidermal growth factor, fibroblast growth factor, and platelet-derived growth factor (PDGF) are released [10].

When inflammation begins neutrophils clear the area for invading microbes and cellular debris around the wound and macrophages clear the area for apoptotic cells. Macrophages also stimulate other cells to promote tissue regeneration, thereby playing a role in promoting the next stage of wound healing, the proliferation and migration of cells [10].

Both endothelial cells and fibroblasts are present in the reparative dermis of the skin [10]. Fibroblasts and endothelial cells are attracted by mediators produced by inflammatory cells in the wound, and the cells proliferate to expand and migrate into the wounded area [11, 12]. Within the wounded area fibroblasts produce various compounds including collagen, which is a major component of the skin extracellular matrix [10, 11]. Skin fibroblasts can change their character; for example, in a wound they can change their actin gene expression and take on some contractile properties of smooth muscle cells and in this way help to pull together the etches of the wound. Such fibroblasts are called myofibroblasts [11].

Fibroblasts can be arrested in a specialized nondividing state called the G_0 phase until they are triggered to proliferate by a growth factor or other extracellular signals. There are many proteins that act as mitogens, but PDGF is believed to have an important role in stimulating cell division during wound healing [11].

The fourth and last phase of wound healing is scar formation and remodeling of the tissue. An important part of this phase is the extracellular matrix attaining the architecture of normal tissue. Therefore, fibroblasts also have a role in this phase of wound healing [10].

A scratch assay has been used as an in vitro model of wound healing in a few studies of medicinal plants [13–18]. In the present study fibroblasts are used to resemble the third phase of wound healing, proliferation and migration of cells into the wounded area. A monolayer of cells is grown in medium supplemented with serum and the cell layer is scratched with a pipette tip to imitate a wound. Plant extracts are then tested in the assay to see if they increase the proliferation and/or migration of the cells.

The present study aims to investigate the wound healing potentials of plants historically used for this purpose, as a part of a larger research collaboration, which aims to examine historical and contemporary medicinal plants in Ghana [4].

2. Materials and Methods

2.1. Cell Line and Chemicals. NIH 3T3 fibroblasts were purchased from Institute of Pharmacy, University of Copenhagen. The cells were maintained in Dulbecco's modified Eagle's medium supplemented with 10% Fetal bovine serum and kept at 37°C with a CO_2 supply of 5%.

PDGF was purchased from Invitrogen Gibco. Rutin and Sil-A were purchased from Sigma.

2.2. Plant Material. Seventeen plants traditionally used for wound healing in Ghana were collected in Ghana from November 2013 to January 2014. Plant material was air-dried away from sunlight and stored in airtight bags. Voucher specimens were identified by Jens Soelberg and deposited at the Herbarium of University of Copenhagen (C) and Herbarium of University of Ghana (GC). Voucher numbers are given in Table 1.

2.3. Wound Healing Scratch Assay. Migration of NIH 3T3 fibroblasts was assessed using the wound healing scratch assay. The cells were seeded in 24-well tissue culture dishes for 24 hours at 37°C, at a concentration of 7.6×10^4 cells/mL, and cultured in 1 mL medium containing 10% fetal bovine serum to a nearly confluent cell monolayer.

A linear scratch was created in the monolayer with a sterile pipette tip (Fastrak, 1250 μL Macro Tip, FR1250, Alpha Laboratories Ltd.), and the medium was replaced by 500 μL new medium (control group), 20 ng/mL platelet-derived growth factor, PDGF (positive control), and the crude extracts (10 μg/mL). The experiments were made in triplicate. The cells were incubated at 37°C for 21 hours. Three images were photographed of each well under a Leica DMLS microscope at 4x/0.10 magnification before and after incubation to estimate the proliferation and/or migration of cells. The data were analyzed using Leica application suite, LAS. Cell proliferation/migration rate was calculated as percent closure of the scratch within 21 hours:

$$\frac{\text{Cell migration}}{\text{proliferation}} = \frac{\left(\text{gap distance}_{t0} - \text{gap distance}_{t21}\right)}{\text{gap distance}_{t0}} \cdot 100\%. \quad (1)$$

2.4. Reversed-Phase High-Performance Liquid Chromatography. Reversed-phased HPLC was used to separate the active extracts. A Shimadzu apparatus (LC-20AB, Prominence liquid chromatograph and SPD-M20A, Prominence diode array detector) was used for analytical as well as preparative HPLC. For analytical HPLC the column was a Thermo Scientific C-18 column, 150 × 4 mm, particle size 5 μm, flow: 1 mL/min. For preparative HPLC the column was a Supelco C-18 column, 250 × 10 mm, particle size 5 μm, flow: 5 mL/min.

Mobile phase A was methanol : water (95 : 5) supplemented with 0.1% formic acid. Mobile phase B was methanol : water (5 : 95) supplemented with 0.1% formic acid.

Fractions of *P. cyanescens* were collected while using a linear gradient from 10% B to 80% B from 0–30 min. The chromatograms were recorded at 254 nm, 270 nm, and 310 nm.

2.5. NMR. The structural identification of wound healing active compounds was performed using NMR spectroscopy. The fractions were dissolved in 50 μL deuterated methanol and 30 μL was transferred to a 1.7 mm NMR tube. ^{1}H-NMR and HSQC spectra were acquired using a 600 MHz Bruker Avance III equipped with a cryogenically cooled 1.7 mm TCI probe head. All spectra were analyzed with ACD/NMR version 12.0 software.

2.6. GC-MS Sugar Analysis. Approximately 0.2 mg of fraction 3 was incubated with 200 μL 2 M TFA at 120°C for two hours. The sample was evaporated to dryness with nitrogen

Table 1: Plant species historically used for wound healing in Ghana.

Plant species	Family	Voucher	Collection site location	Plant part
Aframomum melegueta K. Schum.	Zingiberaceae	JS 224	N 05°51 17.0, W 00°10 30.2	Semen
Allophylus spicatus (Poir.) Radlk.	Sapindaceae	JS 206	N 05°39 25.3, W 00°11 08.2	Radix Herba
Annona senegalensis Pers.	Annonaceae	JS 253	N 05°39 24.6, W 00°11 29.5	Folium
Cissus quadrangularis L.	Vitaceae	JS 256	N 05°39 14.0, W 00°11 06.6	Herba
Gymnanthemum coloratum (Willd.) H. Rob. & B. Kahn	Asteraceae	JS 268	N 05°49 59.1, W 00°07 03.3	Folium cum Flos Radix
Indigofera pulchra Willd.	Fabaceae	JS 270	N 05°49 59.1, W 00°07 03.3	Herba
Jasminum dichotomum Vahl	Oleaceae	JS 273	N 05°54 21.1, W 00°00 18.5	Folium
Leonotis nepetifolia var. africana (P. Beauv.) J. K. Morton	Lamiaceae	JS 278	N 05°54 21.1, W 00°00 18.5	Herba
Melanthera scandens (Schum. & Thonn.) Roberty	Asteraceae	JS 220	N 05°51 49.8, W 00°10 01.0	Herba
Millettia thonningii (Schumacher) Baker	Fabaceae	JS 294	N 05°39 13.3, W 00°11 12.5	Cortex
Ocimum gratissimum L.	Lamiaceae	JS 223	N 05°51 49.8, W 00°10 01.0	Herba
Philenoptera cyanescens (Schum. & Thonn.) Roberty	Fabaceae	JS 204	N 05°42 59.4, W 00°10 35.5	Folium cum Fructus
Rourea coccinea (Schumach. & Thonn.) Benth.	Connaraceae	JS 248	N 05°39 24.1, W 00°11 11.0	Folium Radix
Thonningia sanguinea Vahl	Balanophoraceae	JS 296	N 05°51 10.6, W 00°10 41.9	Herba
Trichilia monadelpha (Thonn.) J. J. de Wilde	Meliaceae	JS 260	N 05°51 15.9, W 00°10 30.1	Cortex
Triumfetta rhomboidea Jacq.	Malvaceae	JS 272	N 05°54 52.3, W 00°02 17.0	Radix
Uvaria ovata (Vahl ex DC.) Hook. f. & Benth.	Annonaceae	JS 207	N 05°39 26.0, W 00°11 05.4	Folium Cortex Radix Folium cum Flos

and 200 μL of 25 mg/mL hydroxylamine hydrochloride in pyridine was added. After incubation on a water bath at 40°C for 20 min, 100 μL of the resulting sugar-oxime solutions was transferred to an Eppendorf tube and the pyridine was evaporated with nitrogen. Fifty μL Sil-A was added to the tube and it was left for 15 min at 20°C. The resulting solutions were centrifuged in 2 min and 28 μL of the supernatant was diluted with pyridine to 200 μL. Sugar standards of D-glucose, α-L(+)-rhamnose monohydrate were prepared in the same way, but with 35 μL of the supernatant diluted with pyridine to 500 μL.

GC-MS spectra were recorded on an Agilent GC-MS system comprising 5973N Mass Selective Detector, 6890N Network GC-system, 7683 Series Injector, and Autosampler (Agilent Technologies, Santa Clara, USA). The system was operated in EI mode at −69.9 eV, recording masses in the range 35.00–400.00. Sugar standards were injected in 1 μL volumes, fraction 3 in 3 μL volume, on an Agilent 19091S HP-5MS capillary column (5%-phenyl-methylpolysiloxane; 30 m × 250 μm × 0.25 μm). The carrier gas (helium) was set to a flow rate of 1 mL/min and the split ratio was set to 1 : 20. The temperature program comprised 125°C for 3 min followed by 125–270°C at 4°C/min. The injector temperature was held at 250°C.

2.7. Statistical Analysis. Statistical analyses were performed using Microsoft Office Excel 2010 data analysis. Data are expressed as the mean ± SEM. Significant differences between the test solutions and the control group were determined by a t-test or a single-factor ANOVA in Microsoft Office Excel 2010 data analysis with the significance factor $p < 0.05$.

3. Results and Discussion

3.1. Wound Healing Activity of Plant Extracts. Warm and cold water extracts were tested for wound healing activity in the scratch assay. Extracts of five of the 17 plant species tested showed increased proliferation and/or migration of fibroblasts in the scratch assay (Figure 1). The mean proliferation/migration rate of *Allophylus spicatus* (warm and cold extracts of herba), *Philenoptera cyanescens* (warm extract), *Melanthera scandens* (warm extract), *Ocimum gratissimum* (cold extract), and *Jasminum dichotomum* (warm extract) was significantly higher than that of the negative control group.

A minimum of 120% proliferation/migration rate compared to the negative control group was used as inclusion criteria for further analysis. Therefore, the warm water extract of folium/fructus of *P. cyanescens* was chosen for further analysis.

3.2. Isolation of Active Compounds. The warm water extract of folium/fructus of *P. cyanescens* was separated in 6 fractions by analytical HPLC (Figure 2). The fractions were tested in the wound healing scratch assay in concentrations corresponding to 10 μg/mL crude extract (Figure 3).

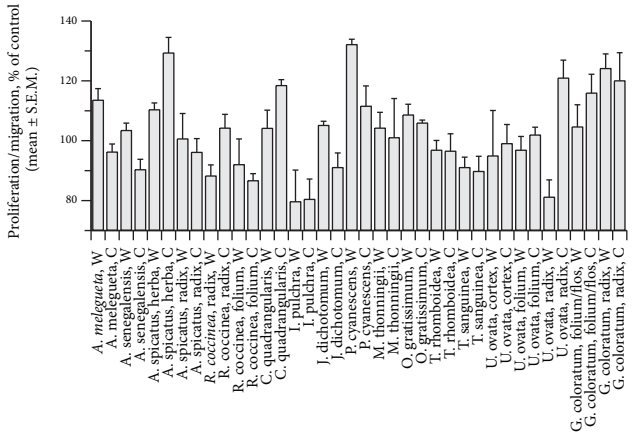

Figure 1: Effect of cold (C) and warm (W) water extracts of plants from Ghana tested for wound healing activity in the scratch assay.

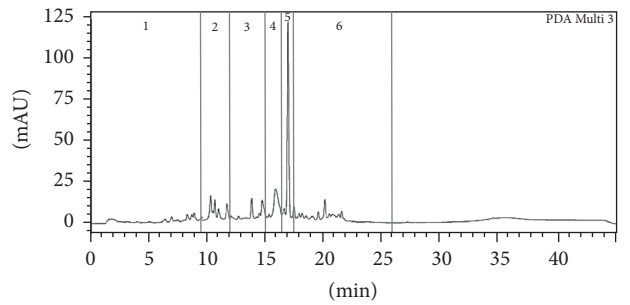

Figure 2: HPLC chromatogram of *Philenoptera cyanescens* at 310 nm separated into fractions 1–6.

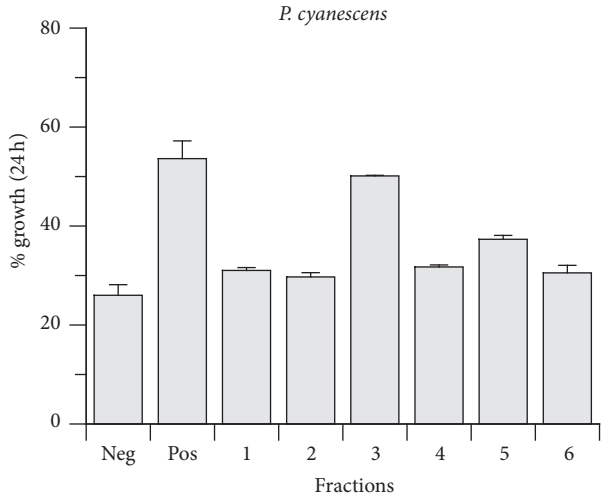

Figure 3: Activity of fractions 1–6 of *Philenoptera cyanescens* tested in the wound healing scratch assay. Neg: negative control, Pos: positive control (20 ng/mL PDGF).

Fractions 3 and 5 of *P. cyanescens* showed significantly more growth than the control group, with fraction 3 showing significantly more growth than fraction 5. The HPLC chromatogram contained two minor peaks in fraction 3, whereas fraction 5 contained the major peak of the HPLC chromatogram. These peaks were isolated by preparative HPLC and tested in the scratch assay, leading to two active compounds, one (**1**) from fraction 3 and the main compound (**2**) from fraction 5.

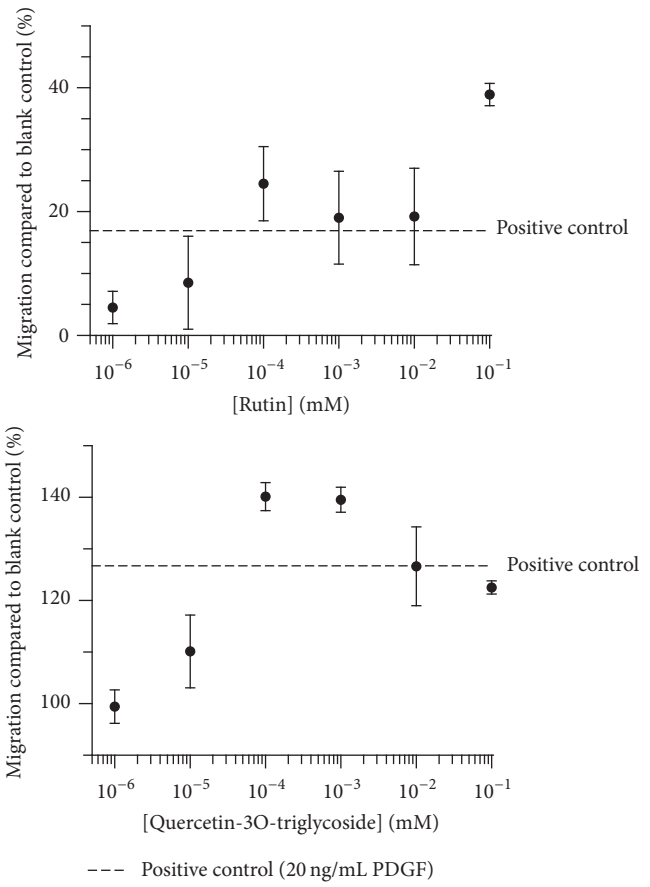

Figure 4: Concentration dependent migration of NIH 3T3 fibroblasts when incubated with rutin or the quercetin-3O-triglucoside from fraction 3.

Compound **2** was identified as rutin (quercetin-3-O-rutinoside). Signals in the proton spectrum were assigned as those of rutin assigned in the literature [19, 20], as well as a 1H-NMR and a HSQC spectrum of standard rutin recorded in this study.

Compound **1** was identified as a glycoside flavonoid composed of the aglycone quercetin by comparison of the proton spectrum with that of rutin, with a triglycoside attached to the O-3 position according to MS and NMR data obtained. The sugar molecules were identified by GC-MS analysis of the hydrolysed sugars, showing that the triglycoside consisted of two sugar molecules of glucose and one of rhamnose. However, we were not able to identify the exact structure of the triglycoside.

Different concentrations of standard rutin and the isolated quercetin-triglycoside were tested in the wound healing scratch assay. The results showed a concentration dependent activity of both compounds (Figure 4), with a concentration of 10 nM giving results comparable to 20 ng/mL PDGF.

In previous studies rutin has shown wound healing activity in vitro [21] as well as in vivo [22]. Rutin has also shown

antioxidant activity [23] as another approach for wound healing. The poor solubility of rutin in aqueous media has been overcome in a study where rutin is formulated as an injectable bioactive hydrogel of rutin-conjugated chitosan. This formulation contributed to improve the healing of dermal wounds [24]. Rutin has also been shown to reduce the healing time for injuries when taken orally in a clinical study [25]. Thus, rutin may hold some promise as an agent in wound healing.

4. Conclusion

Allophylus spicatus, Philenoptera cyanescens, Melanthera scandens, Ocimum gratissimum, and *Jasminum dichotomum* showed proliferation and/or migration of fibroblasts in the scratch assay. Thereby the historical use of these plants as wound healing remedies in Ghana is supported. The wound healing activity was attributed to the glycoside flavonoids rutin and a triglycoside of quercetin in *P. cyanescens*.

Competing Interests

The authors declare that they have no competing interests.

Acknowledgments

The project was funded by the Cand. Pharm. Povl M. Assens Foundation and the Carlsberg Foundation. Thanks are given to Dr. Alex Asase and Mr. J. Y. Amponsah at University of Ghana Herbarium for their assistance in herbarium and field.

References

[1] J. Petiver, "A catalogue of some guinea-plants, with their native names and virtues," *Journal of Philosophical Transactions*, vol. 19, pp. 677–686, 1697.

[2] T. E. Bowdich, *Mission from Cape Coast Castle to Ashantee*, Frank Cass & Co., London, UK, 1819.

[3] C. F. Schumacher, *Beskrivelse af guineiske Planter, som ere fundne af danske Botanikere, især af Etatsraad Thonning*, Hartv. Frid. Popps Bogtrykkerie, Copenhagen, Denmark, 1827.

[4] J. Soelberg, A. Asase, G. Akwetey, and A. K. Jäger, "Historical versus contemporary medicinal plant uses in Ghana," *Journal of Ethnopharmacology*, vol. 160, pp. 109–132, 2015.

[5] WHO, *Dracunculiasis—About Guinea-Worm Disease*, WHO, Geneva, Switzerland, 2014.

[6] D. R. Hopkins and E. Ruiz-Tiben, "Dracunculiasis (guinea worm disease): case study of the effort to eradicate guinea worm," in *Water and Sanitation-Related Diseases and the Environment: Challenges, Interventions, and Preventive Measures*, chapter 10, pp. 125–132, Wiley-Blackwell, Hoboken, NJ, USA, 2011.

[7] WHO, *Dracunculiasis—Epidemiology*, World Health Organization, Geneva, Switzerland, 2014.

[8] C. Agyare, A. Asase, M. Lechtenberg, M. Niehues, A. Deters, and A. Hensel, "An ethnopharmacological survey and in vitro confirmation of ethnopharmacological use of medicinal plants used for wound healing in Bosomtwi-Atwima-Kwanwoma area, Ghana," *Journal of Ethnopharmacology*, vol. 125, no. 3, pp. 393–403, 2009.

[9] A. Hensel, E. Kisseih, M. Lechtenberg, F. Petereit, C. Agyare, and A. Asase, "From ethnopharmacological field study to phytochemistry and preclinical research: the example of Ghanaian medicinal plants for improved wound healing," in *Ethnopharmacology*, M. Heinrich and A. K. Jäger, Eds., John Wiley and Sons; Wiley Blackwell, 2015.

[10] S. Guo and L. A. DiPietro, "Factors affecting wound healing," *Journal of Dental Research*, vol. 89, no. 3, pp. 219–229, 2010.

[11] B. Alberts, A. Johnson, J. Lewis, M. Raff, K. Roberts, and P. Walter, *Molecular Biology of The Cell*, Garland Science, Taylor and Francis, New York, NY, USA, 4th edition, 2002.

[12] T. Schreier, E. Degen, and W. Baschong, "Fibroblast migration and proliferation during in vitro wound healing. A quantitative comparison between various growth factors and a low molecular weight blood dialyzate used in the clinic to normalize impaired wound healing," *Research in Experimental Medicine*, vol. 193, no. 1, pp. 195–205, 1993.

[13] M. Clericuzio, S. Tinello, B. Burlando et al., "Flavonoid oligoglycosides from Ophioglossum vulgatum L. Having wound healing properties," *Planta Medica*, vol. 78, no. 15, pp. 1639–1644, 2012.

[14] M. Fronza, B. Heinzmann, M. Hamburger, S. Laufer, and I. Merfort, "Determination of the wound healing effect of Calendula extracts using the scratch assay with 3T3 fibroblasts," *Journal of Ethnopharmacology*, vol. 126, no. 3, pp. 463–467, 2009.

[15] M. Harishkumar, Y. Masatoshi, S. Hiroshi, I. Tsuyomu, and M. Masugi, "Revealing the mechanism of in vitro wound healing properties of citrus tamurana extract," *BioMed Research International*, vol. 2013, Article ID 963457, 8 pages, 2013.

[16] K. Hostanska, M. Rostock, and R. Saller, "Wound healing potentials of a herbal homeopathic remedy on NIH 3T3 fibroblasts in vitro," *Planta Medica*, vol. 77, no. 12, 2011.

[17] K. Naumann, S. Ebeling, M. Laszczyk, A. Scheffler, and I. Merfort, "Triterpenes from birch bark extract beneficially affect wound healing," *Planta Medica*, vol. 76, no. 12, article 575, 2010.

[18] M. Zubair, A. Ekholm, H. Nybom, S. Renvert, C. Widen, and K. Rumpunen, "Effects of *Plantago major* L. leaf extracts on oral epithelial cells in a scratch assay," *Journal of Ethnopharmacology*, vol. 141, no. 3, pp. 825–830, 2012.

[19] Z. Güvenalp, N. Kiliç, C. Kazaz, Y. Kaya, and L. Ö. Demirezer, "Chemical constituents of Galium tortumense," *Turkish Journal of Chemistry*, vol. 30, no. 4, pp. 515–523, 2006.

[20] J. G. Napolitano, D. C. Lankin, S.-N. Chen, and G. F. Pauli, "Complete ^{1}H NMR spectral analysis of ten chemical markers of *Ginkgo biloba*," *Magnetic Resonance in Chemistry*, vol. 50, no. 8, pp. 569–575, 2012.

[21] M. M. Koganov, O. V. Dueva, and B. L. Tsorin, "Activities of plant-derived phenols in a fibroblast cell culture model," *Journal of Natural Products*, vol. 62, no. 3, pp. 481–483, 1999.

[22] J. S. Almeida, D. M. Benvegnú, N. Boufleur et al., "Hydrogels containing rutin intended for cutaneous administration: efficacy in wound healing in rats," *Drug Development and Industrial Pharmacy*, vol. 38, no. 7, pp. 792–799, 2012.

[23] S. L. Patil, S. H. Mallaiah, and R. K. Patil, "Antioxidative and radioprotective potential of rutin and quercetin in Swiss albino mice exposed to gamma radiation," *Journal of Medical Physics*, vol. 38, no. 2, pp. 87–92, 2013.

[24] N. Q. Tran, Y. K. Joung, E. Lih, and K. D. Park, "In situ forming and rutin-releasing chitosan hydrogels as injectable dressings for dermal wound healing," *Biomacromolecules*, vol. 12, no. 8, pp. 2872–2880, 2011.

[25] S. A. Brown, M. Coimbra, D. M. Coberly, J. J. Chao, and R. J. Rohrich, "Oral nutritional supplementation accelerates skin wound healing: a randomized, placebo-controlled, double-arm, crossover Study," *Plastic and Reconstructive Surgery*, vol. 114, no. 1, pp. 237–244, 2004.

Hindawi Publishing Corporation
Evidence-Based Complementary and Alternative Medicine
Volume 2016, Article ID 6568528, 7 pages
http://dx.doi.org/10.1155/2016/6568528

Research Article

In Vivo Wound Healing Activity of *Abrus cantoniensis* Extract

Qi Zeng, Hui Xie, Hongjin Song, Fayu Nie, Jiahua Wang, Dan Chen, and Fu Wang

School of Life Science and Technology, Xidian University, Xi'an, China

Correspondence should be addressed to Dan Chen; dchen@xidian.edu.cn and Fu Wang; fwang@xidian.edu.cn

Received 4 October 2016; Revised 2 December 2016; Accepted 12 December 2016

Academic Editor: Norazah Basar

Abrus cantoniensis (Leguminosae sp.) is a traditionally used remedy for treating rheumatism, blood stasis, and internal injuries. In order to reveal a new insight of the utilization of the plant, solvent extraction by ethyl acetate (EA) was performed in order to evaluate the plant extracts' in vivo excision and incision-wound potentials with models. The contents of the EA fraction, wound healing activity, acute oral toxicity, and acute dermal toxicity were studied. As a result, the main chemical constituents of the EA fraction were alkaloids, flavonoids, and steroids. The acute oral toxicity test results and assessment of skin hypoallergenicity showed that the plant extract was safe at LD50 as high as 5000 mg/kg. Both excision and incision model tests results indicated that the EA fraction of *A. cantoniensis* showed a significant wound healing capacity at a concentration of 5% (v/w) ($p < 0.01$) as observed by the increased wound contraction, decreased epithelialization time, and increased hydroxyproline content compared to the ones of the controls. The present study showed that the EA fraction of *A. cantoniensis* possesses potential wound healing activities and provided recent results for the use of *A. cantoniensis* for wound curing.

1. Introduction

Wound healing is often considered as a major problem in clinical practice. It is a complex process occurring after injury and is as old as mankind [1]. Wound healing is accomplished by inflammation, proliferation, differentiation, migration, organization, and remodeling of cells inside and around the vicinity of the injury [2]. The proliferative phase consists of angiogenesis, collagen deposition, epithelialization, and wound contraction. The aim of treating wounds is to shorten the time of healing and reduce the risks of undesired complications [3]. Over three-quarters of the world population relies mainly on plants and plant extracts for health care [4]. And for the remedy of wound healing, more than 400 species of plants are identified as potentially useful alternative medicine [5].

Traditional Chinese medicine "Jigucao" belongs to the *Abrus* genus with its Latin name as *Abrus cantoniensis* Hance. *A. cantoniensis* is found in the Hunan, Guangdong, and Guangxi provinces [6]. In China, it is traditionally used against ailments like acute and chronic hepatitis, cirrhosis, cholecystitis, stomach pain, rheumatism, blood stasis, and internal injuries [7, 8]. Previous studies showed that this plant contained various chemical constituents including triterpenoids, steroids, flavonoids, anthraquinones, phenolic acids, and alkaloids [9–17]. Indeed, the medicinal activities of the plant are mainly due to the presence of the constitutive secondary metabolites. However, no study has evaluated the wound healing activity of *A. cantoniensis*. In this context, the aim of the present study was to investigate the wound healing activity of the ethyl acetate fraction of *A. cantoniensis* using the Swiss Albino mice as host for the wound models.

2. Materials and Methods

2.1. Plant Material. Whole plants of *A. cantoniensis* were collected from Meizhou, Guangdong, China, in July 2012, and identified by the pharmacist Yan-rong Li from the Xijiao Hospital of the Meijiang District, Meizhou, China. A voucher specimen (JGC201207) was deposited at the School of Life Science and Technology, Xidian University, Shaanxi, China.

2.2. Animals. Swiss Albino mice (18–22 g, 8–10 weeks of age) were obtained from the animal house of the Xi'an Jiaotong University Health Science Center, China. The mice were housed at room temperature (25 ± 1°C) and were subjected to a 12 h light/12 h dark cycle. All the experiments were

conducted in accordance with the internationally accepted laboratory animal use and care guidelines [18] and the protocol was approved by the School of Pharmacy's Ethics Committee. Mice were acclimatized for one week before the study, and during the experiment the mice were housed individually in their cages so as to avoid biting and possible wound scratch among each other. The mice were provided with water and food pellets before and until the end of the experimental period. The animal study procedures were approved and followed by the Xian Jiaotong University Animal Care and Use Committee (number XJTULAC2016-412).

2.3. Extraction and Fractionation. The air-dried and powdered whole plants of *A. cantoniensis* (5 kg) were extracted with 95% ethanol six times (20 L × 24 h) at room temperature. After evaporation under vacuum, the residue (167.6 g) was then suspended in water and partitioned with petroleum ether (PE), EA, and *n*-butanol (BuOH), respectively. Thus, the extracts from the three different solvents were obtained, submitted separately to solvent evaporation, and named consequently as petroleum ether extract fraction (PE fraction, 42.1 g), ethyl acetate extract fraction (EA fraction, 27.6 g), and n-butanol extract fraction (BuOH fraction, 60.2 g).

2.4. Formulation of the EA Fraction. Two types of formulations (suspension and simple ointment) were prepared. The suspension was prepared following the procedure described by the Encyclopedia of Pharmaceutics Excipient [19] with modifications for the EA fraction. Namely, 2.5 g of the EA fraction was dissolved in 0.75~1.5 mL Tween 80 and grinded until obtaining a white nonhomogenous mixture. Then 100 μL of water was added and the mixture was grinded. The addition of water and grinding step were repeated until the EA fraction was fully dissolved. Finally the volume of the mixture was adjusted to a constant volume of 15 mL. The simple ointment was prepared based on the procedure of Pharmaceutics [20] while using the reduced formula as the base for the EA fraction. More precisely, 5 g of sodium carboxymethylcellulose (Na-CMCC) was mixed in water at 70°C with continuous stirring during 3 hours until no solid particles were found in the mixture. The mixture was then removed from the heating bath and cooled under stirring to obtain the ointment base. In order to obtain the control ointment, 30 mg of nitrofurazone was added to the ointment base resulting in 0.2% (w/v) nitrofurazone ointment. The EA fraction containing ointment was prepared with 10 mL of Na-CMCC in order to form, respectively, 5% and 10% (w/v) EA fraction ointments. All the simple ointments were stored at 4°C.

2.5. Preliminary Phytochemical Analysis. The EA fraction was screened for the presence of secondary metabolites, including alkaloids, saponins, flavonoids, tannins, steroids, and terpenoids by following the procedures described elsewhere [21].

2.5.1. Alkaloids. The test for alkaloids was carried out on 10 mg of EA fraction mixed with 5 mL of ammoniacal chloroform and 2.5 mL of chloroform. After filtration, the supernatant was shaken with drops of 0.5 M sulfuric acid. The appearance of a creamy precipitate indicated the presence of alkaloids.

2.5.2. Saponins. The test for saponins was carried out by adding 10 mg of EA fraction shaken vigorously with 1 mL of ethyl ether and 3 mL of a 2 N solution of hydrochloride (HCl). The appearance of a precipitate indicated the presence of saponins.

2.5.3. Flavonoids. A sample containing 5 mg of the EA fraction was dissolved in 5 mL of absolute ethanol and treated with a few drops of concentrated HCl and 0.2 g of magnesium ribbon. The appearance of a pink-red color indicated the presence of flavanoids.

2.5.4. Tannins. A sample prepared with 5 mg of EA fraction was dissolved in 10 mL of 70% ethanol. The sample was then diluted with sterile distilled water at a ratio of 1 : 2 (v/v). Three drops of 10% (w/v) ferric chloride solution was then added. The appearance of a blue to black precipitate indicated the presence of tannins.

2.5.5. Steroids and Terpenoids. Steroids and terpenoids were detected using the Liebermann-Burchard reaction. A solution containing 5 mg of EA fraction dissolved in chloroform was filtered. The filtrate (2 mL) was added to 2 mL of acetic anhydride and 50% concentrated sulfuric acid. A blue-green ring indicated the presence of steroids while a red color indicated the presence of terpenoids.

2.6. Acute Toxicity Studies

2.6.1. Acute Oral Toxicity Study. Fifteen Swiss Albino mice of both sex weighing between 18 g and 22 g (average weight of 20 g) were used for the acute oral toxicity study. A suspension of the EA fraction was administered following the OECD guideline number 420, starting at a dose level of 2000 mg/kg up to 5000 mg/kg (0, 2000, 3000, 4000, and 5000 mg/kg; five groups of three mice) [22]. Before administration of the EA fraction suspension, all the mice were physically active and consumed food and water regularly. The mice were treated with a suspension of the EA fraction by intragastric administration (0.5 mL) and observed for signs of acute toxicity within 48 h. The mice health was further monitored during the following 7 days in order to detect any general signs of subacute toxicity.

2.6.2. Acute Dermal Toxicity Study. Fifteen mice were used for the skin irritation test. Mice showing normal skin texture were housed individually in a cage. According to the Meeh-Rubner formula, the body surface area of the mice was calculated. Mice were shaved at the dorsal area of the trunk that represented 10% of the skin area 24 h before the study. The mice received a dose of 2000 mg/kg of EA fraction by applying the ointment over the shaved area. The mice were observed for an adverse skin reaction at grading interval of 1, 4, 12, and 24 h.

2.7. Grouping and Dosing of Animals. Mice were divided into four groups: a negative and positive control groups and two test groups. Six mice were used in each group. Mice of the negative control group (group A) were treated with the simple ointment base. Groups B and C were treated with 5% (w/w) and 10% (w/w) of the EA fraction, respectively. The mice in group D were treated with 0.2% (w/v) of nitrofurazone as positive control.

2.8. Wound Healing Studies

2.8.1. Excision Wound Model. Mice were anesthetized by subcutaneous injection of chloral hydrate (1 mL/kg) and 1% atropine. The back of the mice was further shaved. A 215 mm^2 (representing 3.2% of the weight of mice) circular area was marked and the surface of the marked area was carefully excised by using sharp sterilized scissors [23]. After 24 h of wound creation, the ointments were gently applied to cover the wounded area once per day until reaching complete healing [24]. Wound area, wound contraction, epithelialization period, and hydroxyproline content were monitored during the whole healing process.

2.8.2. Wound Area and Wound Contraction. The wound was monitored and the healing area was calculated by using semitransparent tracing paper. The tracing paper was placed on a 1 mm^2 graph sheet and traced out. The area was measured daily and the percentage wound closure was calculated by the following formula:

$$\%\ \text{Wound contraction} = \frac{\text{Wound area on day } 0 - \text{Wound area on day } n}{\text{Wound area on day } 0} \times 100. \quad (1)$$

2.8.3. Estimation of the Hydroxyproline Content. A calibration curve was plotted using standard hydroxyproline solutions in order to determine the hydroxyproline content of the tissue. The hydroxyproline content was determined by following the method described by Leach [25]. The calibration curve of the hydroxyproline content in the EA fraction is depicted in Figure 1. The injured mice were subjected to the ointment formulation treatment during 10 days and then sacrificed on the 11th day using a high dose of diethyl ether. The healed tissue was excised and the water was absorbed with filter paper, before grinding the tissue. A sample weighing 0.15 g of wound tissue was then hydrolyzed with 3 mL of 6 N hydrochloric acid for 24 h at 110°C in a sealed conical glass flask. The pH of the hydrolysate was neutralized to pH 8.0 ± 0.2 [26]. The supernatant solution (1 mL) was removed delicately with a pipette from each of the hydrolysates and submitted to the standard treatment. The hydroxyproline content of the samples was determined based on the equation extracted from the calibration curve.

2.8.4. Incision Wound Model. Anesthetized mice were shaved and a straight line was marked at a distance of 1 cm from the paravertebral ganglia. An incision wound of 3 cm long and of full skin thickness, parallel to the paravertebral region, was made with a sterile scalpel [27]. The wound was then closed by interrupted sutures having 1 cm intervals. The mice were treated with ointments 24 h after the incision and during nine days. The sutures were removed on the 8th day. The tensile strength of the wound was measured on the 10th day [24].

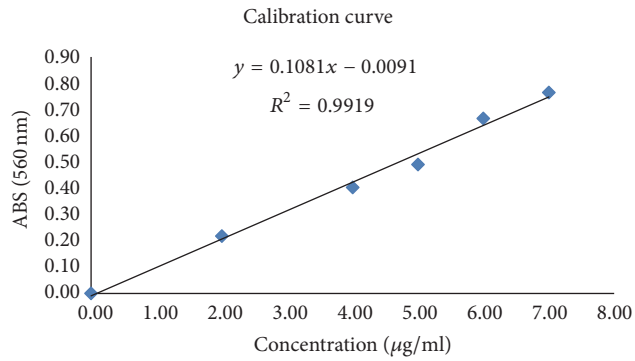

Figure 1: Calibration curve of hydroxyproline specifically plotted for the EA fraction. The standard hydroxyproline solutions had the following concentrations: 7, 6, 5, 4, 2, and 0 μg/mL. The hydroxyproline content was determined by the method described by Leach [25] and using a UV-detection at 560 nm on a spectrophotometer.

2.8.5. Measurement of the Tensile Strength. The breaking strength of the wound on each animal was measured by using the constant water flow method [28].

2.9. Statistical Analysis. The statistical differences were evaluated using the software IBM SPSS Statistics v. 19.0.0 (New York, USA). The normality of the distributions was evaluated through the Kolmogorov-Smirnov's test and the differences were evaluated using the software One-Way ANOVA associated with Scheffe's test (for normal distributions) or the nonparametric Mann–Whitney test for the rest. Differences were considered significant when $p < 0.05$.

3. Results

3.1. Phytochemical Screening. Analyses of the EA fraction of *A. cantoniensis* indicated the presence of alkaloids, flavonoids, and steroids (Table 1) as consistent with former reports [17]. However, our EA fraction did not contain saponins and terpenoids in contrast to previous studies [9–15]. Indeed, the polarity of EA fraction hinders the retention of saponins and terpenoids molecules.

3.2. Acute Toxicity Studies. During the 7 days of the acute oral toxicity observation period, none of the mice died nor showed any adverse reaction such as towering hair, exophthalmos, muscle paralysis, convulsions, breathing difficulties, teeter, coma, or incontinence. The LD_{50} of the EA fraction was greater than 5000 mg/kg. Concerning the skin irritation test, the swelling and erythema did not appear on the test group during the whole experimental period (14 days).

Table 1: Qualitative analysis of bioactive compounds in the EA fraction of *A. cantoniensis*.

	Alkaloids	Saponin	Flavanoids	Tannins	Steroids	Terpenoids
EA fraction	+	−	+	−	+	−

Note: present (+); absent (−).

Table 2: Effect of the EA fraction formulated in ointment on the percentage of wound contraction.

Group ($n = 6$)	Treatment period (day)			
	2nd	4th	6th	8th
0.2 w/v nitrofurazone	58.46 ± 12.05*	74.62 ± 7.15**	82.23 ± 7.25*	92.73 ± 4.28*
10% EA fraction	47.38 ± 19.21	57.85 ± 14.85	71.08 ± 8.21	85.54 ± 7.00
5% EA fraction	53.35 ± 8.12*	66.14 ± 9.41*	83.93 ± 9.16*	94.48 ± 3.04**
Simple ointment	44.04 ± 7.63	56.96 ± 5.58	70.71 ± 8.20	84.92 ± 5.84

Note: *$0.01 < p < 0.05$; **$p < 0.01$.

Table 3: Effect of the EA fraction on the hydroxyproline content of the granulation tissue of the excision wound.

Group ($n = 6$)	Hydroxyproline content (μg/g)
0.2 w/v nitrofurazone	7.448 ± 1.442**
10% EA fraction	3.562 ± 1.109
5% EA fraction	6.264 ± 1.617**
Simple ointment	3.766 ± 0.875

Note: **$p < 0.01$.

Therefore, we estimate a safe dosage of EA fraction superior to 2000 mg/kg.

3.3. Excision Wound Study. The ointment containing 5% (w/v) of the EA fraction showed an increased wound contraction rate compared to the one of the negative control group (e.g., on the 8th day, we observed a wound healing of 94.48% for mice treated with 5% EA against 84.92% for the control group) (Table 2). From the 6th day, the contraction value was even slightly higher for the 5% EA fraction treated mice than for the mice treated with the reference drug nitrofurazone. However, a higher dose of EA fraction (10%, (w/v)) did not show any significant difference compared to the results obtained by the negative control group. Moreover, extrapolation of the results as represented by the trend lines in Figure 2, supports the positive effect of EA fraction in would healing. The excision wound was healed on the 10th day for the mice treated with 5% (w/v) ointment (Figure 3). As showed in Table 3, the hydroxyproline content of the 5% EA fraction was 6.264 μg/g while the one of the reference drug group was 7.448 μg/g. These values are nearly the double of the value detected for the control group (3.766 μg/g). Conversely, the hydroxyproline content of the 10% EA fraction exhibited a lower value as in the case of the control group.

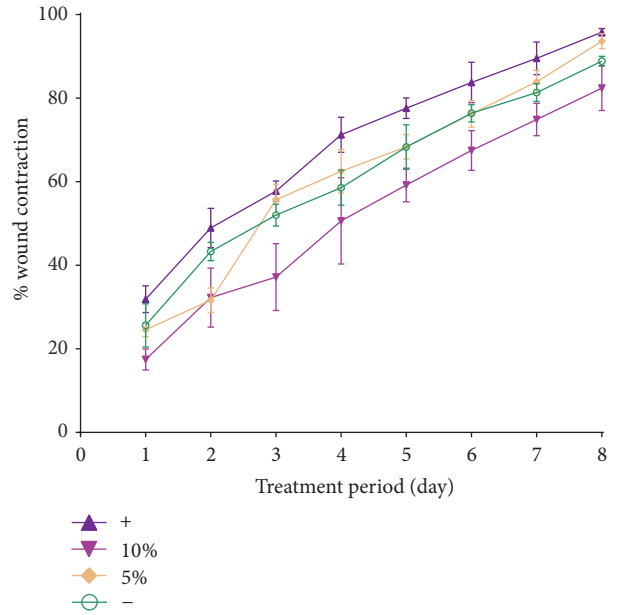

Figure 2: Effect of the EA fraction formulated in ointments on the percentage of wound contraction. The excision wound models were treated with 5% (w/v) and 10% (w/v) of the EA fraction. Negative control group and the blank group were treated with 0.2% (w/v) nitrofurazone and simple ointment.

3.4. Tensile Strength of the Incision Wound. The values of the tensile strength of the incision wound treated with the EA fraction on day 10 are presented in Table 4. Both the high dose (10%, (w/v)) and the low dose (5%, (w/v)) of EA fraction exhibited wound breaking strength values comparable to the one of the control group. The tensile strength of the mice treated with 5% (w/v) EA fraction ointment was higher than the one of the group treated with 10% (w/v) The best healing was observed for the group treated with the EA fraction ointment on the 10th day of treatment.

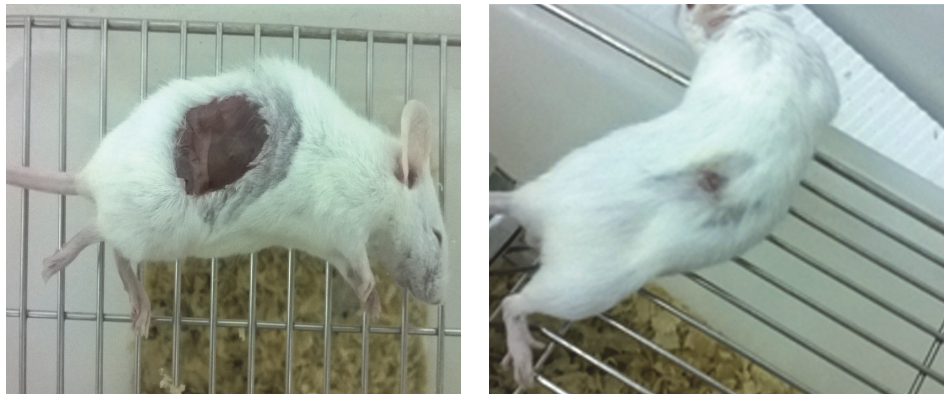

(a) (b)

Figure 3: Photograph of appearance of a healed excision wound: (a) day 0 and (b) day 10.

Table 4: Effect of EA fraction on the tensile strength.

Group	Tensile strength (g) (% tensile strength)
0.2 w/v nitrofurazone	242.83 ± 59.82**
10% EA fraction	171.17 ± 23.30*
5% EA fraction	197.83 ± 46.01**
Simple ointment	134.50 ± 26.37

Note: *$0.01 < p < 0.05$; **$p < 0.01$.

4. Discussion

Wounds are physical injuries of the skin. Healing is a complex process initiated in response to an injury and restores the function and integrity of damaged tissues [3]. Unpublished results showed that the EA fraction showed the highest antibacterial activity among the four other solvent extracts of *A. cantoniensis* (PE, EA, BuOH, and EtOH). Therefore, the aim of this work was to evaluate the wound healing activity of the EA fraction. The results of this study showed, for the first time, the enhancement of the wound contraction rate and reduction of the healing time in mice treated with an ointment containing the EA fraction of *A. cantoniensis*. This result highlights a new possible usage of the traditional medicine plant.

The ointment formulation of the medicinal plant could achieve wound care healing [29]. Therefore, the EA fraction was prepared as an ointment formulation in the excision and incision wound experiments. Moreover, the ointment of the EA fraction showed low allergenicity to the skin. The suspension formulation of the EA fraction was used for the acute toxicity test. An acceptable safety high dosage of 5000 mg/kg bw was determined. These results indicated the safe usage of the EA fraction of *A. cantoniensis* on mice and revealed a potential application for clinical issues.

The lower dose (5%, (w/v)) of the EA fraction accelerated the wound healing ($p < 0.01$) when compared to the results obtained for the negative control groups for both excision and incision tests. Specifically, the 5% EA fraction ointment exhibited a better healing effect than the reference drug (nitrofurazone) in the excision tests. The whole healing period was shortened to ten days when the mice were treated with the ointment containing 5% of EA fraction. Hydroxyproline is a major amino-acid constituent of collagen and serves as marker for collagen content in tissue samples [30]. An increase in the hydroxyproline content indicates an increase in the collagen synthesis, which in turn leads to improved wound healing activity. In this study, the hydroxylproline content of the tissues from mice treated with 5% EA fraction ointment was significantly higher than the ones detected for the negative control mice. This result demonstrated the efficient wound healing activity of a low dose of EA fraction in the excision model. However, a higher dosage of 10% EA fraction in the ointment was not beneficial as shown by the results obtained in both test models and the hydroxyproline content determination. In our previous antibacterial study, the efficient dosage range of EA fraction exhibited a similar trend of this result. In parallel, it could be deduced that the wound healing activity of the EA fraction might be also related to its antimicrobial activity that occurs at a specific dosage interval.

The antimicrobial and wound healing activities might be due to the presence of alkaloids, flavonoids, and steroids in the preliminary phytochemical analysis (Table 1). Other medicinal plants, which were identified as potentially useful for wound healing, contained similar constituents. These metabolites were suggested to play a critical role in the wound healing process by increasing the rate of wound contraction, epithelialization, and prevention of secondary bacterial infections that would have complicated and delayed the wound healing [31–34]. The absence of saponins and terpenoids in the EA fraction might indicate that these compounds do not have affinity with the polar ethyl acetate extraction solvent. As a result, further phytochemical studies should be investigated to pinpoint the active compounds of *A. cantoniensis*.

A. cantoniensis is a basic plant of the traditional medicine "Jigucao." It appears in the daily life as the Guangdong herbal tea or as an ingredient in soups. The ancient and common usage of this plant demonstrated its safe character and indicated the potential development in the medicinal

field. With the rising respect towards "medicine and food homology," we believe that *A. cantoniensis* has a high potential medicinal value. Yet, the substantial constituents of the wound healing activity and action mechanisms were not determined. The next study should be focused on the phytochemistry detection, healing markers analysis, and in vivo dose-effect relationship.

5. Conclusion

The present study revealed the wound healing activity of the EA fraction of *A. cantoniensis*. Wound contraction, increased breaking strength of the repaired tissue, and the increased hydroxylproline content support the observed wound healing. As a conclusion, the results of the study indicated a new view of this medicinal plant for the usage of wounds curing.

Competing Interests

The authors declare that there is no conflict of interests regarding the publication of this paper.

Acknowledgments

This work was supported by The National Basic Research and Development Program of China (no. 2014CB744503), the National Natural Science Foundation of China (no. 81301214; no. 31300268; no. 31400662; no. 31371006; and no. 81571721), and the Natural Science Basic Research Plan from the Shaanxi Province of China (no. 2012JC2-10; no. 2013JQ4040; no. 2016JM8016). Thanks are due to MogoEdit for providing the English language help. Thanks are due also to Xi'an Jiaotong University Health Science Center for the help with animal experiments.

References

[1] D. D. Kokane, R. Y. More, M. B. Kale, M. N. Nehete, P. C. Mehendale, and C. H. Gadgoli, "Evaluation of wound healing activity of root of *Mimosa pudica*," *Journal of Ethnopharmacology*, vol. 124, no. 2, pp. 311–315, 2009.

[2] S. E. Mutsaers, J. E. Bishop, G. McGrouther, and G. J. Laurent, "Mechanisms of tissue repair: from wound healing to fibrosis," *International Journal of Biochemistry and Cell Biology*, vol. 29, no. 1, pp. 5–17, 1997.

[3] D. MacKay and A. L. Miller, "Nutritional support for wound healing," *Alternative Medicine Review*, vol. 8, no. 4, pp. 359–377, 2003.

[4] S. Yogisha and K. A. Raveesha, "*In vitro* antibacterial effect of selected medicinal plant extracts," *Journal of Natural Products*, vol. 2, pp. 64–69, 2009.

[5] P. K. Ghosh and A. Gaba, "Phyto-extracts in wound healing," *Journal of Pharmacy and Pharmaceutical Sciences*, vol. 16, no. 5, pp. 760–820, 2013.

[6] Z. Wei, *Flora of China*, vol. 40, Science Press, Beijing, China, 1994.

[7] L. R. Song, *Chinese Materia Medica*, vol. 4, Shanghai Science and Technology Press, Shanghai, China, 1999.

[8] Y. Q. Yan, C. L. Yu, and T. K. Huang, *Chinese Medicine Dictionary*, vol. 506, China Medical Science Press, Beijing, China, 1996.

[9] T. Takashi, H. Shuichi, and N. Toshihiro, "New triterpenoid sapogenols from *Abrus cantoniensis* (I)," *Chemical and Pharmaceutical Bulletin*, vol. 37, no. 3, pp. 846–848, 1989.

[10] H. Miyao, Y. Sakai, T. Takeshita, J. Kinjo, and T. Nohara, "Triterpene saponins from *Abrus cantoniensis* (Leguminosae). I. Isolation and characterization of four new saponins and a new sapogenol," *Chemical and Pharmaceutical Bulletin*, vol. 44, no. 6, pp. 1222–1227, 1996.

[11] H. Miyao, Y. Sakai, T. Takeshita, Y. Ito, J. Kinjo, and T. Nohara, "Triterpene saponins from *Abrus cantoniensis* (Leguminosae). II. Characterization of six new saponins having a branched-chain sugar," *Chemical and Pharmaceutical Bulletin*, vol. 44, no. 6, pp. 1228–1231, 1996.

[12] Y. Sakai, T. Takeshita, J. Kinjo, Y. Ito, and T. Nohara, "Two new triterpenoid sapogenols and a new saponin from Abrus cantoniensis (II)," *Chemical and Pharmaceutical Bulletin*, vol. 38, no. 3, pp. 824–826, 1990.

[13] T. C. Chiang and H. M. Chang, "Isolation and structural elucidation of some sapogenols from *Abrus cantoniensis*," *Planta Medica*, vol. 46, no. 1, pp. 52–55, 1982.

[14] T. C. W. Mak, T.-C. Chiang, and H.-M. Chang, "X-ray crystal structures of cantoniensistriol and sophoradiol: two oleanane-type triterpenes from the roots of *Abrus cantoniensis* Hance," *Journal of the Chemical Society, Chemical Communications*, no. 14, pp. 785–786, 1982.

[15] H. Miyao, T. Arao, M. Udayama, J. Kinjo, and T. Nohara, "Kaikasaponin III and soyasaponin I, major triterpene saponins of *Abrus cantoniensis*, act on GOT and GPT: influence on transaminase elevation of rat liver cells concomitantly exposed to CCl_4 for one hour," *Planta Medica*, vol. 64, no. 1, pp. 5–7, 1998.

[16] S. M. Wong, T. C. Chiang, and H. M. Chang, "Hydroxyanthraquinones from *Abrus cantoniensis*," *Planta Medica*, vol. 46, no. 3, pp. 191–192, 1982.

[17] H.-M. Shi, J. Wen, and P.-F. Tu, "Chemical constituents of *Abrus cantoniensis*," *Chinese Traditional and Herbal Drugs*, vol. 37, no. 11, pp. 1610–1613, 2006.

[18] Institute for Laboratory Animal Research (ILAR), *Guide for the Care and Use of Laboratory Animals*, The National Academy Press, Washington, DC, USA, 1996.

[19] M. S. Luo and T. H. Gao, "Encyclopedia of pharmaceutics excipient, Sichuan," *Sichuan Publishing House of Science & Technology*, vol. 22, 2006.

[20] D. F. Cui, *Pharmaceutics*, People's Medical Publishing House, Beijing, China, 2011.

[21] M. Malahubban, A. R. Alimon, A. Q. Sazili, S. Fakurazi, and F. A. Zakry, "Phytochemical analysis of *Andrographis paniculata* and *Orthosiphon stamineus* leaf extracts for their antibacterial and antioxidant potential," *Tropical Biomedicine*, vol. 30, no. 3, pp. 467–480, 2013.

[22] The traditional Chinese medicine, natural medicine acute toxicity test technology guiding principle subject group, Chinese medicine, natural medicine acute toxicity research techniques guiding principle, 2005.

[23] E. K. Akkol, U. Koca, I. Peşin, D. Yilmazer, G. Toker, and E. Yeşilada, "Exploring the wound healing activity of *Arnebia densiflora* (Nordm.) Ledeb. by in vivo models," *Journal of Ethnopharmacology*, vol. 124, no. 1, pp. 137–141, 2009.

[24] I. P. Süntar, E. K. Akkol, D. Yilmazer et al., "Investigations on the in vivo wound healing potential of Hypericum perforatum L.," *Journal of Ethnopharmacology*, vol. 127, no. 2, pp. 468–477, 2010.

[25] A. Leach, *Notes on a Modification of the Neuman and Logan Method for the Determination of the Hydroxyproline*, vol. 47, The British Gelatine and Glue Research Association, London, UK, 1960.

[26] R. Sanwal and A. Chaudhary, "Wound healing and antimicrobial potential of *Carissa spinarum* Linn. in albino mice," *Journal of Ethnopharmacology*, vol. 135, no. 3, pp. 792–796, 2011.

[27] P. T. Deshmukh, J. Fernandes, A. Atul, and E. Toppo, "Wound healing activity of Calotropis gigantea root bark in rats," *Journal of Ethnopharmacology*, vol. 125, no. 1, pp. 178–181, 2009.

[28] K. Ilango and V. Chitra, "Wound healing and anti-oxidant activities of the fruit pulp of Limonia acidissima linn (Rutaceae) in rats," *Tropical Journal of Pharmaceutical Research*, vol. 9, no. 3, pp. 223–230, 2010.

[29] D. C. Odimegwu, E. C. Ibezim, C. O. Esimone, C. S. Nworu, and F. B. C. Okoye, "Wound healing and antibacterial activities of the extract of Dissotis theifolia (Melastomataceae) stem formulated in a simple ointment base," *Journal of Medicinal Plants Research*, vol. 2, no. 1, pp. 11–16, 2008.

[30] Z.-Q. Lin, T. Kondo, Y. Ishida, T. Takayasu, and N. Mukaida, "Essential involvement of IL-6 in the skin wound-healing process as evidenced by delayed wound healing in IL-6-deficient mice," *Journal of Leukocyte Biology*, vol. 73, no. 6, pp. 713–721, 2003.

[31] A. Mekonnen, T. Sidamo, K. Asres, and E. Engidawork, "In vivo wound healing activity and phytochemical screening of the crude extract and various fractions of Kalanchoe petitiana A. Rich (Crassulaceae) leaves in mice," *Journal of Ethnopharmacology*, vol. 145, no. 2, pp. 638–646, 2013.

[32] S. Shailajan, S. Menon, S. Pednekar, and A. Singh, "Wound healing efficacy of *Jatyadi Taila*: *In vivo* evaluation in rat using excision wound model," *Journal of Ethnopharmacology*, vol. 138, no. 1, pp. 99–104, 2011.

[33] S. Sasidharan, R. Nilawatyi, R. Xavier, L. Y. Latha, and R. Amala, "Wound healing potential of Elaeis guineensis Jacq leaves in an infected albino rat model," *Molecules*, vol. 15, no. 5, pp. 3186–3199, 2010.

[34] J. S. Reddy, P. R. Rao, and M. S. Reddy, "Wound healing effects of *Heliotropium indicum*, *Plumbago zeylanicum* and *Acalypha indica* in rats," *Journal of Ethnopharmacology*, vol. 79, no. 2, pp. 249–251, 2002.

Hindawi Publishing Corporation
Evidence-Based Complementary and Alternative Medicine
Volume 2016, Article ID 1621894, 10 pages
http://dx.doi.org/10.1155/2016/1621894

Research Article

Preventive Effects of the Intestine Function Recovery Decoction, a Traditional Chinese Medicine, on Postoperative Intra-Abdominal Adhesion Formation in a Rat Model

Cancan Zhou,[1] Pengbo Jia,[2] Zhengdong Jiang,[1] Ke Chen,[1] Guanghui Wang,[3] Kang Wang,[3] Guangbing Wei,[3] and Xuqi Li[3]

[1]*Department of Hepatobiliary Surgery, The First Affiliated Hospital of Xi'an Jiaotong University, Xi'an, Shaanxi 710061, China*
[2]*Department of General Surgery, The First People's Hospital of Xianyang City, Xianyang, Shaanxi 712000, China*
[3]*Department of General Surgery, The First Affiliated Hospital of Xi'an Jiaotong University, Xi'an, Shaanxi 710061, China*

Correspondence should be addressed to Xuqi Li; lixuqi@163.com

Received 5 August 2016; Revised 18 November 2016; Accepted 5 December 2016

Academic Editor: Ipek Suntar

The intestine function recovery decoction (IFRD) is a traditional Chinese medicine that has been used for the treatment of adhesive intestinal obstruction. In this study, the preventative effects and probable mechanism of the IFRD were investigated in a rat model. We randomly assigned rats to five groups: normal, model, control, low dose IFRD, and high dose IFRD. In the animal model, the caecum wall and parietal peritoneum were abraded to induce intra-abdominal adhesion formation. Seven days after surgery, adhesion scores were assessed using a visual scoring system, and histopathological samples were examined. The levels of serum interleukin-6 (IL-6) and transforming growth factor beta-1 (TGF-β1) were analysed by an enzyme-linked immunosorbent assay (ELISA). The results showed that a high dose of IFRD reduced the grade of intra-abdominal adhesion in rats. Furthermore, the grades of inflammation, fibrosis, and neovascularization in the high dose IFRD group were significantly lower than those in the control group. The results indicate that the IFRD can prevent intra-abdominal adhesion formation in a rat model. These data suggest that the IFRD may be an effective antiadhesion agent.

1. Introduction

Intra-abdominal adhesions are a common complication that occurs in 90–95% of patients who undergo abdominal surgery [1, 2]. Intra-abdominal adhesion can cause abdominal and pelvic pain, adhesive intestinal obstruction, infertility, and other severe complications [3]. Approximately 10% of bowel obstructions caused by adhesions require surgery to release the adhesions, with resulting mortality rates of 5–20% [4]. Operative adhesiolysis results in increased surgical difficulty, prolonged operative duration, and increased risk of bleeding. The situation is even more complicated because approximately 30% of patients require reoperation for adhesion recurrence [5].

The recurrence rate of adhesive bowel obstruction after treatment using a surgical method is high. Without effective precautions, the recurrence rate is 12% within 41 months of the initial surgery. The risk of relapse is present even after 20 years [6]. Adhesive bowel obstruction causes endless pain in patients and places a considerable burden on already overtaxed healthcare systems [7]. To date, there is no effective method for preventing intra-abdominal adhesion [8]. Therefore, finding an effective agent or strategy to prevent intra-abdominal adhesion is critical [9].

In China and other parts of East Asia, traditional Chinese medicine (TCM) has been used to treat disease for thousands of years. TCM usually works by mixing different types of herbs, which are called formulas or "Fufang." As a complementary treatment, TCM may offer an option for prevention of intra-abdominal adhesion formation. According to TCM theory, intestine function recovery decoction (IFRD) has been used clinically with substantial benefits in treating adhesive intestinal obstruction. However, there is no in vivo experimental evidence showing this effect or likely

Table 1: Constituents of intestine function recovery decoction.

Chinese name	Latin name	Family	Plant part	Dry weight (g)
Dangshen	*Codonopsis pilosula* Franch.	Campanulaceae	Radix	15
Baizhu	*Atractylodes macrocephala* Koidz.	Asteraceae	Rhizoma	15
Taoren	*Prunus persica* Batsch	Rosaceae	Semen	10
Chishao	*Paeonia lactiflora* Pall.	Ranunculaceae	Radix	15
Zhiqiao	*Citrus aurantium* L.	Rutaceae	Fructus	12
Houpu	*Magnolia officinalis* Rehd. et Wils.	Magnoliaceae	Cortex	15
Muxiang	*Aucklandia lappa* Decne.	Asteraceae	Radix	15
Huomaren	*Cannabis sativa* L.	Moraceae	Fructus	30
Daihuang	*Rheum palmatum* L.	Polygonaceae	Radix and Rhizoma	20
Total				147

pharmacological mechanisms of adhesion prevention. In this study, we demonstrate the effects of the IFRD and explain a likely mechanism for intra-abdominal adhesion prevention in a rat model.

2. Materials and Methods

2.1. Preparation of the IFRD. The constituents of the IFRD are shown in Table 1. All of the TCM herbs were purchased from the pharmacy of the First Affiliated Hospital of Xi'an Jiaotong University. Each herb was identified and authenticated by the head of the department and herbal medicinal botanist. Per the Pharmacopoeia of China (version 2010), exact amounts of component herbs were weighed according to the classic percentages and mixed well. The mixture was soaked in distilled water for 30 min and then boiled in eight volumes of water (v/w) for 1 h in herb-extracting machine. This preparation followed the ancient method and was also identical to the clinical preparation. The supernatant was orally administered to the rats in the experiments. The concentration of the IFRD is expressed as the total dry weight of the crude herbs per millilitre in decoction.

2.2. Operation and Postoperative Intervention. Sprague–Dawley rats weighing 200–250 g were purchased from the Experimental Animal Centre of Xi'an Jiaotong University (SYXK2012-003). All the rats were fed at room temperature (22 ± 2°C). They were allowed to drink freely and were provided with standard rat chow. All the procedures were authorized by the Animal Ethics Committee of Xi'an Jiaotong University (XJTULAC2016-410). The animals were randomly divided into five groups: normal, model, control, low dose, and high dose IFRD groups. All the rats were anesthetized using methoxyflurane prior to surgery. The skin was shaved and sterilized using iodine solution. As previously described [10], a 2 to 3 cm incision was made. The caecum wall and corresponding parietal peritoneum were scrubbed with sterile gauze until punctate haemorrhage occurred. The area of the injured wall of the caecum was approximately 2-3 cm^2. After exposure to air for 5 min, the bowel loop was arranged and returned to its original position. In the normal group, the caecum wall and corresponding parietal peritoneum were not scrubbed.

Table 2: Steps of operation and postoperative intervention for each group.

Groups	Abdominal incision	Peritoneum abraded	Gastric infusion
Normal	Yes	No	No
Model	Yes	Yes	No
Control	Yes	Yes	10 mL/kg normal saline
Low dose IFRD	Yes	Yes	10 mL/kg IFRD (equivalent to 7.55 g of herbs/kg)
High dose IFRD	Yes	Yes	10 mL/kg IFRD (equivalent to 15.1 g of herbs/kg)

The IFRD was administered to the rats twice a day via gastric infusion from postoperative day 0 to day 7 with 10 mL/kg/day solution. In the high dose IFRD group, the dosage is equivalent to 15.1 g of crude herbs/kg/day, which was calculated from the body surface area and is generally used clinically for humans [11]. In the low dose IFRD group, the dosage per rat is 7.55 g of crude herb/kg/day, which is equal to approximately half of the human dose. For rats in the control group, normal saline was administered at the same volume for rats in the IFRD groups. Each rat was monitored for changes in body weight. Every step of the operation and the postoperative interventions for each group are shown in Table 2.

2.3. Assessment of Adhesion Grade. Seven days after the operation, all the rats were anesthetized, and the abdominal cavities were opened with U-like incisions. The intra-abdominal adhesion evaluation was performed by a single researcher blinded to the treatment data according to the standard adhesion grades by Nair et al. [12]. These standard grades are listed in Table 3.

2.4. Haematoxylin and Eosin (HE) Staining and Microscopic Histological Grading. The injured peritoneum and adhesion tissues were excised after assessment of the adhesion grade. Specimen fixation and section preparation were carried out

Table 3: The numerical scoring of adhesion described by Nair et al.

Grade	Criteria
0	No adhesion band is present
1	A single adhesion band forms between the viscera or between a viscus and the abdominal wall
2	Two bands form between the viscera or between the viscera and abdominal wall
3	More than two bands form between the viscera or between the viscera and abdominal wall, or the whole intestine forms a mass without adhering to the abdominal wall
4	The viscera have directly adhered to the abdominal wall, irrespective of the number of bands

and then HE staining was performed. The tissues were evaluated under a microscope as previously reported [13]. The evaluation standards were as follows: degree of inflammation (grade 0: absent or normal in number; grade 1: slight increase; grade 2: moderate infiltration; and grade 3: massive infiltration), fibrosis (grade 0: none; grade 1: slight; grade 2: moderate; and grade 3: dense), and neovascularization (grade 0: none; grade 1: 1-2 vessels; grade 2: 3–9 vessels; and grade 3: 10 or more vessels).

2.5. Immunohistochemistry. The samples were fixed with 4% paraformaldehyde and then embedded in paraffin. After cutting the paraffin-embedded samples into sections, immunohistochemical staining was performed. The expression level of α-SMA (sc-53015, 1 : 800 dilution; Santa Cruz Biotechnology, Dallas, TX, USA) was detected. An image signal acquisition and analysis system (Leica, Wetzlar, Germany) was used for image acquisition.

2.6. Enzyme-Linked Immunosorbent Assay (ELISA). Seven days after surgery, blood samples from the rats were obtained. After centrifugation at 3,000 rpm for 30 min, only the serum was retained and stored at −20°C. The serum levels of TNF-α and IL-6 were examined using the ELISA kit (R&D, Minneapolis, MN, USA) according to the manufacturer's recommendations.

2.7. Statistical Analysis. All the data are expressed as the mean ± standard error or the median. A one-way ANOVA was performed followed by the *LSD* method for multiple comparisons to compare differences between the groups. A Kruskal-Wallis analysis was applied for assessing the adhesion grades. A Mann–Whitney U analysis was used to compare intergroup differences. The statistical analysis was performed using SPSS software version 13.0. $P < 0.05$ was considered to be statistically significant.

3. Results

3.1. The IFRD Reduced the Macroscopic Grades of Intra-Abdominal Adhesion in Rat Models. None of the rats died and all completed the experiment. The grades of adhesion showed significant differences between the different groups. There was almost no adhesion in the normal group (Figure 1(a)), whereas the rats in the model group (Figure 1(b)) and in the control group (Figure 1(c)) demonstrated patchy adhesion that could not be separated; the adhesion appeared at the injured areas of the peritoneum and caecum surface as well as the omentum. In contrast, the adhesions in the animals of the low dose IFRD group appeared to be loose and easy to separate (Figure 1(d)). The rats in the high dose IFRD group showed slight adhesions or even no adhesions. After grading the adhesions, the five groups showed significant differences ($P < 0.05$) (Table 4 and Figure 1(e)). There was no obvious difference in the adhesion grades between the model group and the control group, excluding the possibility of gastric infusion with an equal volume of saline for adhesion prevention. Compared to the control group, we found that the IFRD, especially the high dose of IFRD, significantly reduced the grades of adhesion. Thus, the results showed that the IFRD was able to prevent intra-abdominal adhesion in rats.

3.2. The IFRD Inhibited Inflammation, Fibrosis, and Neovascularization in Rat Models. By assessing the HE staining of the adhesion and peritoneum wound tissue slices, the grades of inflammation, fibrosis, and neovascularization were observed (Figure 2). We found that compared with the normal group the grades of inflammation, fibrosis, and neovascularization in the model and control groups were improved. However, compared to the control group, the high dose IFRD group distinctly presented less inflammation, fibrosis, and neovascularization (Figure 3). There is a trend to reduce inflammation, fibrosis, or neovascularization in the low dose IFRD group compared with the control group. Therefore, the data indicate that the IFRD inhibited inflammation, fibrosis, and neovascularization in the progression of adhesion induced by abrasion.

3.3. The IFRD Inhibited α-SMA, an Activated Fibroblast Marker, in Adhesion Tissues in the Rat Model. To further study the degree of fibrosis of adhesion tissues in the rat model, immunohistochemical staining of α-SMA, an activated fibroblast marker, was performed. In the normal group, no positive staining in the intact peritoneum was observed. In the model and control groups, there were a large number of fusiform fibroblasts with positive brown staining in the thick adhesive tissue. However, in the high dose IFRD group, the expression of α-SMA in the injured peritoneum and/or adhesion tissues was remarkably decreased compared to the model and control groups (Figure 4).

3.4. The IFRD Suppressed the Blood Levels of TGF-β and IL-6 in the Rat Model. We used ELISA to analyse the levels of TGF-β1 and IL-6 in the serum. The results indicate that the serum levels of TGF-β (Figure 5(a)) and IL-6 (Figure 5(b)) were notably higher in the model and control groups than that in the normal group, suggesting that operative injury-induced adhesion formation was accompanied by significant inflammatory response. A high dose of IFRD can markedly inhibit the increase of TGF-β and IL-6 ($P < 0.05$).

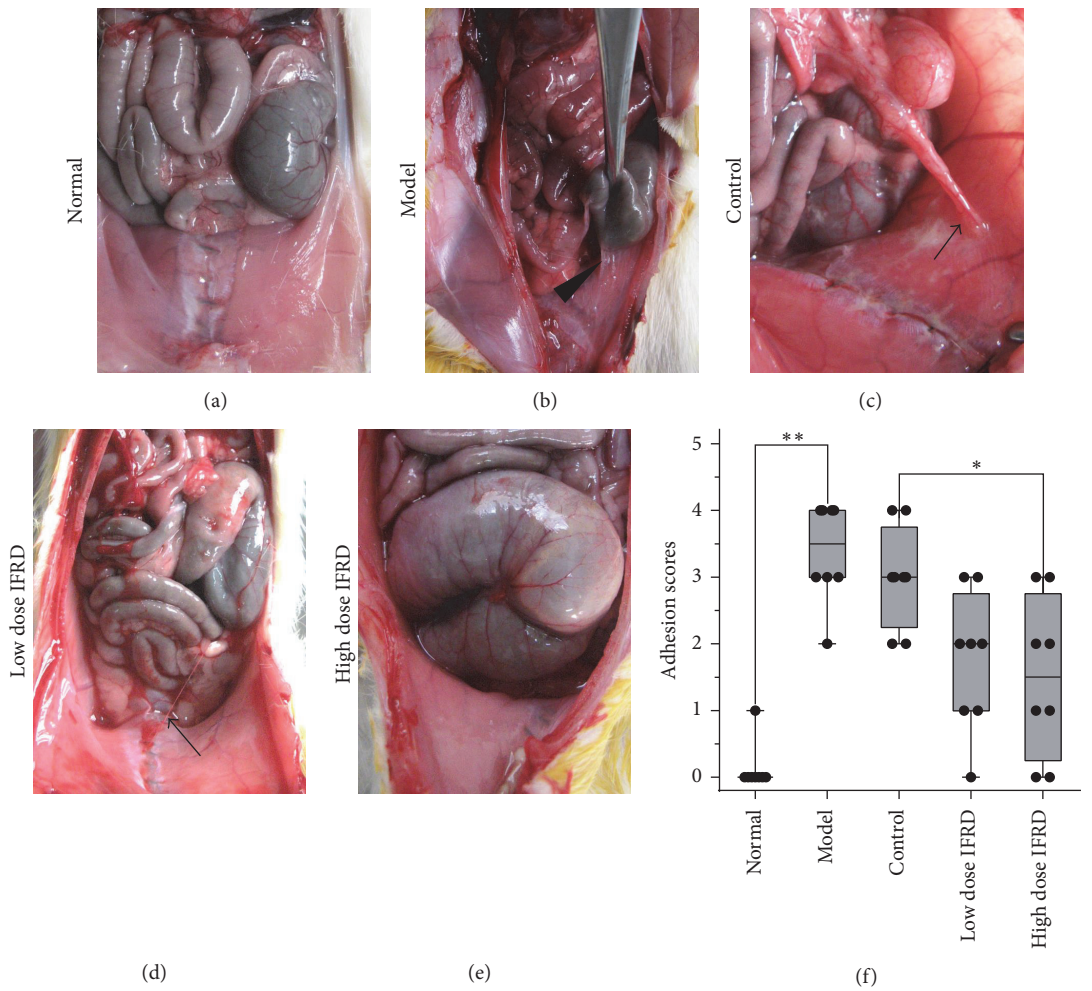

Figure 1: The intestine function recovery decoction (IFRD) prevented intra-abdominal adhesion formation in rats. (a) Normal group animals had intra-abdominal adhesions. (b) Model group animals developed a large number of extensive, thick adhesions, which were difficult to separate (black triangle). (c) Intra-abdominal adhesions occurred only slightly less in control group animals (black arrow). (d) The low dose IFRD group exhibited fewer intra-abdominal adhesions (black arrow) than the control group. (e) In the high dose IFRD group, some animals had no intra-abdominal adhesions. (f) Adhesion scores for the acroscopic classification ($n = 8$). The IFRD groups had the lowest scores of adhesions ($^{*}P < 0.05$; $^{**}P < 0.01$).

Table 4: Effect of IFRD on rat abdominal adhesions after operation.

Group	n	Adhesions degree classification					Mean ± SD	Median adhesion score
		0	1	2	3	4		
Normal	8	7	1	0	0	0	0.125 ± 0.331	0
Model	8	0	0	1	3	4	3.375 ± 0.696	3.5
Control	8	0	0	2	4	2	3 ± 0.707	3
Low dose IFRD	8	1	2	3	2	0	1.75 ± 0.968	2
High dose IFRD	8	2	2	2	2	0	1.5 ± 1.118	1.5
$P^{\#}$								<0.01

$^{\#}$*Kruskal-Wallis analysis.*

4. Discussion

Intra-abdominal adhesions are a common complication after abdominal and pelvic surgery [5]. Our study showed that the TCM IFRD could effectively prevent postoperative intra-abdominal adhesions in a rat model, likely resulting from the inhibition of inflammation, fibrosis, and neovascularization during adhesion formation.

An abdominal adhesion forms between two wound surfaces of the peritoneum. The formation of an adhesion depends on whether the deposited fibrous tissue is absorbed or undergoes organization [14]. The factors resulting in

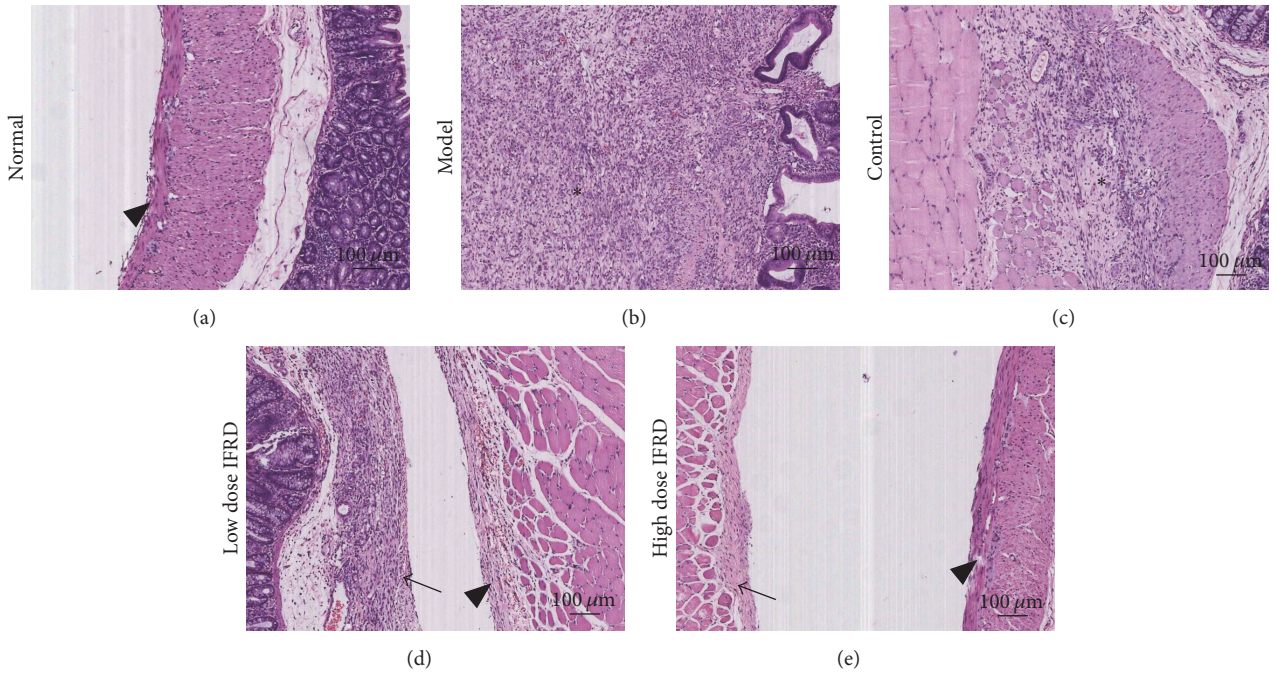

Figure 2: Representative images of HE staining in each group (100x). (a) Normal group; (b) model group; (c) control group; (d) low dose IFRD group; and (e) high dose IFRD group (∗ indicates the area of adhesion tissue; black triangle indicates visceral peritoneum; black arrow indicates parietal peritoneum).

adhesion formation include peritoneal mechanical trauma and peritoneal ischaemia caused by operation, traction, or residue from foreign matter, such as a suture. All these factors cause damage to the peritoneum and an inflammatory response. The cytokines released by inflammatory cells and oxidative stress are considered triggers and important initial events. The inflammatory reaction caused by peritoneal damage will produce fibrous exudation and deposition; meanwhile, the dissolving capacity of wound tissue will decrease. Ultimately, the deposition of extracellular matrix results in the formation of an adhesion [15, 16] Thus, the formation of an adhesion is a complex process caused by different cells, inflammatory mediators, and cytokines.

With the mechanism of adhesion formation elucidated, many preventative methods have emerged. Several barrier materials have been used clinically, including hyaluronic acid, carboxymethyl chitin, and oxidized regenerated cellulose, to prevent adhesion by separating the wounded tissues and promoting the repair of mesothelium cells [17–19]. Furthermore, researchers have attempted to prevent postoperative adhesion by inhibiting the inflammatory response [20], regulating fibrinolysis [21], and using antiangiogenesis [22] and antifibrosis [23] methods. However, verification of the value, effectiveness, and safety of these applications requires clinical trials and evidence-based medicine.

The IFRD consists of nine different herbs that have complex chemical components. According to the TCM theory [24, 25], the IFRD plays an important role in the special therapeutic method of "removing stasis by purgation and promoting blood circulation to remove blood stasis." The IFRD works effectively in treating severe abnormal infection and bowel motility dysfunction. In essence, the IFRD promotes tissue repair, decreases the inflammatory reaction and exudation, improves circulation in the intestine, and eventually improves intestinal functional recovery. Our study shows that the grades of intra-abdominal adhesion were reduced and the nonadhesion percentage was elevated in rats given the IFRD. Consequently, the IFRD may have an advantage in potentially preventing intra-abdominal adhesion.

Studies have demonstrated that inhibiting the inflammatory reaction can prevent intra-abdominal adhesion in animals [26, 27]. Thus, it may be effective in preventing adhesion by inhibiting the inflammatory reaction and cytokines induction caused by injury. In the IFRD, some constituents including Codonopsis Radix (Dangshen) [28], Atractylodes Rhizoma (Baizhu) [29], and Paeoniae Rubra Radix (Chishao) [30] were reported to have anti-inflammatory and antioxidative effects. Jia and He [31] indicated that paeoniflorin, a chemical constituent of Paeoniae Rubra Radix, ameliorated disease in rat models of rheumatoid arthritis by suppressing oxidative stress and inflammation and reducing COX-2 protein expression. Wei et al. [32] and other researchers [20, 33] have provided evidence that hypoxia-induced COX-2 expression in peritoneal fibroblasts is involved in the formation of intra-abdominal adhesions. In the current study, the grade of inflammation in the IFRD group was lower than that in the control group, which demonstrates that the IFRD possesses potent anti-inflammatory properties.

Cytokines such as IL-6 and TGF-β are of vital importance during the formation of adhesions. IL-6 is a key cytokine for regulating the proliferation of epithelial cells and promoting the deposition of inflammatory cells and fibrosis at damage

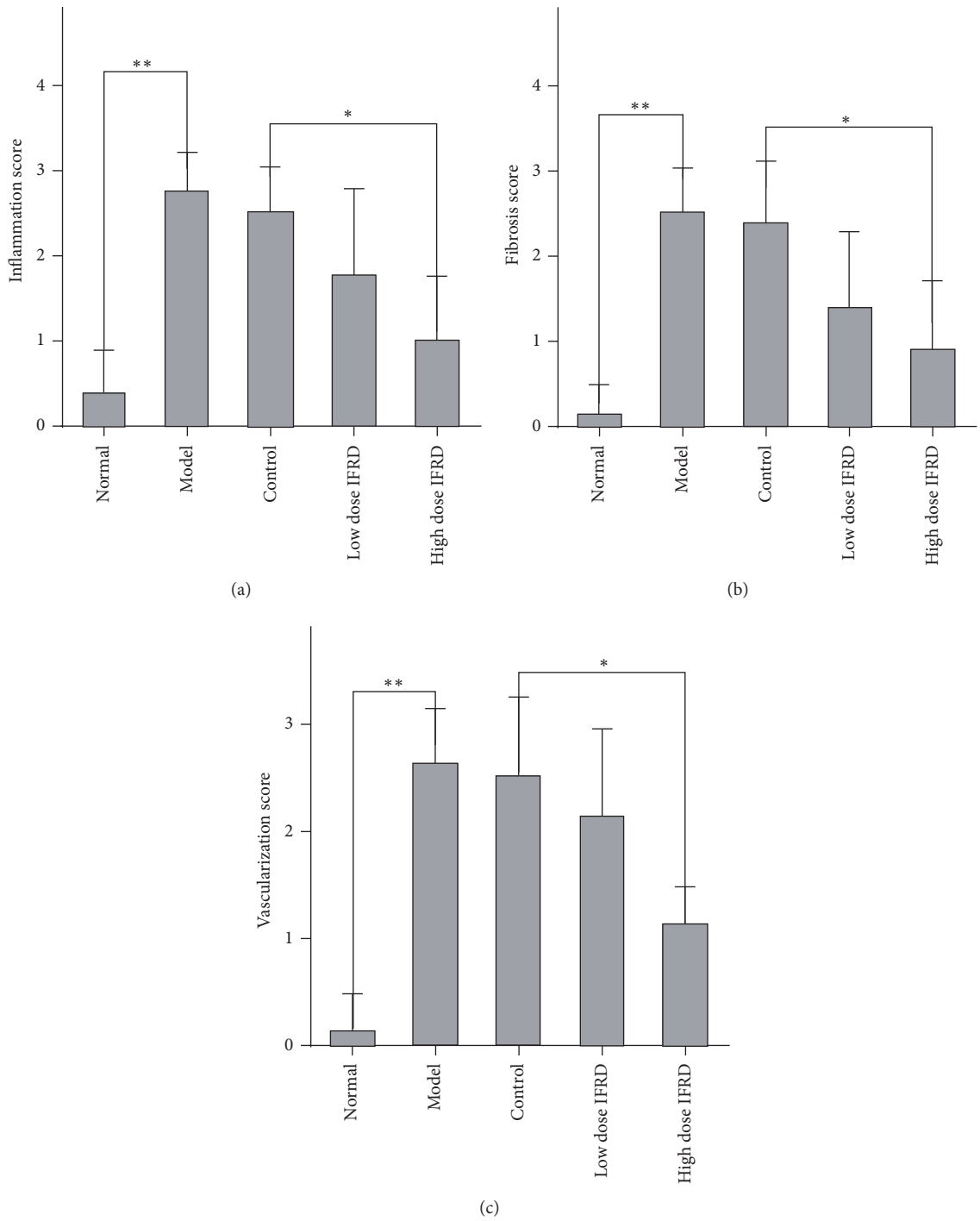

Figure 3: Inflammation, fibrosis, and neovascularization scores for each group ($^{*}P < 0.05$; $^{**}P < 0.01$). (a) Inflammation scores, (b) fibrosis scores, and (c) neovascularization scores are shown.

sites [34]. TGF-β promotes peritoneal mesothelial cells to increase the synthesis of plasminogen activator inhibitor-1 by regulating the activity of various cytokines [35] and accelerates the migration and proliferation of adhesion fibroblasts [23]. The expression levels of IL-6 and TGF-β positively regulate the formation of adhesions. Our present study suggests that the preventative effects of the IFRD on intra-abdominal adhesion formation are involved in inhibition of inflammatory cytokines IL-6 and TGF-β release.

Because the overexpression of cytokines induced by inflammation correlates with hyperplasia of fibrous connective tissue, the IFRD may work by inhibiting the expression of cytokines and decreasing hyperplasia of fibrous connective tissue. Fibroblast cells are crucial for ECM deposition; once

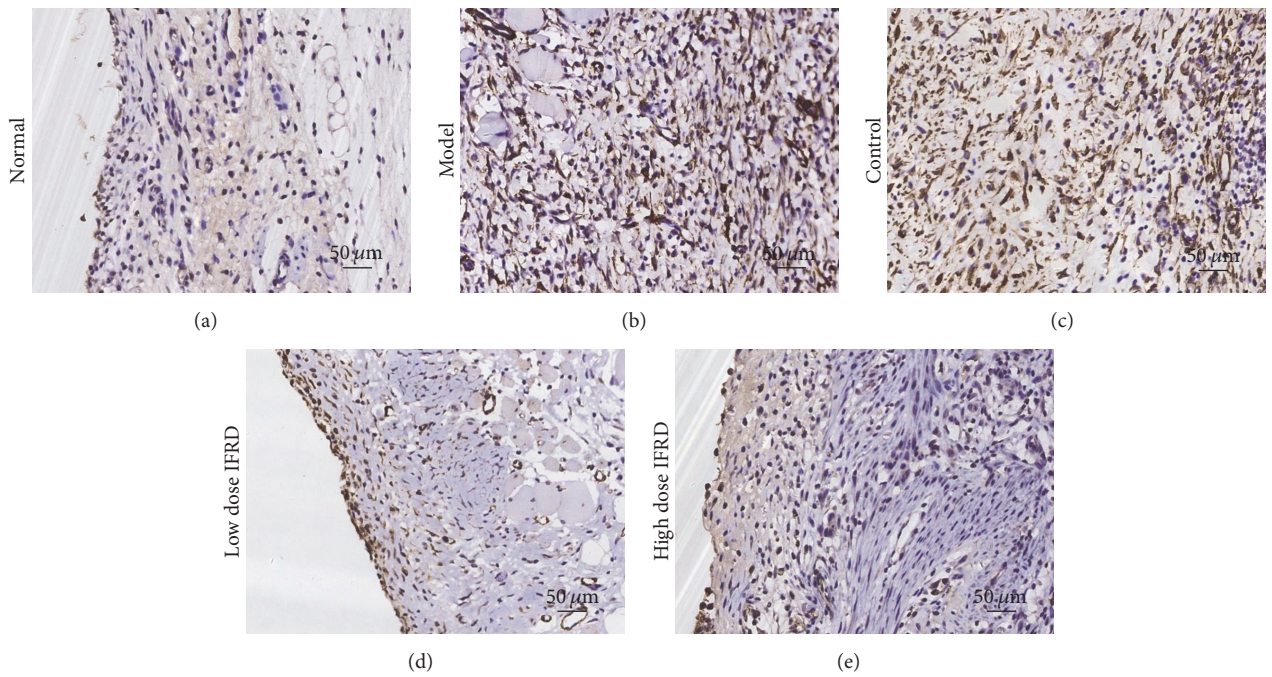

Figure 4: Immunohistochemical analysis of α-SMA in intra-abdominal adhesion tissues from all groups (200x). (a) Normal group; (b) model group; (c) control group; (d) low dose IFRD group; and (e) high dose IFRD group.

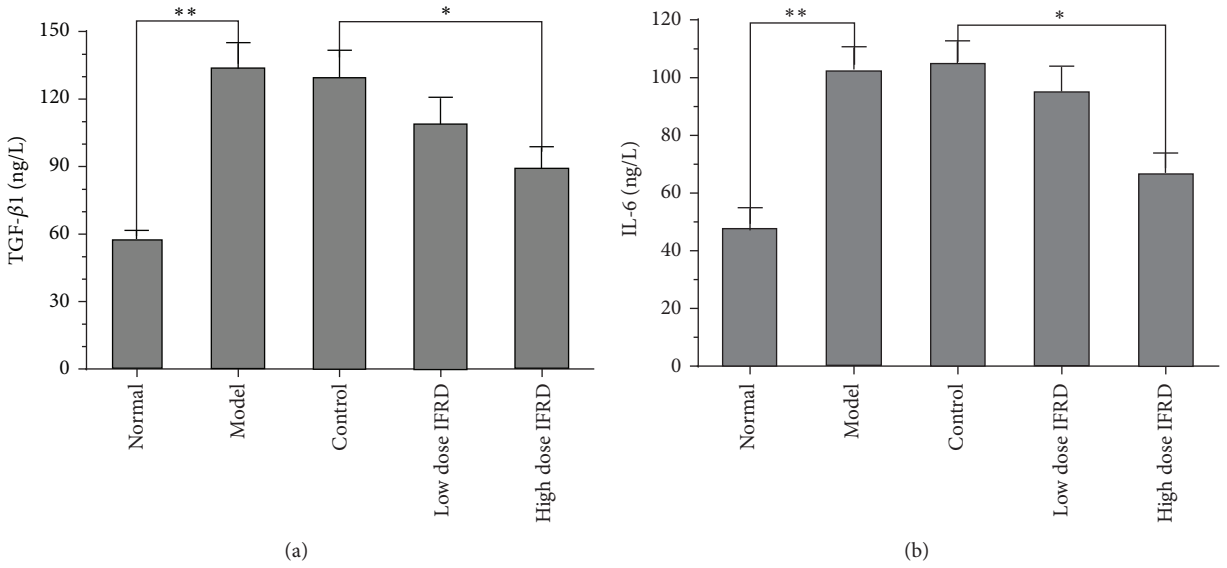

Figure 5: Effects of the IFRD on the serum levels of TGF-β1 (a) and IL-6 (b) ($^{*}P < 0.05$; $^{**}P < 0.01$).

activated, they differentiate into myofibroblasts that express α-SMA [30]. A hallmark of myofibroblast activation, α-SMA, is typically used to assess the level of fibrosis [36], and positive staining of α-SMA reveals the development of fibrosis. In our results, the observation of decreased fibrosis grades and α-SMA expression in the IFRD group demonstrated that the IFRD notably inhibited fibrosis and activated fibroblasts in adhesion formation.

Operative injury damages the balance between the production and degradation of fibrous protein while inducing the deposition of ECM, which forms the foundation of the adhesion. Persicae Semen (Taoren) in the IFRD is a representative herb for invigorating blood circulation and eliminating stasis; after thousands of years of clinical application and observation in China, its therapeutic effects are indeed certain, and its pharmacoactivity is defined [37]. Persicae Semen (Taoren) significantly decreased fibrinogen content, prolonged thrombin time and thromboplastin time, and increased prothrombin time in an animal model [38]. Therefore, the mechanism of action of the IFRD for adhesion

prevention may be related to activating the fibrinolytic system and decreasing the deposition of fibrous protein.

An intra-abdominal adhesion may have restricted motility in the slow postoperative recovery of intestinal function caused by injury from the abdominal operation and anesthetization [39]. Inhibition of postoperative intestinal motility by inhibitors of gastrointestinal motility can result in increased numbers of adhesions. Therefore, the possibility of preventing postoperative adhesions by promoting gastrointestinal transit has been suggested [40]. Bove and Chapelle [41] have shown that visceral massage immediately following surgery interfered with postoperative adhesion formation by promoting normal peristaltic movements in a rat model. Some components of the IFRD have important effects on improving the peristalsis and movement of gastrointestinal smooth muscle. Rhei Radix et Rhizoma (Daihuang), Aucklandiae Radix (Muxiang), and Cannabis Fructus (Huomaren) have been used extensively for treating gastrointestinal motor dysfunction [42, 43]. Emodin, an anthraquinone derivative of Rhei Radix et Rhizoma (Daihuang), has also been reported to possess an anti-inflammatory effect [44]. Furthermore, Aurantii Fructus (Zhiqiao) and Magnoliae Officinalis Cortex (Houpu) used together can synergistically increase gut motor function by involving muscarinic receptors and secondarily alpha-receptors [45]. Therefore, the IFRD is applied to promote the recovery of dynamic intestinal function and shorten the contact time with impaired peritoneum lining, thus preventing intra-abdominal adhesion in rats.

The present study has some limitations that should be noted and further explored to elucidate precise mechanisms. Further studies are required. In a future study, we will try to elucidate these mechanisms and identify which constituents or pure compounds serve as active ingredients for adhesion prevention in the IFRD.

5. Conclusion

Our study found that the IFRD effectively prevented the formation of adhesions by decreasing inflammatory infiltration of the injured peritoneum and by reducing collagen deposition and fibrosis (Figure 6). This study demonstrated the wide-ranging potential value of the IFRD, a traditional Chinese medicine, in preventing postoperative adhesions, which could improve patient quality of life.

Competing Interests

The authors declare that there is no conflict of interests related to this work.

Acknowledgments

This study was supported by the National Natural Science Foundation of China (no. 81572734), the Scientific and Technological Development Research Project Foundation by Shaanxi Province (2016SF-121), and the Fundamental Research Funds for the Central Universities in Xi'an Jiaotong University (no. 2013jdhz33).

Figure 6: Preventative effects of the intestine function recovery decoction, a traditional Chinese medicine, on postoperative intra-abdominal adhesion formation in a rat model. The outermost circle illustrates the nine traditional Chinese medicinal (TCM) herbs, which are components of the intestine function recovery decoction (IFRD). The second circle shows that the IFRD possesses two types of TCM pharmacology, namely, "removing stasis by purgation" and "promoting blood circulation to remove blood stasis." The third circle illustrates four types of underlying pharmacological action of the IFRD for preventing adhesive formation, including anti-inflammation, antifibrosis, profibrinolysis, and prointestinal motility. The kernel shows that the IFRD can effectively prevent adhesive formation independent of complementary TCM.

References

[1] R. T. Beyene, S. L. Kavalukas, and A. Barbul, "Intra-abdominal adhesions: anatomy, physiology, pathophysiology, and treatment," *Current Problems in Surgery*, vol. 52, no. 7, pp. 271–319, 2015.

[2] A. Barbul, "In brief. Abdominal adhesions," *Current Problems in Surgery*, vol. 52, no. 7, pp. 266–269, 2015.

[3] W. Arung, M. Meurisse, and O. Detry, "Pathophysiology and prevention of postoperative peritoneal adhesions," *World Journal of Gastroenterology*, vol. 17, no. 41, pp. 4545–4553, 2011.

[4] K. Okabayashi, H. Ashrafian, E. Zacharakis et al., "Adhesions after abdominal surgery: a systematic review of the incidence, distribution and severity," *Surgery Today*, vol. 44, no. 3, pp. 405–420, 2014.

[5] J.-J. Duron, N. J.-D. Silva, S. T. Du Montcel et al., "Adhesive postoperative small bowel obstruction: incidence and risk factors of recurrence after surgical treatment: a multicenter prospective study," *Annals of Surgery*, vol. 244, no. 5, pp. 750–757, 2006.

[6] B.-T. S. Fevang, J. Fevang, S. A. Lie, O. Søreide, K. Svanes, and A. Viste, "Long-term prognosis after operation for adhesive small bowel obstruction," *Annals of Surgery*, vol. 240, no. 2, pp. 193–201, 2004.

[7] R. P. G. ten Broek, Y. Issa, E. J. P. van Santbrink et al., "Burden of adhesions in abdominal and pelvic surgery: systematic review and met-analysis," *British Medical Journal*, vol. 347, no. 7929, Article ID f5588, 2013.

[8] J. M. Becker and A. F. Stucchi, "Intra-abdominal adhesion prevention: are we getting any closer?" *Annals of Surgery*, vol. 240, no. 2, pp. 202–204, 2004.

[9] W. B. Robb and C. Mariette, "Strategies in the prevention of the formation of postoperative adhesions in digestive surgery: a systematic review of the literature," *Diseases of the Colon and Rectum*, vol. 57, no. 10, pp. 1228–1240, 2014.

[10] C. C. Peyton, T. Keys, S. Tomblyn et al., "Halofuginone infused keratin hydrogel attenuates adhesions in a rodent cecal abrasion model," *Journal of Surgical Research*, vol. 178, no. 2, pp. 545–552, 2012.

[11] S. Reagan-Shaw, M. Nihal, and N. Ahmad, "Dose translation from animal to human studies revisited," *FASEB Journal*, vol. 22, no. 3, pp. 659–661, 2008.

[12] S. K. Nair, I. K. Bhat, and A. L. Aurora, "Role of proteolytic enzyme in the prevention of postoperative intraperitoneal adhesions," *Archives of Surgery*, vol. 108, no. 6, pp. 849–853, 1974.

[13] A. Sahbaz, O. Aynioglu, H. Isik, B. D. Gun, O. Cengil, and O. Erol, "Pycnogenol prevents peritoneal adhesions," *Archives of Gynecology and Obstetrics*, vol. 292, no. 6, pp. 1279–1284, 2015.

[14] N. Chegini, "Peritoneal molecular environment, adhesion formation and clinical implication," *Frontiers in Bioscience*, vol. 7, pp. e91–e115, 2002.

[15] G. S. DiZerega and J. D. Campeau, "Peritoneal repair and post-surgical adhesion formation," *Human Reproduction Update*, vol. 7, no. 6, pp. 547–555, 2001.

[16] Y. C. Cheong, S. M. Laird, T. C. Li, J. B. Shelton, W. L. Ledger, and I. D. Cooke, "Peritoneal healing and adhesion formation/reformation," *Human Reproduction Update*, vol. 7, no. 6, pp. 556–566, 2001.

[17] U. S. Ha, J. S. Koh, K. J. Cho et al., "Hyaluronic acid-carboxymethylcellulose reduced postoperative bowel adhesions following laparoscopic urologic pelvic surgery: a prospective, randomized, controlled, single-blind study," *BMC Urology*, vol. 16, no. 1, article 28, 2016.

[18] X. Wu, J. Hu, D. Fan et al., "Safety and efficacy of sodium hyaluronate gel and chitosan in preventing postoperative peristomal adhesions after defunctioning enterostomy: a prospective randomized controlled trials," *Medicine (United States)*, vol. 94, no. 51, article no. e2354, 2015.

[19] G. Wei, C. Zhou, G. Wang, L. Fan, K. Wang, and X. Li, "Keratinocyte growth factor combined with a sodium hyaluronate gel inhibits postoperative intra-abdominal adhesions," *International Journal of Molecular Sciences*, vol. 17, no. 10, 2016.

[20] Y. I. Kim, "Comparative study for preventive effects of intra-abdominal adhesion using cyclo-oxygenase-2 enzyme (COX-2) inhibitor, low molecular weight heparin (LMWH), and synthetic barrier," *Yonsei Medical Journal*, vol. 54, no. 6, pp. 1491–1497, 2013.

[21] P. Dinarvand, S. M. Hassanian, H. Weiler, and A. R. Rezaie, "Intraperitoneal administration of activated protein C prevents postsurgical adhesion band formation," *Blood*, vol. 125, no. 8, pp. 1339–1348, 2015.

[22] S. Kim, S. Lee, A. K. Greene et al., "Inhibition of intra-abdominal adhesion formation with the angiogenesis inhibitor sunitinib," *Journal of Surgical Research*, vol. 149, no. 1, pp. 115–119, 2008.

[23] L. Deng, Q. Li, G. Lin et al., "P-glycoprotein mediates postoperative peritoneal adhesion formation by enhancing phosphorylation of the chloride channel-3," *Theranostics*, vol. 6, no. 2, pp. 204–218, 2016.

[24] R. Teschke, A. Wolff, C. Frenzel, A. Eickhoff, and J. Schulze, "Herbal traditional Chinese medicine and its evidence base in gastrointestinal disorders," *World Journal of Gastroenterology*, vol. 21, no. 15, pp. 4466–4490, 2015.

[25] K.-J. Chen, "Blood stasis syndrome and its treatment with activating blood circulation to remove blood stasis therapy," *Chinese Journal of Integrative Medicine*, vol. 18, no. 12, pp. 891–896, 2012.

[26] T. Dalgic, E. Oymaci, E. B. Bostanci et al., "Effects of carbon dioxide pneumoperitoneum on postoperative adhesion formation and oxidative stress in a rat cecal abrasion model," *International Journal of Surgery*, vol. 21, pp. 57–62, 2015.

[27] G. Wei, X. Chen, G. Wang, L. Fan, K. Wang, and X. Li, "Effect of resveratrol on the prevention of intra-abdominal adhesion formation in a rat model," *Cellular Physiology and Biochemistry*, vol. 39, no. 1, pp. 33–46, 2016.

[28] J. Y.-W. Chan, F.-C. Lam, P.-C. Leung, C.-T. Che, and K.-P. Fung, "Antihyperglycemic and antioxidative effects of a herbal formulation of Radix Astragali, Radix Codonopsis and Cortex Lycii in a mouse model of type 2 diabetes mellitus," *Phytotherapy Research*, vol. 23, no. 5, pp. 658–665, 2009.

[29] S. Ahmed, C. Zhan, Y. Yang et al., "The transcript profile of a traditional chinese medicine, *Atractylodes lancea*, revealing its sesquiterpenoid biosynthesis of the major active components," *PLOS ONE*, vol. 11, no. 3, Article ID e0151975, 2016.

[30] Y. Ji, Y. Dou, Q. Zhao et al., "Paeoniflorin suppresses TGF-β mediated epithelial-mesenchymal transition in pulmonary fibrosis through a Smad-dependent pathway," *Acta Pharmacologica Sinica*, vol. 37, no. 6, pp. 794–804, 2016.

[31] Z. Jia and J. He, "Paeoniflorin ameliorates rheumatoid arthritis in rat models through oxidative stress, inflammation and cyclooxygenase 2," *Experimental and Therapeutic Medicine*, vol. 11, no. 2, pp. 655–659, 2016.

[32] G. Wei, X. Chen, G. Wang et al., "Inhibition of cyclooxygenase-2 prevents intra-abdominal adhesions by decreasing activity of peritoneal fibroblasts," *Drug Design, Development and Therapy*, vol. 9, pp. 3083–3098, 2015.

[33] A. K. Greene, I. P. J. Alwayn, V. Nose et al., "Prevention of intra-abdominal adhesions using the antiangiogenic COX-2 inhibitor celecoxib," *Annals of Surgery*, vol. 242, no. 1, pp. 140–146, 2005.

[34] D. R. Ambler, N. M. Fletcher, M. P. Diamond, and G. M. Saed, "Effects of hypoxia on the expression of inflammatory markers IL-6 and TNF-a in human normal peritoneal and adhesion fibroblasts," *Systems Biology in Reproductive Medicine*, vol. 58, no. 6, pp. 324–329, 2012.

[35] G. Wang, K. Wu, W. Li et al., "Role of IL-17 and TGF-β in peritoneal adhesion formation after surgical trauma," *Wound Repair and Regeneration*, vol. 22, no. 5, pp. 631–639, 2014.

[36] M. Kitamura, T. Nishino, Y. Obata et al., "The kampo medicine Daikenchuto inhibits peritoneal fibrosis in mice," *Biological & Pharmaceutical Bulletin*, vol. 38, no. 2, pp. 193–200, 2015.

[37] S. Xi, L. Qian, H. Tong et al., "Toxicity and clinical reasonable application of Taoren (*Semen Persicae*) based on ancient and modern literature research," *Journal of Traditional Chinese Medicine*, vol. 33, no. 2, pp. 272–279, 2013.

[38] L. Liu, J.-A. Duan, Y. Tang et al., "Taoren-Honghua herb pair and its main components promoting blood circulation through

influencing on hemorheology, plasma coagulation and platelet aggregation," *Journal of Ethnopharmacology*, vol. 139, no. 2, pp. 381–387, 2012.

[39] D. M. Scott-Coombes, M. N. Vipond, and J. N. Thompson, "Small bowel transit time in patients with intra-abdominal adhesions," *The British Journal of Surgery*, vol. 79, no. 10, p. 1076, 1992.

[40] F. Fu, Y. Hou, W. Jiang, R. Wang, and K. Liu, "Escin: inhibiting inflammation and promoting gastrointestinal transit to attenuate formation of postoperative adhesions," *World Journal of Surgery*, vol. 29, no. 12, pp. 1614–1622, 2005.

[41] G. M. Bove and S. L. Chapelle, "Visceral mobilization can lyse and prevent peritoneal adhesions in a rat model," *Journal of Bodywork and Movement Therapies*, vol. 16, no. 1, pp. 76–82, 2012.

[42] H. Guo, J. Zhang, W. Gao, Z. Qu, and C. Liu, "Gastrointestinal effect of methanol extract of Radix Aucklandiae and selected active substances on the transit activity of rat isolated intestinal strips," *Pharmaceutical Biology*, vol. 52, no. 9, pp. 1141–1149, 2014.

[43] R. L. Whiting and A. C. Ford, "Efficacy of traditional chinese medicine in functional constipation," *The American Journal of Gastroenterology*, vol. 106, no. 5, pp. 1003–1004, 2011.

[44] M. Xiao, T. Zhu, W. Zhang et al., "Emodin ameliorates LPS-induced acute lung injury, involving the inactivation of NF-κB in mice," *International Journal of Molecular Sciences*, vol. 15, no. 11, pp. 19355–19368, 2014.

[45] X. Xiong, W. Peng, L. Chen et al., "Traditional Chinese medicine Zhiqiao-Houpu herb-pair induce bidirectional effects on gastric motility in rats," *Journal of Ethnopharmacology*, vol. 175, pp. 444–450, 2015.

Hindawi Publishing Corporation
Evidence-Based Complementary and Alternative Medicine
Volume 2016, Article ID 7965689, 12 pages
http://dx.doi.org/10.1155/2016/7965689

Research Article

Evaluation of Wound Healing Properties of Grape Seed, Sesame, and Fenugreek Oils

Dorsaf Moalla Rekik,[1] Sameh Ben Khedir,[2] Kamilia Ksouda Moalla,[1] Naziha Grati Kammoun,[3] Tarek Rebai,[2] and Zouheir Sahnoun[1]

[1]*Laboratory of Pharmacology, Faculty of Medicine of Sfax, University of Sfax, Sfax, Tunisia*
[2]*Laboratories of Histology and Embryology, Faculty of Medicine of Sfax, University of Sfax, Sfax, Tunisia*
[3]*Olivier Institute, BP 1087, 3000 Sfax, Tunisia*

Correspondence should be addressed to Dorsaf Moalla Rekik; rmdorsaf@gmail.com

Received 18 August 2016; Accepted 4 October 2016

Academic Editor: Lutfun Nahar

Background. Medicinal plants have proved at all times to be a powerful remedy for health care. Accordingly, grape seed, sesame, and fenugreek extracted oils with pharmacological properties are investigated as wound treatments. This study assesses the potential of our oils for healing wounds induced on rats. *Methods*. Phytochemical analyses of oils have involved: quality value, polyphenol, chlorophylls, carotene, and fatty acids. Antibacterial activity was carried out. Antioxidant activity was evaluated: the scavenging effect on DPPH radicals, the reducing power, and β-carotene discoloration. Uniform wound excision was induced on rats dorsum randomly divided into five groups: groups treated with "*CICAFLORA®*" and tested oils and untreated one. The posthealing biopsies were histologically assessed. *Results*. Wound biopsies treated with oils showed the best tissue regeneration compared to control groups. Groups treated with our oils and "*CICAFLORA*" had higher wound contraction percentage. Polyunsaturated fatty acids in oils act as inflammatory mediators increasing neovascularization, extracellular remodeling, migration, and cell differentiation. Wound healing effect was attributed to antibacterial and antioxidant synergy. *Conclusion*. According to findings, oils showed better activity in wound healing compared to "*CICAFLORA*" due to a phytoconstituents synergy. However, clinical trials on humans are necessary to confirm efficacy on human pathology.

1. Background

Wounds regardless of their types and causes are common diseases that constitute a major problem of public health at the global level and mainly in countries in the process of development. However, despite the impressive progress in modern medicine, drugs dispensed to treat the skin represent 3% of the intended ones and are not yet really effective.

Various medicinal plants, mainly their oils, have always been used to treat different kinds of wounds. The literature presents various herbal formulations and natural extracts with several phytochemical compounds (vitamins, phenols, sterols, etc.), in healing plants for the application of wound care. A whole list of those medicinal plants are traditionally used in folk medicine, including our three selected plants, grape seed, fenugreek, and sesame, which are investigated in this study in order to explore their phytochemical compositions, to evaluate their wound healing effect and to better explain the mechanism on wound healing.

Trigonella foenum graecum L. (Fenugreek) is an annual herb that belongs to the *Fabaceae* family, commonly used in oriental countries as a spice in food preparations. The seeds are reported to have nutritive and restorative properties and can stimulate digestive processes [1]; moreover, they are used as a traditional remedy for the treatment of diabetes [2].

Sesamum indicum L. (Sesame) is a pioneer cultivated self-pollinating annual plant, originating from Africa, belonging to the *Pedaliaceae* family. Sesame takes an important role in human nutrition and the seeds are essentially used for the production of oil.

The fruit is a micronized and oblong capsule containing numerous seeds [3]. This oilseed has numerous nutritional

[4], ethnobotanical, pharmaceutical, and medical applications. In fact, it is laxative, emollient, and demulcent [5]. This urges us to further explore this oilseed and focus our concern on dermal repair, stressing our research on wound healing in particular.

Vitis vinifera L. (grapes) belongs to the *Vitaceae* family. Grapes have been a traditional treatment in Europe for thousands of years. The grape seed oil is rich in unsaturated fatty acids, especially linoleic acid [6] which constitutes a considerable proportion of the seed.

Wound healing, the significant concern in pathology like in postsurgeries, burns, and scars, is a dynamic and complex process that involves biochemical and physiological phenomena from inflammation to proliferation to remodeling, behaving in a harmonious way to ensure tissue repair [7]. During the inflammatory phase, this process is hampered by the production of a high level of free radicals. If not controlled by the antioxidative capacity of the host, the inhibition of both the cell migration and the proliferation takes place, which can damage the surrounding, wound tissue [8]. So, the present study evaluates the wound healing effect of three medicinal plants previously referred to (the fenugreek seed oil, the sesame seed oil, and the grape seed oil) via the exploration of phytochemical composition and the different parameters of antibacterial and antioxidant activities to explain the crucial mechanism of wound healing.

2. Methods

2.1. Plant Material and Reagents

2.1.1. Reagents. The (DPPH) 1,1-diphenyl-2-picrylhydrazyl was purchased from Sigma Chemical Co. (St. Louis, MO, USA). Butylated-hydroxytoluen (BHT) and all the other chemicals were of analytical grade.

For the evaluation of the wound healing, "*CICAFLORA*" was used as a reference product. It consists in an emulsion oil-water that contains *Mimosa* as a main active component and is marketed in a cream form.

2.1.2. Materials. The analysis of the methyl esters of fatty acids was made by chromatography in gas phase (C.P.G) by means of a UNICAM 610 chromatograph, equipped with a detector (FID) allowing the detection of compounds, a column (15 m in length and 0.22 mm in diameter) lined with a film (0.25 μm thick) of a polar phase (50% cyanopropylmethyl and 50% phenylmethyl-polysiloxane), and an injector divisor. The detector was at a temperature of 250°C, the column at 180°C, and the injector at 220°C. The quantity of injected oil was 0.2 μL.

2.2. Analytical Methods

2.2.1. Phytochemical Analysis

(1) Quality Value and Fatty Acids

(i) Peroxide Value. The peroxide value of any oil is an important indicator of primary oxidation level according to ISO 3960/2001 method. The index of peroxide of a fatty acid is the number of milliequivalents of active oxygen contents in 1 kg of the product and oxidizing the iodine of potassium with the liberation of iodine and titration of this one by the thiosulfate of sodium.

(ii) Acidity Value. The acidity value indicates the content of free fatty acids present in the tested oils, expressed in oleic acid. It represents an important quality parameter for the commercial classification of the product according to ISO 660/2003 method. 5 g of oil was dissolved in 30 mL of equal volumes of ethanol/ether (1/1) neutralized. The free carboxylic functions were measured by a solution of potassium hydroxide in the presence of 1% phenolphthalein. The end of the experience is marked by the appearance of a pink color.

(iii) The Saponification Value. The saponification value is an indirect measure that allows classifying the oil according to the length of fatty acid chains; the criterion was bound to the molecular weight of fatty acids. This measure can turn out useful because this value gives an idea about the quality of oils according to ISO 3657/2002 method. The value of saponification represents the quantity in milligrams of necessary potassium hydroxide to transform the free fatty acids and the glycerides contained in 1 g of fat into soap and is determined by mixing a volume of oil with potassium hydroxide and titrated with hydrochloric acid.

(iv) Specific Extinction Coefficient at 232 nm and 270 nm. The determination of the UV-specific extinction values gives an approximation of the oxidation process in unsaturated oils [9] according to COI/T.20/Doc (No 19/Rev.2 of November 2008) method. 0.25 g of the oil was dissolved in 25 mL of cyclohexane. The absorbance of the solution of fatty oil was measured by UV/visible spectrophotometer at specific wave length of 270 nm. The extinction at 270 nm of a raw fat can give an idea about the level of secondary oxidation.

(v) Free Fatty Acid Percentage. The free fatty acid method, COI/T.20/Doc (No 34, November 2015), determines the free fatty acids in oils by chromatography in gas phase. The content of free fatty acids is expressed in acidity, calculated as the percentage of oleic acid. It consists in diluting 0.2 g of extracted oil in 3 mL hexane and 0.3 mL of methanolic potassium hydroxide. The reactive mixture is shaken in a hanging whirlpool for 2 min and then spin-dried. Thus, the upper phase contains the esters of fatty acids dissolved in the hexane and the lower phase is trained by the fraction of glycerin and the minor constituents of the blank oil.

(2) Quantification of Polyphenols. The content of total phenols of the various samples is determined according to the method described by Tsai et al. [10]. In this method Folin-Ciocalteu reagent was added to the test oil. After agitation, a solution of washing soda is added. After 2 h of incubation, the absorbance is measured at 760 nm.

(3) Chlorophylls and Carotene. The contents of chlorophylls pigments and carotenoids in oils were calculated after the reading of the optical densities at 670 nm and 470 nm using

coefficients of extinction for carotene and total chlorophylls [11].

2.2.2. Antioxidant Activities

(1) DPPH Free Radical-Scavenging Assay. This assay has been used to investigate the scavenging activity of antioxidant compounds. In fact, DPPH is a stable free radical that can be reduced by a proton-donating substrate like an antioxidant, causing the discoloration of DPPH and reduction of the absorbance at 517 nm.

The DPPH free radical-scavenging potential of the three studied oils was determined according to the reports of Bersuder et al. [12]. Radical-scavenging activity was expressed as the inhibition percentage and was calculated using the equation of DPPH radical scavenging activity.

$$\text{DPPH radical-scavenging activity (\%)} = \frac{A_{\text{control}} - A_{\text{sample}}}{A_{\text{control}}} \times 100. \quad (1)$$

A_{control} is the absorbance of the control reaction and A_{sample} is the absorbance of oils/standard BHT samples. The IC50 value (mg sample/mL) is the effective concentration at which the DPPH radicals are scavenged by 50%. The test was carried out in duplicate.

(2) Ferric Reducing Antioxidant Power FRAP. The ability of the oils (0.06 mg/mL to 1 mg/mL) to reduce iron (III) was determined according to the method of Yildirim et al. [13]. The IC50 value (mg sample/mL) is the effective concentration at which the absorbance is 0.5 for the reducing power. BHT is used for comparison and all data values are the mean of duplicate analysis.

(3) β-Carotene Bleaching Assay. This spectrophotometric technique in the ultraviolet ray was developed by Marco [14] and then slightly modified by Miller [15]. It consists in a measurement at 470 nm. The discoloration of β-carotene results from an oxidation by the linoleic acid.

2.2.3. Antibacterial Activity

(1) Microbial Strains. The antimicrobial activity of the studied oils was evaluated using a range of laboratory control stains: two Gram-positive bacteria: *Bacillus subtilis* (JN 934392) and *Staphylococcus aureus* (ATCC 6538); two Gram-negative bacteria: *Escherichia coli* (ATCC 25922) and *Salmonella enteritidis* (ATCC 43972).

(2) Determination of Antibacterial Activity by the Disc Diffusion Method. The oils were tested for antibacterial activity by the method of disc diffusion according to the National Committee for Clinical Laboratory Standards (NCCLS, 2001) using suspension of the tested microorganisms. Mueller-Hinton agar (MHA), sterilized in a flask and cooled, was distributed to sterilized Petri dishes. The filter paper discs (6 mm in diameter) were individually impregnated with oil and then placed onto the agar plates which had previously been inoculated with the tested microorganisms. The Petri dishes were kept at 4°C for 2 h. The plates were inoculated with the bacteria and incubated at 37°C for 24 h. The diameters of all the inhibition zones were measured in millimeters. All the tests were performed in duplicate.

(3) Determinations of the Minimum Inhibitory Concentration (MIC) and Minimum Bactericidal Concentration (MBC). The microdilution method was used to investigate the minimum inhibitory concentration (MIC) and the minimum bactericidal concentration (MBC) according to the National Committee for Clinical Laboratory Standards (NCCLS, 2001). All tests were performed in Mueller Hinton Broth (MHB). The oils were dissolved in 20% dimethylsulfoxide (DMSO) and then diluted from the highest concentration to the lowest one. A serial doubling dilution of the oils was prepared in a 96-well plate. Overnight broth cultures of each strain were prepared. Petri dishes were kept at 4°C for 2 h. Then, bacteria were incubated at 37°C for 24 h. The microbial growth was determined by absorbance at 600 nm using the universal microplate reader [16]. To evaluate MBC, broth from each well was taken and inoculated in Mueller Hinton Agar (MHA) at 37°C for 48 h for the bacteria.

(4) MBC/MIC Ratio. The MBC/MIC ratio [17] can give a clear idea about the effect of oils under study on bacteria. Indeed, if the ratio is higher than 4, the oil is said to be bacteriostatic and if the oil is endowed with a bactericide effect, the ratio is lower than 4.

2.2.4. Wound Healing Activity Test

(1) Experimental Animals. Thirty Wistar male rats weighing 175 ± 3.98 g were used for the experiment. They were randomly housed in clean polyethylene cages individually under controlled conditions of 22–25°C, 60–70% relative humidity, and 12 hours of dark-light cycle with free access to water and food. Procedures and animal comfort were controlled by the International Guidelines for Animal Care.

(2) Circular Excision Wound Model. After anesthesia with ketamine (100 mg/kg body weight) by intramuscular injection, a full thickness of elliptic area of approximately 200 mm^2 wound was induced on the shaved rats' dorsal interscapular region [18]. The day on which wound was created was considered as day 0 and all the wounds were covered with a gauze dressing and were treated until they completely healed.

(3) Excision Wounds Treatment. The rats were divided into five groups consisting of six rats each. Group number (I) was untreated and served as a control (the wounds were just cleaned with a physiologic saline). Group (II) was treated with fenugreek oil, group (III) with sesame oil, and group (IV) with grape seed oil and served as the test groups, while group (V) was treated with "*CICAFLORA*" cream and served as a standard reference (positive control).

After rinsing the wounds with the physiologic saline, the test samples (fenugreek oil, grape seed oil, and sesame oil) and the "*CICAFLORA*" cream were applied, in a fine

Table 1: Values of phytochemical tests.

Oils	Phytochemical test				
	Acidity value	UV constants		Peroxide value	Saponification value
	%	K_{232}	K_{270}	Meq O_2/Kg	$170 < x < 255$
Grape seed	1.83	3.0113	2.1710	12	175.32
Sesame	0.4	3.0103	1.1547	0.9	173.91
Fenugreek	0.2	3.0079	0.4373	11	172.32

layer covering all over the surface of the wound, every two days until the wound completely healed. So, the treatment was stopped when the wounds of any first group completely healed; then the rats were sacrificed and the granulation tissues were excised from animals. A part of wet tissue was fixed in formalin at 10% (v/v), embedded in paraffin, and presented for histological observation.

(4) Wound Healing Evaluation Parameters. To evaluate the process of wound healing for the 5 study groups, we relied on two clinical macroscopic criteria including the qualitative (color of wound) and the quantitative criteria (wound closure rate) and one microscopic criterion (histological evaluation).

(5) Chromatic Study. Superficial wounds tend to lighten from red to pale pink and become more homogeneous and more consistent in texture when they heal. The chromatic evaluation of the healing process was done through photography of wounds. This study consists of coding the wound of each rat: bright red for blood that covers the wound, dark red for coagulated blood in epidermis, red for granulation tissue, and finally pink for epithelialization phase [19].

(6) Rate of Wound Closure and Epithelialization Time. The rate of closure of each individual wound from both controls and the treated groups was used as an indicator of wound healing. A wound margin was traced after the wound incision using transparent paper and then the area was measured through the Mayrovitz rule [20]. Wound contraction was measured on the 3rd, 5th, 7th, 9th, and 10th days until complete wound healing and expressed in percentage of healed area. Wound contraction, the percentage of reduction of the original wound size, was calculated using the following expression:

$$\text{Wound closure}\,(\%) = \frac{(A_T - A_D)}{A_T} \times 100. \quad (2)$$

The initial wound area on day 0 and the wound area on all the following days are represented as A_T and A_D, respectively.

The epithelization period was considered as the number of required days to fall of scab without any residual raw wound [21].

(7) Histological Examination. All of the skin samples were fixed in 10% neutral buffered formalin. Following the fixation, 3 μm sections of paraffin were perpendicularly made to the surface of skin including the whole thickness of skin. Serial sections were stained with hematoxylin-eosin (HE) [22] to show the morphology of tissues: organization, epithelial proliferation and granuloma tissue formation, collagenisation, newly capillaries formed, and scar formation in dermis.

The studied criteria in histopathological sections consisted in the reepithelialization, cornification of the epithelium, fibroblast, and collagen contents. Furthermore, histological biopsies examined for advanced tissue regeneration were characterized by the presence of well-organized stratum of both epidermis and derma.

2.2.5. Statistical Analysis. Statistical analyses were performed using SPSS version 17 (SPSS Inc., Chicago, Il, USA).

Student test was applied to compare weights averages before and after treatment between oil-treated groups and both negative and positive control groups to detect ascertain significant differences. Nonparametric tests, Kruskal Wallis test, and Mann Whitney test were used to compare different groups. Raw data were shown with median IQR for each group. Differences were considered to be statistically significant at $p < 0.05$.

3. Results

3.1. Phytochemical Analysis

3.1.1. Quality Value and Fatty Acids. Table 1 presents the values of acidity, specific extinction coefficient, peroxide, and the saponification.

Table 2 shows a different percentage of polyunsatured acids especially oleic, linoleic, and linolenic acids that reach together 89.37%, 82.5%, and 84.28%, respectively, for grape seed oil, sesame oil, and fenugreek oil.

3.1.2. Quantitative Polyphenols, Chlorophylls, and Carotene. The quantitative dosage of total phenolic compounds of oils shows high values for oils, but grape seed oil and fenugreek oil have a higher level of chlorophylls (8.078 ppm) and carotene (56.78 ppm) (Table 3).

3.2. Antioxidant Activities

3.2.1. DPPH Free Radical-Scavenging Assay. The antioxidizing efficiency increases with the concentration of the oil (Figure 1). The three oils seem to have a potential antioxidant activity compared to the BHT activity. The percentages of inhibition are 68.12%, 84.59%, and 84.6% for grape seed oil, sesame oil, and fenugreek oil, respectively, and 54.6% for BHT at a concentration of 1 mg/g.

Table 2: Fatty acids components.

Oil	Fatty acid				
	C16:0 Palmitic acid%	C18:0 Stearic acid%	C18:1 Oleic acid% (Ω9)	C18:2 Linoleic acid% (Ω6)	C18:3 α-Linolenic acid% (Ω3)
Grape seed	6.69	3.57	19.75	69.33	0.29
Sesame	10.44	3.18	40.19	41.94	0.37
Fenugreek	8.36	3.60	19.19	37.71	27.38

Table 3: Polyphenols, chlorophylls, and carotene values.

Oils	Polyphenols (ppm)	Chlorophylls (ppm)	Carotene (ppm)
Grape seed	191.1	8.078	15.24
Sesame	191.3	0.005	3.98
Fenugreek	210.3	0.229	56.78

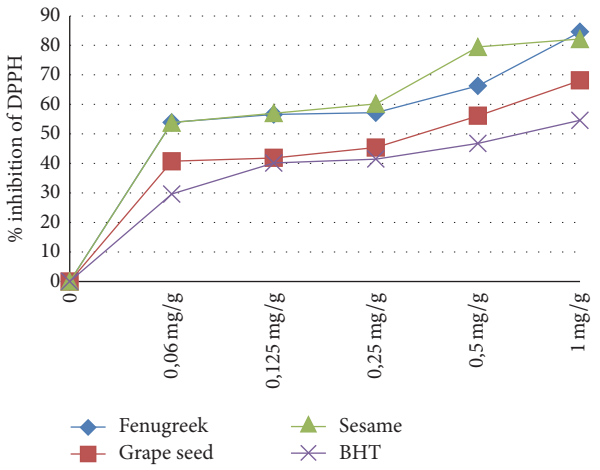

Figure 1: Activity of DPPH free radical scavenging.

3.2.2. Ferric Reducing Antioxidant Power FRAP. Figure 2 illustrates the reducing capacity of oils on iron III.

3.2.3. β-Carotene Bleaching Assay. Figure 3 demonstrates the β-carotene bleaching assays results.

3.3. Antibacterial Activity

3.3.1. Diameter of Inhibition Zone. The antimicrobial activity of oils tested on different bacteria gram(+) and gram(−) was presented in Table 4.

3.3.2. Determination of Minimum Inhibitory and Bactericidal Concentrations (MIC and MBC µg/mL MH). Table 5 points to the concentrations of MIC and MBC.

3.3.3. Ratio = MBC/MIC. This ratio was used in order to verify the antimicrobial potential of oils, and the ratio MBC/MIC is required (Table 6).

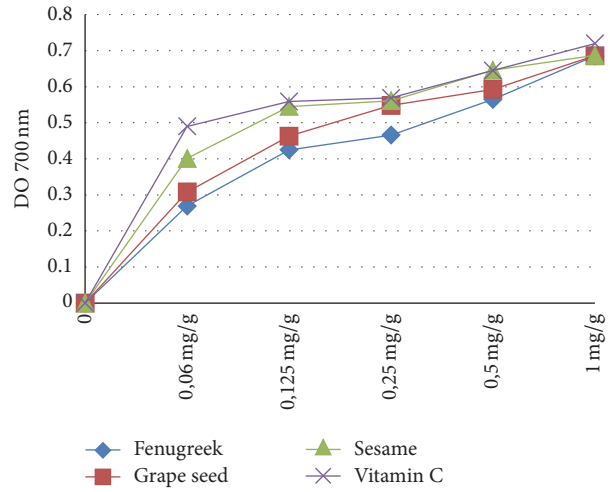

Figure 2: Ferric reducing power assay.

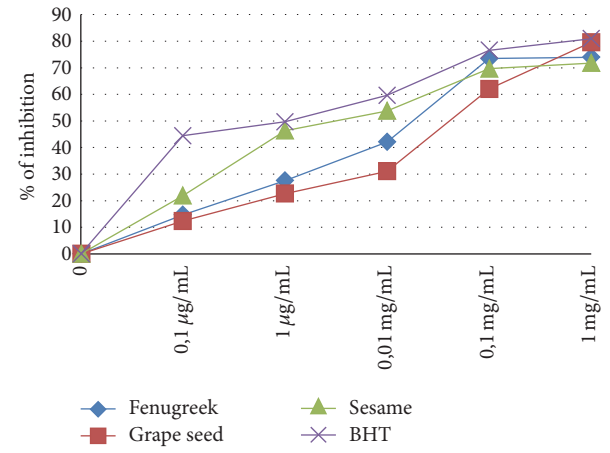

Figure 3: Activity of inhibition of bleaching of β-carotene.

3.4. Wound Healing Activity Test. The wound healing process was carried out by a chromatic study on the basis of the progressive changes in wound color during the different phases of cicatrization for each group: fenugreek oil, grape seed oil, sesame oil, "*CICAFLORA*," and physiologic serum.

3.4.1. Wound Healing Evaluation Parameters. Weights of Wistar rats were illustrated in Table 7. The statistical comparison of their average weight for the same group before and after treatment was not significant ($p < 0.05$).

Table 4: Diameter of inhibition zone (mm).

Oils	Stains			
	Gram(+)		Gram(−)	
	Bacillus subtilis JN 934392	*Staphylococcus aureus* ATCC 6538	*Escherichia coli* ATCC 25922	*Salmonella enteritidis* ATCC 43972
Grape seed	17 ± 1.0	—	11 ± 1.0	11 ± 1.0
Sesame	12 ± 0.5	—	—	—
Fenugreek	10 ± 1.0	—	—	—

Table 5: Concentration of bacteria (μg/mL MH).

Oils	Stains							
	Gram(+)				Gram(−)			
	Bacillus subtilis JN 934392		*Staphylococcus aureus* ATCC 6538		*Escherichia coli* ATCC 25922		*Salmonella enteritidis* ATCC 43972	
	MIC	MBC	MIC	MBC	MIC	MBC	MIC	MBC
Grape seed	6.25	12.5	—		6.25	12.5	6.25	12.5
Sesame	6.25	25	—		—		—	
Fenugreek	3.125	25	—		—		—	

MIC: minimal inhibitory concentration, MBC: minimal bactericide concentration.

Table 6: Bactericide effect of tested oils.

Oils	Stains			
	Gram(+)		Gram(−)	
	Bacillus subtilis JN 934392	*Staphylococcus aureus* ATCC 6538	*Escherichia coli* ATCC 25922	*Salmonella enteritidis* ATCC 43972
Grape seed	Bactericide	—	Bactericide	Bactericide
Sesame	Bacteriostatic	—	—	—
Fenugreek	Bacteriostatic	—	—	—

Table 7: Average weights before and after treatment with controls and oils.

Day	Average weight, untreated (g)	Average weight, CICAFLORA (g)	Average weight, grape seed oil (g)	Average weight, fenugreek (g)	Average weight, sesame (g)
Before treatment	182,5 ± 2.271	184.5 ± 2,271	176.5 ± 2.121	193,5 ± 2,121	172,33 ± 2,926
After treatment	183 ± 2.265	184.33 ± 2.559	176 ± 2.212	193 ± 2.265	171 ± 2.849
p value	0.25	0.085	0.25	0.25	0.66

Student's t-test was applied to detect and ascertain significant differences.

3.4.2. Chromatic Study. Wound photography of the same group rats was illustrated in Figure 4. The chosen days (0/3/5/7/9 and 10) were corresponding to the wound induction day, inflammatory phase, granulation tissue formation, and reepithelialization, respectively.

The chromatic study of the wounds showed a similar coloration during the first three days. In fact, the bright red coloration observed on the wounding day reflected the color of the blood covering the underlying muscles after excision of the skin. This coloration became dark red on the second day which gave evidence of the formation of a blood clot. This clot enabled the blood coagulation. From the 3rd day, the blood clot was converted to a scab which retracted in the treated rats.

Towards the 7th day, the scabs allowed the apparition of a red coloration that corresponded to the tissue granulation with spread sides of the wound for the rats of the control group (untreated group).

From the 10th day, these scabs in rats treated with oils and reference product began to fall to let a pinkish color appear that characterized an epithelialization ending after 11 days. The wound contracting ability of the oils and "*CICAFLORA*" was more significant than those of the control groups. The rate of wound closure by fenugreek oil, sesame oil, grape seed oil, and CICAFLORA and in the control group is illustrated in Table 8 and Figure 5. Their rates of wound closure at 11th day were, respectively, 99.84%, 99.83%, 99.84%, 94.82%, and 86.05%.

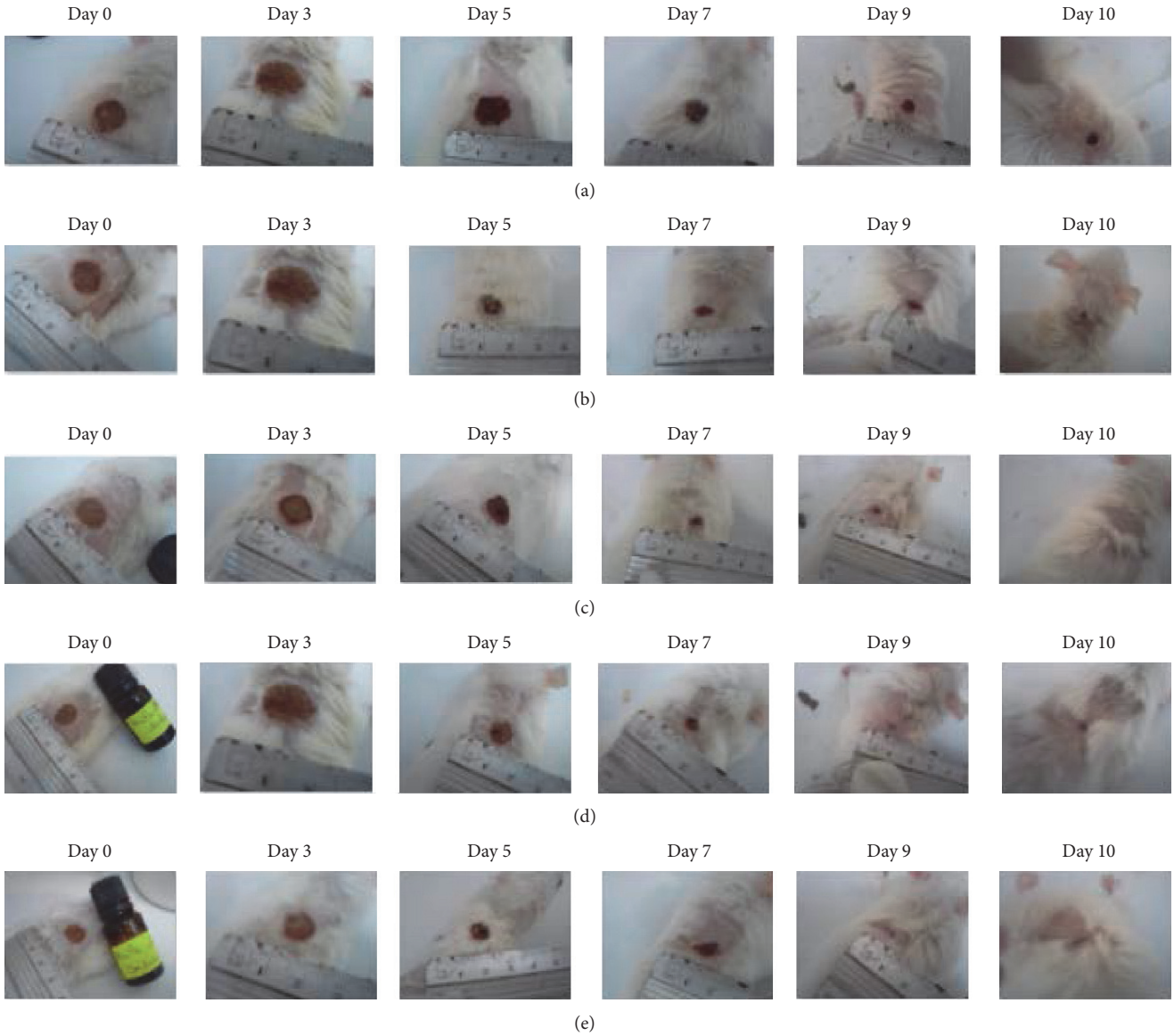

Figure 4: Visual observation of the wound healing experiment on days 0, 3, 5, 7, 9, and 10. (a) Untreated group, (b) group treated with "CICAFLORA," (c) group treated with grape seed oil, (d) group treated with sesame oil, and (e) group treated with fenugreek oil.

3.4.3. Histological Examination. Epidermal regeneration covering over the wound surface treated by the fenugreek, grape seed, and sesame oils was colored by the hematoxylin-eosin to investigate the epithelium and tissue organization (Figure 6).

We noticed fibroconnective tissue regeneration in the reference biopsies and those of the three tested oils, without hairy adnexal or glandular structures. However, this tissue regeneration was lower in the biopsies of control rats. The microscopic examination of the scar zones handled by various oils highlighted an epidermic complete regeneration and well organized, which was considered normal. Also, the thickness of the epithelium was more important for the grape seed oil, sesame oil, and fenugreek oil than "*CICAFLORA*" cream.

4. Discussion

Various plants, essentially their oils, have been used to treat wounds. The literature presents several phytochemical constituents, various herbal formulations, and natural extracts from medicinal plants to the application for wound care. Some of those medicinal plants are traditionally used in folk medicine, including our plants, grape, fenugreek, and sesame, which are investigated in this study in order to explore their phytochemical compositions, to evaluate their wound healing effect, and to better understand their mechanism on wound healing. Consequently, topical application of the tested oils and the cicatrizing reference drug seems to accelerate the healing of wounds and the contraction of the skin borders to a

Table 8: Statistical study: median IQR and nonparametric tests.

	1	3	5	7	9	11
Grape seed	1.29 (1.12–1.38)	0.90 (0.84–1.12) (b*)	0.56 (0.56–0.60) (b**)	0.18 (0.15–0.18) (a**, b**)	0.04 (0.02–0.06) (a**, b**)	0.002 (0.002–0.003) (a**, b**)
Fenugreek	1.38 (1.17–1.38)	0.94 (0.84–0.97) (a*, b**)	0.42 (0.42–0.43) (a**, b**)	0.18 (0.18–0.21) (a**, b**)	0.08 (0.04–0.09) (a**, b**)	0.003 (0.001–0.003) (a**, b**)
Sesame	1.29 (1.03–1.31)	0.94 (0.94–1.12) (b*)	0.56 (0.56–0.84) (b*)	0.18 (0.16–0.21) (a**, b**)	0.05 (0.023–0.094) (a**, b**)	0.002 (0.001–0.003) (a**, b**)
CICAFLORA	1.17 (1.00–1.50)	1.03 (0.96–1.12)	0.77 (0.56–0.77) (b*)	0.38 (0.37–0.41) (b*)	0.18 (0.17–0.19) (b**)	0.06 (0.06–0.07) (b**)
Untreated	1.17 (1.15–1.41)	1.22 (0.99–1.38)	0.91 (0.81–0.96)	0.50 (0.38–0.50)	0.32 (0.27–0.32)	0.21 (0.11–0.21)

Nonparametric tests: Kruskal Wallis and Mann Whitney tests. Raw data shown with median IQR ($n = 6$) for each group.
* $p < 0.05$, ** $p < 0.001$. a: compared to CICAFLORA; b: compared to untreated.

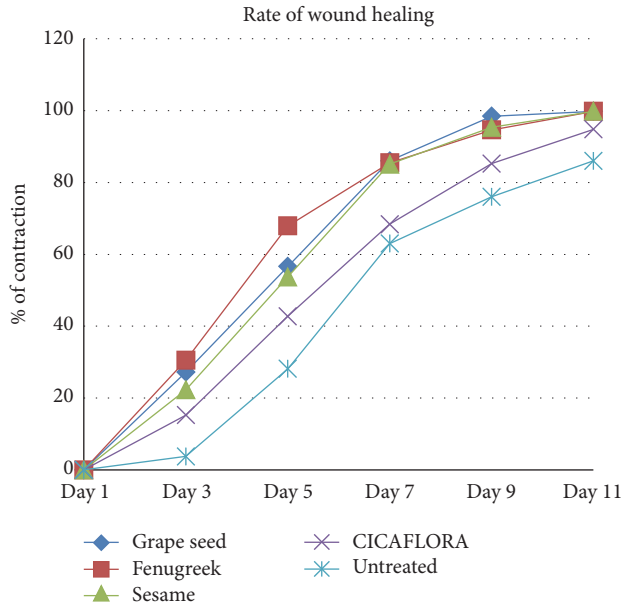

Figure 5: Rate of wound closure.

fast recovery compared to the control. The best healing activity would be attributed to their physicochemical properties, antioxidant, and antibacterial activities.

So, oil acidity is the result of the degree of triacylglycerol distribution due to a lipolysis reaction, in which free fatty acids are formed. The acidity measured in the oil samples was low in the order of 0.2% for the fenugreek oil, 0.4% for the sesame oil, and 1.83% for the grape seed oil. All the studied oils were of acidic pH that promoted the inhibition capacity of bacteria growth and accelerated the wound healing process [23].

Peroxidation is a beginning to fat autoxidation, which is an inevitably slow phenomenon. The manipulation of oils and the manner of storage can reduce autooxidation effects. According to common regulations, the peroxide values of extra virgin olive oil must be under 20 Meq O_2/kg [24], which concords with the results of the three oils. Those low peroxide values indicate that the tested oils were newly harvested and extracted and then stored in good conditions, suggesting that they kept a good quality over this work. The specific UV absorbance values at 232 nm, a primary oxidation indicator of oils, were 3.01 and the K_{270} values were lower. According to common standards, the UV absorbance at 232 nm for extra virgin olive oil must be under 2.5 [25]. These findings were concordant with the previous peroxide values. Both parameters, reflecting the degree of the oil autooxidation, can increase with the age of oils and their exposure to sunlight or high temperatures.

Tested oils contain a significant amount of unsaturated fatty acids that reach 89.37%, 82.5%, and 84.28% for grape seed oil, sesame oil, and fenugreek oil, respectively. The high level of polyunsaturated fatty acids can make it extremely susceptible to oxidation [26]. However, the oils were very stable due to the presence of a number of antioxidants like polyphenols, carotene, and chlorophylls. The antioxidants described in the present study can explain the lower values of the autooxidation parameters. In fact, several researches reported that many vegetable oils were an important natural source of carotenoids such as *Pistacia lentiscus* that presented a value ranging between 5.8 and 10.57 mg/kg oil [27], but our studied oils have substantially higher amounts especially in fenugreek and sesame oils 56.78 mg/kg and 15.24 mg/kg, respectively. Carotenoids are the most important source of vitamin A.

The autooxidation is the major cause of the deterioration of oil during the storage. It depends on several factors as the initial composition of the oil and the presence in minor compounds with pro- or antioxidizing activities like chlorophylls [28]. In our study, grape seed oil presented the highest value (8.078 mg/kg).

The autooxidation distorts edible oils by degradation of the essential fatty acids and consequently the reduction in the nutritional value and the formation of products of decomposition [29, 30]. The phenolic compounds in the three oils (197.56 ± 11.2 mg/kg), due to their antioxidizing activity, can contribute to the preservation of the quality of this one [31]. DPPH is a stable free radical which is reduced in the presence of an antioxidant, mostly by the phenolic compounds [32]. Indeed, the chemical structure of polyphenols enables them to trap this free radical by hydrogen transfer. Our results demonstrated that our tested oils reacted strongly against the DPPH radicals. This finding would be related to high

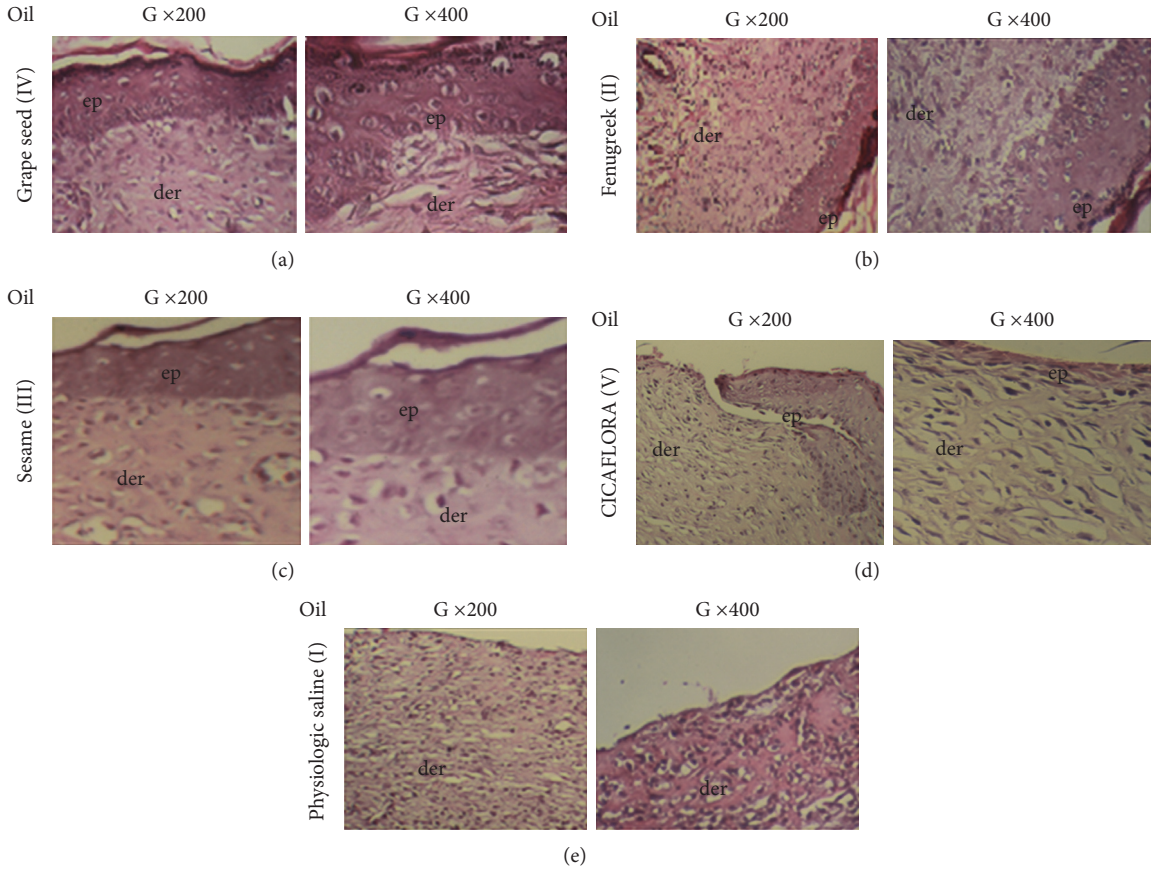

Figure 6: Histological investigation of treated and untreated biopsies: epidermal (ep) and dermal (der) architecture of wounds after the 11th day. (a) Group treated with grape seed oil, (b) group treated with fenugreek oil, (c) group treated with sesame oil, (d) group treated with "CICAFLORA," and (e) untreated group (Gr200 and Gr400).

concentrations of polyphenols in oils and explain their relative stability and lower autooxidation.

Other antioxidants in our studied oils described in literature can also contribute to their stability and to the wound healing phenomenon such as vitamin E and sterols [33].

Our study showed a total closure of the wounds treated by the oils and "*CICAFLORA*" after 11 days with an advanced tissue regeneration characterized by the presence of well-organized stratum of derma and epidermis in comparison with those of the control biopsies whose tissue neoformation was incomplete. According to literature, the natural contraction of wounds takes place by the 21st day [34]. This finding underlines the capacity of studied oils to accelerate the proliferation contributing to a fast recovery. The same healing period was also observed with two medicinal plant oils: *Cucurbita pepo. L* (Cucurbitaceae) and *Linum usitatissimum* (Linaceae) [35].

The chromatic study of the wounds showed a similar coloration during the first three days corresponding to the formation of a blood clot with debris of cell filling the breach in the course of the initial inflammatory phase. So, fibrin, once stabilized in blood clot, is a key element in the initial process of skin healing. It allows the recruitment of fibroblasts by chemotactic effect and stimulates the production of collagen [36]. When inflammatory cells arrive at the site of injury, they initiate a prolonged inflammatory phase that results in delayed deposition of matrix components, wound remodeling, and closure [37].

From the 3rd day, a proliferative phase has been triggered and characterized by the formation of granulation tissue, including angiogenesis, the migration of fibroblasts, and collagen synthesis [38]. In our study, from the 3rd day, the blood clot was converted to a scab which retracted in the treated rats. But an inflammatory reaction, manifested by an edema and oozing on wounds, seems more important in the rats of the control groups than those of all the three treated ones. Towards the 7th day, the scabs allowed the apparition of a red coloration that corresponded to the tissue granulation with spread sides of the wound for the rats of the control groups. In the treated groups, an important wound contraction was observed with an advanced reepithelization. The epithelial cells of the wound borders proliferated towards the center and led a complete wound closure towards the 11th day (Figure 5).

The phytoconstituents of the studied oils could explain the mechanisms of the skin wound healing process. So, their considerable amount of polyunsaturated fatty acids included oleic acid, linoleic acid, and linolenic acid. Linoleic acid, a precursor of arachidonic acid, is important in the inflammatory cascade (prostaglandins, thromboxanes, and

leukotrienes) [39]. These substances act as inflammatory mediators and accelerate the inflammatory process. Thus, they increase local neovascularization, the remodeling of the extracellular matrix, migration, and fibroblastic cell differentiation [38], which accelerates the healing of wounds. Fatty acids have been reported to have the ability to reduce transepidermal water loss and increase skin hydration and supportive environment for accelerated skin wound healing [40].

In addition, the wound healing effect would also be attributed to a synergy between an antibacterial and antioxidant action observed in our study and described in the literature.

Generally, bacterial species have optimum moisture content closed to neutrality ($6.5 < pH < 7.5$). Habitually, bacteria need a pH ranging from 5.5 to 8.0 to grow; otherwise, there is a slowdown in their development activity, reaching a complete growth cessation at a pH under 4.5 or above 9.0. All the oils showed acidic pH that promoted the inhibition of bacterial growth and accelerated the wound healing process especially in the inflammation phase. Acidic pH contributed to the ideal environment for fibroblastic activity, cell migration, cell proliferation, and reorganization of collagen, which resulted in the stimulation of wound healing [41].

Polyphenols and carotenoids together with vitamin E and sterols demonstrated a beneficial effect on wound healing and collagen synthesis by preventing damaging effects of free radicals and ensuring the stability and integrity of biological membranes [42]. Palmieri et al. [43] also described how vitamin E has a humectant effect on skin wound scarring.

In addition, sterols are powerful compounds that can help to reduce systemic inflammation [44]. They can speed new skin growth by stimulating macrophages and increasing fibroblast and collagen production.

5. Conclusions

In conclusion, according to our experimental results, fenugreek, grape seed, and sesame oils proved to have a better activity on the wound healing compared to the "*CICAFLORA*." This might be due to the synergistic effect of the phytoconstituents present in the oils. However it is necessary to initiate clinical trials on humans to confirm their efficacy in human pathology.

Additional Points

Availability of Data and Materials. The published and the software applications/tools were readily available to any scientist wishing to use them for noncommercial purposes, without restrictions.

Ethical Approval

The experimental protocols were conducted in accordance with the guide for the care and use of laboratory animals and have therefore been performed in accordance with the ethical standards laid down in the 1964 Declaration of Helsinki and its later amendments and approved by the Committee of Animal Ethics (Protocol no. 94-1939).

Competing Interests

The authors declare that they have no competing interests.

Authors' Contributions

Dorsaf Moalla Rekik and Sameh Ben Khedir conceived and designed the experiments. Dorsaf Moalla Rekik, Sameh Ben Khedir, Naziha Grati Kammoun, and Kamilia Ksouda Moalla performed the experiments. Dorsaf Moalla Rekik, Sameh Ben Khedir, Naziha Grati Kammoun, and Kamilia Ksouda Moalla analyzed the data. Dorsaf Moalla Rekik, Sameh Ben Khedir, Naziha Grati Kammoun, Kamilia Ksouda Moalla, and Zouheir Sahnoun contributed reagents/materials/analysis tools. Dorsaf Moalla Rekik, Kamilia Ksouda Moalla, and Sameh Ben Khedir wrote the paper. All authors read and approved the final manuscript.

Acknowledgments

This work was supported by the Ministry of Higher Education and Scientific Research, Tunisia. The authors are grateful to Madiha JALLOULI, English Professor at the Faculty of Medicine of Sfax, for having proofread the manuscript. This research was supported by the Tunisian Ministry of Higher Education and Scientific Research via Sfax University.

References

[1] M. Smith, "Therapeutic applications of fenugreek," *Alternative Medicine Review*, vol. 8, pp. 20–27, 2003.

[2] R. Ram, D. Catlin, J. Romero, C. Cowley, J. Janick, and J. E. Simon, "Sesame: new approaches for crop improvement," in *Advances in New Crops. Proceedings of the First National Symposium "New Crops: Research, Development, Economics", Indianapolis, Ind, USA, October 1988*, Timber Press, 1990.

[3] H. W. Felter and J. U. Lloyd, *Eclectic Medical Publications*, King's American Dispensatory, 1983.

[4] K. R. Anilakumar, A. Pal, F. Khanum, and A. S. Bawa, "Nutritional, medicinal and industrial uses of sesame (*Sesamum indicum* L.) seeds—an overview," *Agriculturae Conspectus Scientificus*, vol. 75, no. 4, pp. 159–168, 2010.

[5] B. S. Nayak, M. R. Marshall, and G. Isitor, "Wound healing potential of ethanolic extract of *Kalanchoe pinnata* Lam. leaf-a preliminary study," *Indian Journal of Experimental Biology*, vol. 48, no. 6, pp. 572–576, 2010.

[6] T. Maier, A. Schieber, D. R. Kammerer, and R. Carle, "Residues of grape (*Vitis vinifera* L.) seed oil production as a valuable source of phenolic antioxidants," *Food Chemistry*, vol. 112, no. 3, pp. 551–559, 2009.

[7] S. Enoch and D. J. Leaper, "Basic science of wound healing," *Surgery*, vol. 26, no. 2, pp. 31–37, 2008.

[8] G. Mohammad, V. K. Mishra, and H. P. Pandey, "Antioxidant properties of some nanoparticle may enhance wound healing in T2DM patient," *Digest Journal of Nanomaterials and Biostructures*, vol. 3, pp. 159–162, 2008.

[9] F. Gutiérrez, M. J. Villafranca, and J. M. Castellano, "Changes in the main components and quality indices of virgin olive oil during oxidation," *Journal of the American Oil Chemists' Society*, vol. 79, no. 7, pp. 669–676, 2002.

[10] T.-H. Tsai, T.-H. Tsai, Y.-C. Chien, C.-W. Lee, and P.-J. Tsai, "In vitro antimicrobial activities against cariogenic streptococci and their antioxidant capacities: a comparative study of green tea versus different herbs," *Food Chemistry*, vol. 110, no. 4, pp. 859–864, 2008.

[11] M. I. Minguez-Mosquera, L. Rejano-Navarro, B. Gandul-Rojas, A. H. Sanchez-Gomez, and J. Garrido-Fernandez, "Color-pigment correlation in virgin olive oil," *Journal of the American Oil Chemists' Society*, vol. 68, no. 5, pp. 332–336, 1991.

[12] P. Bersuder, M. Hole, and G. Smith, "Antioxidants from a heated histidine-glucose model system. I: investigation of the antioxidant role of histidine and isolation of antioxidants by high-performance liquid chromatography," *Journal of the American Oil Chemists' Society*, vol. 75, no. 2, pp. 181–187, 1998.

[13] A. Yildirim, A. Mavi, and A. A. Kara, "Determination of antioxidant and antimicrobial activities of *Rumex crispus* L. extracts," *Journal of Agricultural and Food Chemistry*, vol. 49, no. 8, pp. 4083–4089, 2001.

[14] G. J. Marco, "A rapid method for evaluation of antioxidants," *Journal of the American Oil Chemists' Society*, vol. 45, no. 9, pp. 594–598, 1968.

[15] H. E. Miller, "A simplified method for the evaluation of antioxidants," *Journal of the American Oil Chemists' Society*, vol. 48, no. 2, p. 91, 1971.

[16] M. Skočibušić, N. Bezić, and V. Dunkić, "Phytochemical composition and antimicrobial activities of the essential oils from *Satureja subspicata* Vis. growing in Croatia," *Food Chemistry*, vol. 96, no. 1, pp. 20–28, 2006.

[17] N. Canillac and A. Mourey, "Antibacterial activity of the essential oil of *Picea excelsa* on *Listeria, Staphylococcus aureus* and coliform bacteria," *Food Microbiology*, vol. 18, no. 3, pp. 261–268, 2001.

[18] L. A. DiPietro and A. L. Burns, *Wound Healing. Methods and protocols. 156 × 235 mm*, Humana Press, Totowa, NJ, USA, 2003.

[19] P. Albertin and F. Alric, *Plaies et Cicatrisations au Quotidien*, Sauramps Médical, 2001.

[20] N. Ohura, S. Ichioka, T. Nakatsuka, and M. Shibata, "Evaluating dressing materials for the prevention of shear force in the treatment of pressure ulcers," *Journal of Wound Care*, vol. 14, no. 9, pp. 401–404, 2005.

[21] A. Fikru, E. Makonnen, T. Eguale, A. Debella, and G. Abie Mekonnen, "Evaluation of in vivo wound healing activity of methanol extract of Achyranthes aspera L," *Journal of Ethnopharmacology*, vol. 143, no. 2, pp. 469–474, 2012.

[22] J. F. A. McManus and R. W. Mowry, *Staining Methods-Histologic and Histochemical*, Academic Medicine, 1961.

[23] P. G. Bowler, B. I. Duerden, and D. G. Armstrong, "Wound microbiology and associated approaches to wound management," *Clinical Microbiology Reviews*, vol. 14, no. 2, pp. 244–269, 2001.

[24] M. Deiana, A. Rosa, C. F. Cao, F. M. Pirisi, G. Bandino, and M. A. Dessi, "Novel approach to study oxidative stability of extra virgin olive oils: importance of α-tocopherol concentration," *Journal of Agricultural and Food Chemistry*, vol. 50, no. 15, pp. 4342–4346, 2002.

[25] M. J. Berenguer, P. M. Vossen, S. R. Grattan, J. H. Connell, and V. S. Polito, "Tree irrigation levels for optimum chemical and sensory properties of olive oil," *Hort Science*, vol. 41, pp. 427–432, 2006.

[26] M. Bravi, F. Spinoglio, and N. Verdone, "Improving the extraction of a-tocopherol-enriched oil from grape seeds by supercritical CO_2. Optimization of the extraction conditions," *Journal of Food Engineering*, vol. 78, pp. 488–493, 2007.

[27] F. Mezni, M. L. Khouja, S. Gregoire, L. Martine, A. Khaldi, and O. Berdeaux, "Effect of growing area on tocopherols, carotenoids and fatty acid composition of *Pistacia lentiscus* edible oil," *Natural Product Research*, vol. 28, no. 16, pp. 1225–1230, 2014.

[28] A. A. Dandjouma, C. Tchiegang, and M. Parmentier, "Evolution de quelques paramètres de qualité physico-chimique de l'huile de la pulpe des fruits de *Canarium schweinfurthii* Engl. au cours du stockage," *International Journal of Biological and Chemical Sciences*, vol. 2, no. 3, pp. 249–257, 2008.

[29] E. Psomiadou and M. Tsimidou, "Stability of virgin olive oil. 1. Autoxidation studies," *Journal of the Science of Food and Agriculture*, vol. 41, pp. 640–647, 2002.

[30] E. Psomiadou and M. Tsimidou, "Stability of virgin olive oil. 2. Photo-oxidation studies," *Journal of Agricultural and Food Chemistry*, vol. 50, no. 4, pp. 722–727, 2002.

[31] W. Wang, X. Weng, and D. Cheng, "Antioxidant activities of natural phenolic components from *Dalbergia odorifera T. Chen*," *Food Chemistry*, vol. 71, no. 1, pp. 45–49, 2000.

[32] L. Almela, B. Sánchez-Muñoz, J. A. Fernández-López, M. J. Roca, and V. Rabe, "Liquid chromatograpic-mass spectrometric analysis of phenolics and free radical scavenging activity of rosemary extract from different raw material," *Journal of Chromatography A*, vol. 1120, no. 1-2, pp. 221–229, 2006.

[33] D. M. Luzia and N. Jorge, "Oxidative stability and alpha-tocopherol retention in soybean oil with lemon seed extract (*Citrus limon*) under thermoxidation," *Natural Product Communications*, vol. 4, pp. 1553–1556, 2009.

[34] W. T. Lawrence, "Physiology of the acute wound," *Clinics in Plastic Surgery*, vol. 25, no. 3, pp. 321–340, 1998.

[35] S. Bardaa, D. Moalla, S. Ben Khedir, T. Rebai, and Z. Sahnoun, "The evaluation of the healing proprieties of pumpkin and linseed oils on deep second-degree burns in rats," *Pharmaceutical Biology*, vol. 54, no. 4, pp. 581–587, 2015.

[36] R. W. Colman, A. W. Clowes, and J. N. George, "Overview of hemostasis," in *Hemostasis and Thrombosis: Basic Principles and Clinical Practice*, pp. 1–16, Williams & Wilkins, Philadelphia, Pa, USA, 5th edition, 2006.

[37] J. E. Albina, "Nutrition and wound healing," *Journal of Parenteral and Enteral Nutrition*, vol. 18, no. 4, pp. 367–376, 1994.

[38] T. Velnar, T. Bailey, and V. Smrkolj, "The wound healing process: an overview of the cellular and molecular mechanisms," *Journal of International Medical Research*, vol. 37, no. 5, pp. 1528–1542, 2009.

[39] J. W. Fetterman Jr. and M. M. Zdanowicz, "Therapeutic potential of n-3 polyunsaturated fatty acids in disease," *American Journal of Health-System Pharmacy*, vol. 66, no. 13, pp. 1169–1179, 2009.

[40] M. A. Farage, K. W. Miller, and H. I. Maibach, "Degenerative changes in aging skin," in *Textbook of Aging Skin*, pp. 25–35, Springer, Berlin, Germany, 2010.

[41] B. P. Mwipatayi, D. Angel, J. Norrish, M. J. Hamilton, A. Scott, and K. Sieunarine, "The use of honey in chronic leg ulcers: a literature review," *Primary Intention*, vol. 12, pp. 107–112, 2004.

[42] J. A. Lucy and J. T. Dingle, "Fat-soluble vitamins and biological membranes," *Nature*, vol. 204, no. 4954, pp. 156–160, 1964.

[43] B. Palmieri, G. Gozzi, and G. Palmieri, "Vitamin E added silicone gel sheets for treatment of hypertrophic scars and keloids," *International Journal of Dermatology*, vol. 34, no. 7, pp. 506–509, 1995.

[44] A. De Jong, J. Plat, A. Bast, R. W. L. Godschalk, S. Basu, and R. P. Mensink, "Effects of plant sterol and stanol ester consumption on lipid metabolism, antioxidant status and markers of oxidative stress, endothelial function and low-grade inflammation in patients on current statin treatment," *European Journal of Clinical Nutrition*, vol. 62, no. 2, pp. 263–273, 2008.